Copyright Warning & Restrictions

The copyright law of the United States (Title 17, United States Code) governs the making of photocopies or other reproductions of copyrighted material.

Under certain conditions specified in the law, libraries and archives are authorized to furnish a photocopy or other reproduction. One of these specified conditions is that the photocopy or reproduction is not to be "used for any purpose other than private study, scholarship, or research." If a, user makes a request for, or later uses, a photocopy or reproduction for purposes in excess of "fair use" that user may be liable for copyright infringement,

This institution reserves the right to refuse to accept a copying order if, in its judgment, fulfillment of the order would involve violation of copyright law.

Please Note: The author retains the copyright while the New Jersey Institute of Technology reserves the right to distribute this thesis or dissertation

Printing note: If you do not wish to print this page, then select "Pages from: first page # to: last page #" on the print dialog screen

Order Number 8816821

Assessment of autonomic regulation of heart rate variability

Shin, Shaw-Jyh, D.Eng.Sc.

New Jersey Institute of Technology, 1988

U·M·I
300 N. Zeeb Rd.
Ann Arbor, MI 48106

ASSESSMENT OF AUTONOMIC REGULATION

OF

HEART RATE VARIABILITY

by
Shaw-Jyh Shin

Dissertation submitted to the Faculty of the Graduate School
of the New Jersey Institute of Technology in partial
fulfillment of the requirements for the degree of
Doctor of Engineering Science
1988

APPROVAL OF DISSERTATION

Title of Dissertaion: Assessment of Autonomic Regulation of Heart Rate Variability

Name of Candidate: Shaw-Jyh Shin

Doctor of Engineering Science, 1988

Dissertaion and Abstract Approved:

Dr. Stanley S. Reisman Professor and Associate Chairman Electrical Engineering Department	Date
Dr. Walter M. Tapp	Date
Dr. Andrew U. Meyer	Date
Dr. Peter Engler	Date

VITA

Name: Shaw-Jyh Shin

Degree and date to be conferred: D. Eng. Sc., 1988

Secondary education: Kao Hsiung Senior High School

College attended	Date	Degree	Date of degree
Tamkang Univ.	1973	BSEE	1977
N. J. I. T.	1982	MSEE	1983
N. J. I. T.	1983	DES	1988

Major: Electrical Engineering

Minor: Mathematics

Publications: S. S. Reisman, H. E. Pawel, M. Korurek, S. Shin, T. G. Lynch, R. W. Hobson
Microcomputer Simulation of an Arterial Circulation System.
Proceedings of IEEE/Eighth Conference of the Engineering in Medicine and Biology Society, 1986, pp. 843-846

Positions held: Special Lecturer, N. J. I. T., Newark, N.J.

ABSTRACT

Title of Dissertation: Assessment of Autonomic Regulation of Heart Rate Variability

Shaw-Jyh Shin, Doctor of Engineering Science, 1988

Dissertation directed by: Dr. Stanley S. Reisman

Complex demodulation, accompanied by the techniques of interpolation, detrending and zero-phase-shift lowpass filtering were used to examine the effect of both divisions of the autonomic nervous system (sympathetic and parasympathetic) on heart rate by analyzing the heart rate variability signal from dogs under two different classical conditionings: CS+ and CS-, which cause different dynamic pattern changes in the autonomic nervous system to regulate the heart rate.

Unlike power spectral analysis, complex demodulation gives results in the time domain and shows the variation of amplitude and phase over time at a given frequency. The variation of phase indicates the frequency deviation from the center frequency while the variation of amplitude indicates the intensity of the frequency components in the signal around the center frequency.

The complex demodulation results from the study of dogs which are classically conditioned clearly show the

activities of both sections of the autonomic nervous system in regulating heart rate, and this allows us to understand more about the relationship between the heart rate and the autonomic nervous system in both conditioned and nonconditioned animals.

ASSESSMENT OF AUTONOMIC REGULATION

OF

HEART RATE VARIABILITY

ACKNOWLEDGEMENTS

I wish to express my deep sense of gratitude to my advisor, Dr. Stanley S. Reisman, and Dr. Walter N. Tapp, for their valuable suggestions, criticisms, and patience. Additional thanks need to be expressed to Dr. Benjamin H. Natelson for his personal and sincere care.

Special thanks are due to Mr. Tom Pritzel for his assistance in computer software.

Finally, I would like to thank my parents for their endless love and care.

TABLE OF CONTENTS

LIST OF FIGURES

LIST OF TABLES

CHAPTER I

INTRODUCTION

1-1 INTRODUCTION TO THE MECHANISM OF HEART CONTRACTION

The contraction of the heart is initiated by a depolarization process along the cardiac conduction system which consists of four specialized structures: the sino-atrial node (SA node), the atrioventricular node (AV node), the bundle of His, and the Purkinje system (18). In four-chambered mammalian hearts, the SA node is located at the junction of the superior vena cava with the right atrium.

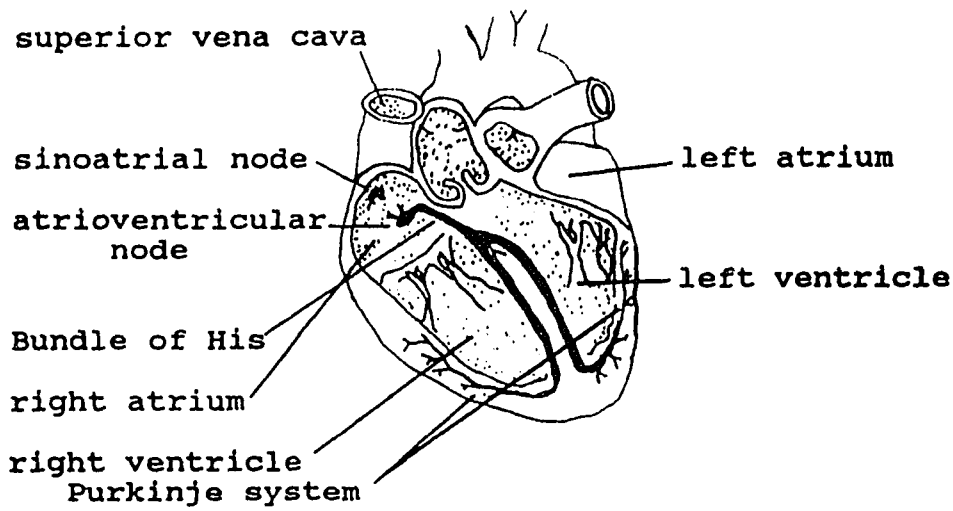

FIGURE 1.1 Conducting system of the heart.

The AV node is located in the right posterior portion of the interatrial septum. There is no specialized conducting

tissue connecting the two nodes, but the atrial muscle fibers converge on and interdigitate with the fibers in the AV node. The AV node is continuous with the bundle of His, which divides at the top of the interventricular septum into right and left branches. The branches run subendocardially down either side of the septum, and come into contact with the Purkinje system, the fibers of which spread to all parts of the ventricular myocardium (Figure 1.1).

The SA node normally discharges most rapidly, depolarization spreading from it to the other regions before those regions discharge spontaneously. The SA node is therefore the normal cardiac pacemaker, its rate of discharge determining the rate at which the heart beats. Impulses generated in the SA node pass through the atrial muscle to the AV node, through this node to the bundle of His, and through the branches of the bundle of His via the Purkinje system to the ventricular muscle. The orderly depolarization process triggers a coordinated wave of contraction that spreads through the myocardium.

1-2 THE ELECTROCARDIOGRAM

Because the body fluids are good conductors, fluctuations in potential that represent the action of potentials of myocardial fibers can be recorded from the surface of the body. The record of these potential functions during the cardiac cycle is the electrocardiogram, or ECG

(18).

Figure 1.2 shows a typical ECG signal. After the discharge of the SA node, a wave of excitation spreads over the atria, producing the P wave and causing the atria to contract. The excitation is delayed in the AV node, resulting in the P-R interval. The wave of excitation then spreads over the ventricles, causing them to contract and producing the QRS complex. Recovery of ventricular deporization produces the T wave (37).

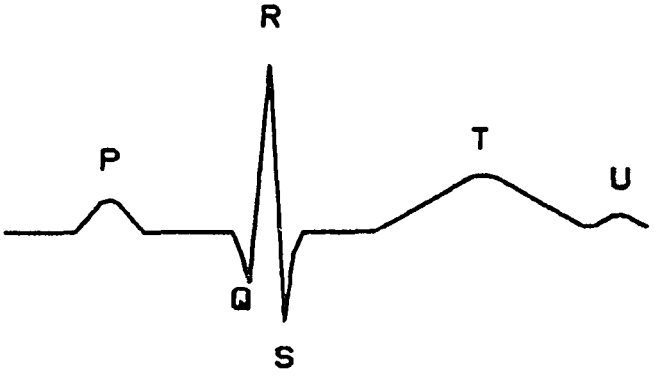

FIGURE 1.2 A typical ECG signal.

1-3 GENERAL DISCUSSION OF THE REGULATION OF THE HEARTBEAT

There are many factors which contribute to the regulation of the heart rhythm. For example: the respiratory effect - Cardiac rate accelerates during inspiration and decelerates during expiration (respiratory cardiac arrhythmia); the blood pressure effect - The alterations in heart rate evoked by changes in blood pressure depends on

baroreceptors located in the aortic arch and carotid sinuses. An abrupt rise in pressure in the aortic arch results in bradycardia (the heart rate is slowed). A subsequent decline of pressure is followed by return of the heart rate to control levels (3).

In the intact organism, a change in the behavior of one of these features of cardiac activity almost invariably produces an alteration in another. Experimentally it has been shown that certain local factors, such as temperature changes and tissue stretch, can affect the discharge frequency of the SA node. However, under natural conditions, the principal control of heart rate is relegated to the autonomic nervous system. As in the case of the respiratory effect on the cardiac rate, the neural activity increases in the sympathetic fibers during inspiration, and the neural activity in the parasympathetic (vagal) fibers increases during expiration (3). Also in the case of the blood pressure effect on the cardiac rate, an increase of blood pressure would increase the parasympathetic activity and decrease the sympathetic activity, and a decrease of blood pressure would increase the sympathetic activity and decrease the parasympathetic activity. Figure 1.3 shows a simplified block diagram which describes the regulation of the heart rate. Also, the regulation of heart rate can be described by using an integral pulse frequency modulation (IPFM) model, in which the instantaneous heart rate signal

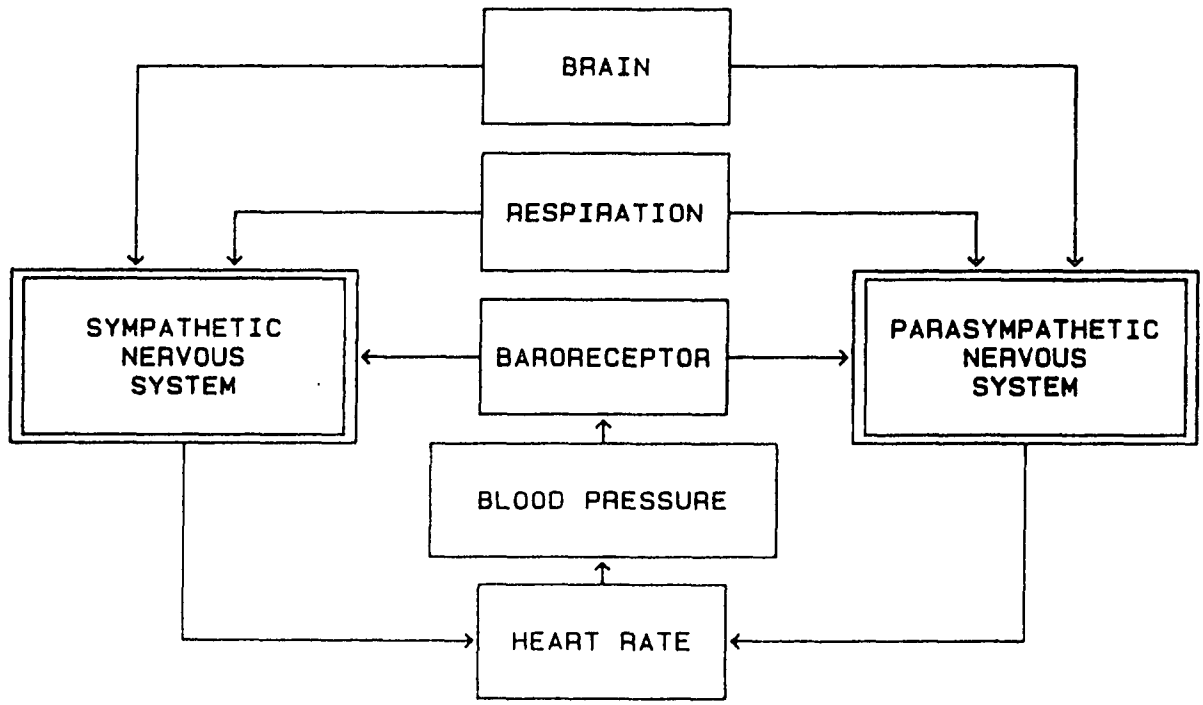

FIGURE 1.3 A SIMPLIFIED BLOCK DIAGRAM WHICH DESCRIBES THE REGULATION OF THE HEART RATE.

may be considered as an approximation of the autonomic (sympathetic and parasympathetic) influence on the pacemaker (12).

1-4 INTRODUCTION TO THE AUTONOMIC NERVOUS SYSTEM

Both divisions of the autonomic nervous system usually influence the heart rate: the sympathetic system enhances automaticity (the ability for the heart to initiate beats), whereas the parasympathetic system inhibits it. Changes in heart rate usually involve a reciprocal action of the two divisions of the autonomic nervous system.

1-4-1 THE PATHWAY OF THE PARASYMPATHETIC NERVES TO THE HEART

The cardiac parasympathetic fibers originate in the melulla oblongata, in cells that lie in the dorsal motor nucleus or the nucleus ambiguus. The precise location varies from species to species. Centrifugal vagal fibers pass inferiorly through the neck in close proximity to the common carotid arteries and then through the mediastinum to synapse with postganglionic cells within the heart itself. Most of the cardiac ganglion cells are located near the SA node and the AV conduction tissue. The right and left vagi are usually distributed differentially to the various cardiac structures. The right vagus nerve predominantly affects the SA node. Stimulation of the right vagus nerve produces sinus

bradycardia or even complete cessation of SA nodal activity for several seconds. The left vagus nerve mainly influences AV conduction tissue to produce various degrees of AV block. However, there is considerable overlap, such that left vagal stimulation also depresses the SA node activity and right vagal stimulation impedes AV conduction (3).

1-4-2 THE PATHWAY OF THE SYMPATHETIC NERVES TO THE HEART

The cardiac sympathetic fibers originate in the intermediolateral columns of the upper five or six thoracic and lower one or two cervical segments of the spinal cord. They emerge from the spinal column through the white communicating branches and enter the paravertebral chain of ganglia. In the dog, virtually all of the preganglionic neurons ascend in the paravertebral chain and funnel through the stellate ganglia. The preganglionic neurons traverse the two limbs of the ansa subclavia and then synapse with the postganglionic neurons in the caudal cervical ganglia. These latter ganglia lie close to the vagus nerves in the superior portion of the mediastinum. Sympathetic and parasympathetic fibers then join to form a complex network of mixed efferent nerves to the heart. The postganglionic cardiac sympathetic fibers approach the base of the heart along the adventitial surface of the great vessels. On reaching the base of the heart, these fibers are distributed to the various chambers as an extensive epicardial plexus. They then penetrate the

myocardium, usually accompanying the branches of the coronary vessels. As with the vagus nerves, there is a differential distribution of the left and right sympathetic fibers. In the dog, the fibers on the left side have more pronounced effects on myocardial contractility than on heart rate. In some dogs, left cardiac sympathetic nerve stimulation may not affect heart rate, even though it may exert pronounced facilitative effects on ventricular performance (3).

1-4-3 INTRODUCTION TO NERVE CELL PHYSIOLOGY AND NERVE CONDUCTION

The size of the nerve cells and the length of their processes vary considerably in different parts of the nervous system. A typical spinal motor neuron shown in Fig. 1.4 has many processes called "dendrites" which extend out

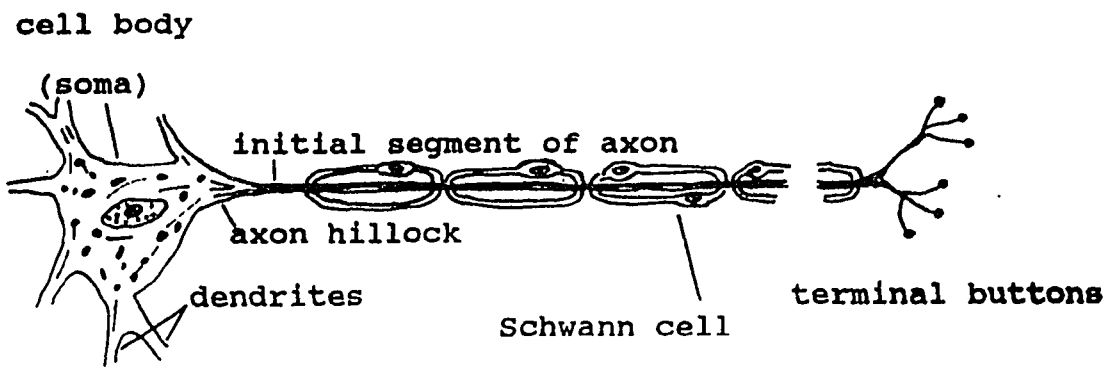

FIGURE 1.4 A motor neuron with myelinated axon.

from the cell body and arborize extensively. It also has a long fibrous "axon" which originates from a somewhat thickened area of the cell body, the axon hillock. The "dendritic zone" of the neuron is the receptor membrane of the neuron. The axon is the single, elongated cytoplasmic neuronal extension with the specialized function of conducting impulses away from the dendritic zone. The axon ends in a number of "terminal buttons", or "axon telodendria" (18).

Impulses are transmitted from one nerve cell to another at synapses, the junctions where the axon of one cell (the presynaptic cell) terminates on the soma or dendrites (or both) of another cell (the postsynaptic cell).

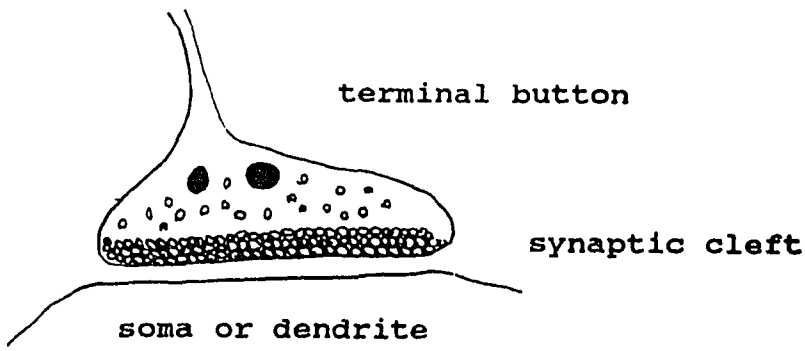

FIGURE 1.5 Relation of the terminal button to the postsynaptic nerve cell membrane.

The terminal buttons are separated from the soma of the postsynaptic cell by a synaptic cleft (Fig. 1.5). Inside the terminal button, there are many mitochondria and small vesicles or granules, the latter being especially numerous in the part of the terminal button closest to the synaptic cleft. It has been claimed that the vesicles contain small "packets" of the chemical neuro-transmitter responsible for synaptic transmission (18). There are also receptors on the dendrites of the post synaptic cell which receive the chemical transmitted from the terminal button. The chemical transmitter released at the parasympathetic (vagal) endings is acetylcholine while the chemical transmitter released at the sympathetic endings is norepinephrine (18).

1-5 NEURAL CONTROL OF HEART RATE CONDITIONING

Under certain conditions, the heart rate may change by selective action of just one division of the autonomic nervous system. In other words, specific autonomic inputs cause the heart to deviate from its average rate by characteristic patterns over time. The best understood of these patterns is the so-called respiratory cardiac arrythmia (as discussed in section 1-3) associated with respiration that produces decreases and increases in beat-to-beat interval [interbeat interval (IBI)], with each inspiration and expiration.

In order to understand more about the regulation of the

heart rate due to the autonomic nervous system, the heart rate variability signal with and without conditioning will be studied.

1-5-1 NATURE OF CONDITIONED CARDIOVASCULAR RESPONSES

Classical conditioning of heart rate can be deemed an experimental model for studying the relationship between behavior and cardiovascular responses. Classical conditioning uses precise stimulus control so that the stimulus-locked cardiovascular responses and the rapid establishment of reliable cardiovascular responses can be observed and investigated.

Generally speaking, there are two kinds of stimuli when classical conditioning is used to investigate the regulation of the heart rate by the two divisions of the autonomic nervous system. One is the conditioned stimulus (CS), the other is the unconditioned stimulus (US). Initially, the conditioned stimulus elicits either no cardiovascular response or a minimal one while the unconditioned stimulus evokes a vigorous cardiovascular response. However, after a sufficient number of CS-US pairings, the dog learns that the CS predicts the occurrence of the US and the CS acquires the capability of reliably eliciting a cardiovascular response. For example, if an innocuous CS such as sound is paired with a nociceptive US such as shock, the CS would reliably elicit a tachycardia after several CS-US pairings. From the

experiments performed under pharmacological neural blockade or peripheral nerve ablation conditions, this tachycardia is believed to be due to an increase of the sympathetic activity and a decrease of parasympathetic activity. This tachycardia reflects the escape or avoidance behavior of the dog during a CS period, even though the experimental situation may not permit achievement of that goal. Simply stated, a temporal contingency in CS-US pairing has been learned, so that the CS which used to evoke no cardiovascular response or a minimal one, now elicits large cardiovascular changes (8).

1-5-2 DRUG TREATMENT CONDITIONS

In the past, the different divisions of the autonomic nervous system have been investigated by using drugs. Drug treatments are used to selectively inhibit the effect of the sympathetic and parasympathetic nervous systems to the heart.

As discussed earier, most neural transmission is chemical. In chemical transmission, the neural cell that transmits the impulse releases chemicals known as neurotransmitters into the synaptic cleft. The neurotransmitter molecules bind to specific receptors on the post-synaptic cell. Atropine methylnitrate is an agent that is used to block the parasympathetic receptors which respond to acetylcholine, and propranolol is used to block the

sympathetic beta-adrenergic receptors which respond to norepinephrine. Selective blockade of a specific portion of the autonomic nervous system by drugs has been the main method used to assess the regulation of the heart by the autonomic nervous system. Ordinarily, abolition of parasympathetic influences by the administration of atropine elicits a pronounced tachycardia, whereas abrogation of sympathetic effects by the administration of propranolol usually results in slowing of the heart beat. However, these drug effects can be complicated by autonomic reflex effects. For example, after propranolol is administrated, the blood pressure might drop, causing the baroreceptor reflex from the aortic arch and carotic sinuses to deactivate parasympathetic activity. The resulting heart rate would then show either no change or an actual increase. Problems with this method are also discussed in section 1-7.

1-6 DESCRIPTION OF AVAILABLE METHODS TO ASSESS THE REGULATION OF THE HEART BY THE AUTONOMIC NERVOUS SYSTEM

Traditionally, the effect of the autonomic nervous system on heart rate has been investigated through two approaches. First, the average heart rate was measured under normal conditions as a reference, and then the average heart rate was measured under different drug treatments - atropine to block the parasympathetic nervous system and propranolol

to block the sympathetic nervous system. By comparing the average heart rate from different drug treatments with the average heart rate under normal conditions, it had been found that the average heart rate under sympathetic blockade was slower than that under normal conditions, and the average heart rate under parasympathetic blockade was faster than that under normal conditions. Those facts imply that the parasympathetic nervous system inhibits the ability for the heart to initiate beats and the sympathetic nervous system tends to enhance it.

The second approach was to use power spectrum analysis to analyze the heart rate variability signal (HRV) under normal conditions and under different drug treatment conditions. By comparing the power spectra, the effect of each division of the autonomic nervous system on heart rate regulation can be assessed. Sayers and others (6,11,26,30,34) used power spectrum analysis to analyze the heart rate variability signal and showed that in addition to the well-known fluctuations in heart rate associated with the respiratory cycle, there are also fluctuations in heart rate at lower frequencies. Akselrod et al (1) showed that sympathetic and parasympathetic nervous activity make frequency-specific contributions to the heart rate power spectrum: the parasympathetic nervous system mediates respiration frequency peaks and mid-frequency peaks of the spectrum because the respiration frequency peaks and mid-

frequency (between the respiration frequency and low frequency) peaks of the spectrum can be abolished by muscarinic antagonists or by vagotomy (6), and both sympathetic and parasympathetic systems mediate heart rate fluctuations in the range of the low frequency peak. Figure 1.6 shows a power spectrum of heart rate variability from a normal dog for a data sample of 204.8 seconds. In this figure, only the low frequency and respiration frequency peaks are visible. The respiration frequency peak at 0.343 Hz is mediated only by the parasympathetic nervous system, and the low frequency peak at 0.119 Hz is mediated by both parasympathetic and sympathetic nervous systems.

Classical conditioning of the heart rate response has been studied for many years because it gives some information about how environmental stimuli alter the activity of the autonomic nervous system. The pattern of the conditioned heart rate response varies from species to species with rodents usually showing heart rate slowing (15,16,20,22,41) and dogs and primates heart rate acceleration (13,27,32) as a result of different behavior to the classical conditioning. Because heart rate provides an integrated measure of autonomic nervous system activity, one can not be sure how much of the conditioned effect is due to sympathetic activation or withdrawal and how much is due to parasympathetic activation or withdrawal. Therefore, behavioral neuroscientists have used a number of strategies

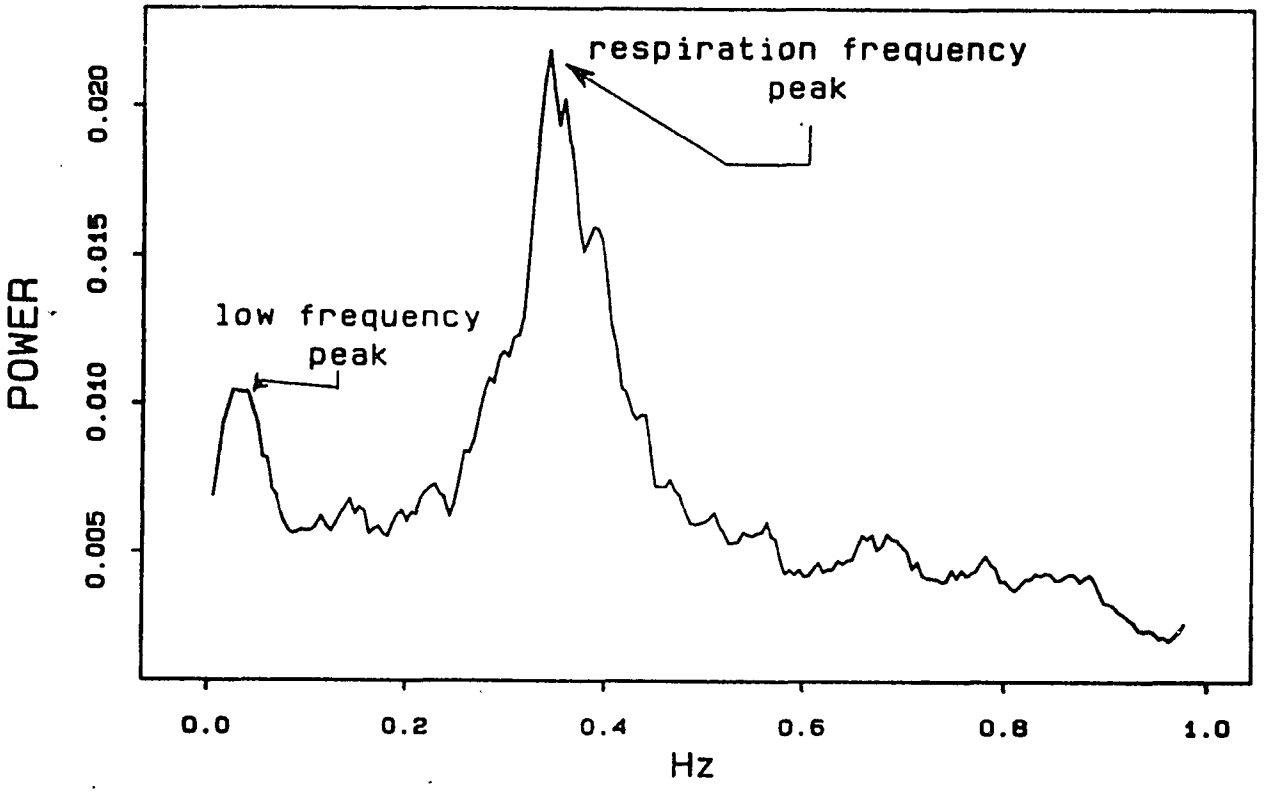

FIGURE 1.6 A POWER SPECTRUM OF THE HEART RATE VARIABILITY SIGNAL OF 204.8 SECOND DURATION FROM A NORMAL DOG.

to try to learn the contributions of the individual components of the autonomic nervous system in producing the conditioned heart rate response. In general, these have consisted of peripheral nerve ablations (6,24) and pharmacological neural blockade (13,14,17,27,32,35,39).

1-7 STATEMENT OF THE PROBLEMS

The two traditional approaches (heart rate averaging and power spectral analysis of HRV) to assess the regulation of the heart rate by the autonomic nervous system and the two ways (neural blockade and ablation) to investigate the contribution of the individual components of the autonomic nervous system in producing the conditioned heart rate response may have three major drawbacks.

First, those methods assess the contribution of the autonomic nervous system to the heart rate regulation either by averaging the heart rate over a period of time or by taking the power spectrum of the HRV signal over a period of time. In other words, both methods show their data in the form of an average over a time period, and can not display what really happens within that time period. For example, if the average heart rate within a 3-minute time period is 70 beat/min., it could actually be 60 beat/min. in the 1st minute, 70 beat/min. in the 2nd minute and 80 beat/min. in the 3rd minute, or it could be 40 beat/min. in the first 1.5 minutes and 100 beat/min. in the 2nd 1.5 minute. Also if the

power spectrum of the HRV signal in 3 minutes shows a dominant peak at the frequency of 0.3 Hz, that 0.3 Hz dominant frequency could occur in the whole 3-minute period, or it just occur in the first 1 minute and disappear.

Second, reciprocal control of the heart rate is an important feature of the autonomic nervous system. In other words, there is an interaction between the two divisions of the autonomic nervous system in the regulation of the heart rate. Therefore, when one section of the nervous system is blocked or cut, the interaction between the two sections can not be observed.

Third, most drugs have more than one effect. For example, in addition to its sympathetic blocking activity, propranolol has a local anesthetic effect. Therefore, when using a drug like propranolol, one cannot always be sure which of the drug effects is producing the experimental effect that is being observed. Also, drugs may have some unknown effects.

1-8 DESCRIPTION OF METHODS USED IN THIS DISSERTATION

Because of the drawbacks mentioned above, it is desirable to have a method to investigate the regulation of the conditioned heart rate in the time domain that does not involve drugs. The complex demodulation method allows us to examine both sections of the autonomic nervous system acting in concert without any effect of drugs. It enables us to

track changes of magnitude in the low and respiration frequency responses as a function of time. The respiration frequency response reflects the activity of the parasympathetic nervous system, and the low frequency response reflects the activities of both the parasympathetic and sympathetic nervous systems.

Also, in an experiment of conditioned or unconditioned response of heart rate (8), and with no drug treatment, complex demodulation shows the changes of the low and the respiration frequency responses due to the classical conditioning. By monitoring these changes, we are able to monitor the time-locked dynamic activities of the sympathetic and parasympathetic nervous systems separately under some circumstances. This will be discussed in section 4-3.

In addition to complex demodulation, other signal processing techniques, like interpolation, detrending and zero-phase-shift lowpass filtering are necessary to process the signal; these will be described in chapter III.

CHAPTER II

DATA ACQUISITION SYSTEM DESCRIPTION

2-1 INTRODUCTION

Signal processing of the heart rate variability (HRV) signal can provide information about the activity of the autonomic nervous system in regulating the heart rate. As discussed in section 1-7, there are several drawbacks to the traditional approaches. In order to avoid these drawbacks, we used the method of complex demodulation on the heart rate variability signal.

Besides the HRV signal, the respiration signal is also needed. The respiratory sinus arrhythmia derived from spectral analysis can be used as a non-invasive estimate of vagal influence to the heart (29,31,42). Because respiration is driving this component of HRV, it is important to know the respiratory pattern and frequency. Therefore, we need to collect the respiration signal. Neural activity increases in the sympathetic fibers during inspiration, and the neural activity in the parasympathetic (vagal) fibers increases during expiration. The acetylcholine released at the vagal endings is removed so rapidly that the rhythmic changes in activity are able to elicit rhythmic variations in heart rate. Conversely, the norepinephrine released at the sympathetic endings is removed more slowly, thus damping out the effects of rhythmic variations in transmitter release on

heart rate.

In order to efficiently assess the contribution of the autonomic nervous system to regulate heart rate, the HRV signal and the corresponding respiration signal were taken from dogs under normal conditions and under classical conditioning.

This chapter will introduce the method of acquisition of the HRV and respiration signals.

2-2 EXPERIMENTAL PROCEDURE

Four male mongrel dogs weighing 10 to 14 kg were randomly assigned to one of the two groups: conditioned (COND) and non-conditioned (NCOND). The basic task of the conditioning is for the animal to learn that a signal (tone) predicts the occurrence of a small shock. In order to make sure that the animal is not responding to the tone, we use a differential conditioning where one tone predicts the occurrence of the shock (CS+) and another tone predicts that no shock will occur (CS-). Once the animal is conditioned, that is, once he has learned that the CS+ tone reliably predicts a shock, then the occurrence of the CS+ tone itself serves to produce a reliable sequence of autonomic events. This is the sequence of events that the project was set up to study.

For the COND dogs, the CS+ was a 30 second, 90 dB continuous tone followed by a 0.5 second, 3 to 5 mA flank

shock, while the CS- was a tone pulsed at 10 Hz. A fifteen-minute baseline period preceded each day's data collection. All dogs received 16 trials per day and each trial consisted of a 3-minute baseline, a 30-second pre-CS period, a 30-second CS period, and a 30 second post-CS period as shown in Fig. 2.1 (a) and (b).

All dogs were placed in a double sound-attenuated chamber for the same period each day. However, for dogs in the NCOND groups only tones were presented. We use REF to indicate the period which corresponds to the CS in COND dogs as shown in Fig. 2.1 (c).

ECG, arterial blood pressure and respiration signals were displayed on a Grass polygraph. Presentation of stimuli and control of the chart recorder were performed by a PDP-8 computer (DEC) using a SKED (Snapper et al., 1984) (36) system which consists of a two-pass compiler with an optional third pass listing, a set of programs for identifying and merging data acquisition files and a sophisticated system monitor that can be used to start, stop, load and modify as many as 12 independent stations, where each station can acquire every event time of interest and can record these sequentially on mass-storage devices for later processing using standard FORTRAN, BASIC or FOCAL programs. An eight channel SONY tape recorder recorded the baseline and trial 6, 7 and 8 of the ECG signal as well as the corresponding respiration signal.

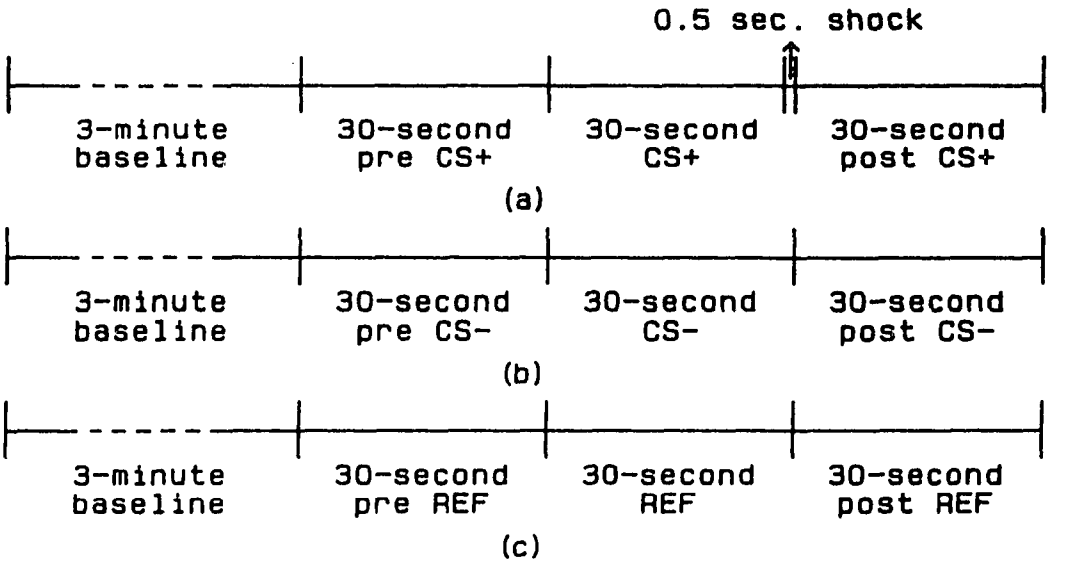

FIGURE 2.1 (a) A CS+ TRIAL WHICH CONTAINS A 3-MINUTE BASELINE, A 30-SEC. PRE-CS+ PERIOD, A 30-SEC. CS+ PERIOD, AND A 30-SEC. POST-CS+ PERIOD. A 0.5 SECOND SHOCK WAS DELIVERED AT THE END OF THE 30-SEC. CS+ PERIOD.

(b) A CS- TRIAL WHICH CONTAINS A 3-MINUTE BASELINE, A 30-SEC. PRE-CS- PERIOD, A 30-SEC. CS- PERIOD, AND A 30-SEC. POST-CS- PERIOD.

(C) A REF TRIAL WHICH CONTAINS A 3-MINUTE BASELINE, A 30-SEC. PRE-REF PERIOD, A 30-SEC. REF PERIOD, AND A 30-SEC. POST-REF PERIOD.

Figure 2.2 shows the block diagram of the system. The following sections will introduce the function and circuitry of the subsystems.

2-3 SIGNAL ACQUISITION CIRCUIT

The fuction of this subsystem is to acquire the ECG and respiration signals from dogs or humans and pass them through an isolation circuit in order to save them on tape.

The respiration signal was acquired by using an impedance technique (2): During inspiration, the lung tissue fills with air and becomes more resistive. Also, the chest wall becomes thinner and its circumference increases. Both effects increase the impedance across the chest. During expiration, the opposite occurs. Basically, this technique requires the passage of a low intensity, high frequency, constant amplitude sinusoidal current across the chest of the subject by means of two electrodes attached to the body surface. Because of the respiratory movement, the chest skin impedance will change accordingly, and the voltage across the chest will vary. From the variation of voltage, the respiration signal is acquired.

Figure 2.3 is the block diagram of this subsystem. The circuitry of this subsystem and the description of this circuit is in Appendix A.

In figure 2.3, there are four electrodes attached to the subject. The inner two electrodes are pick-up electrodes

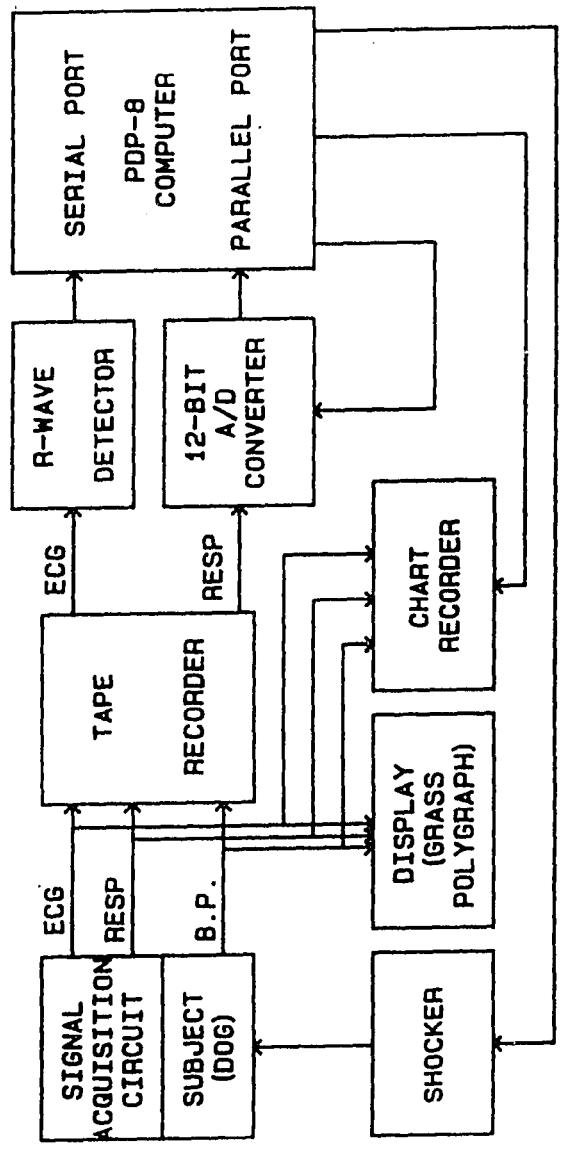

FIGURE 2.2 THE BLOCK DIAGRAM OF THE SYSTEM.

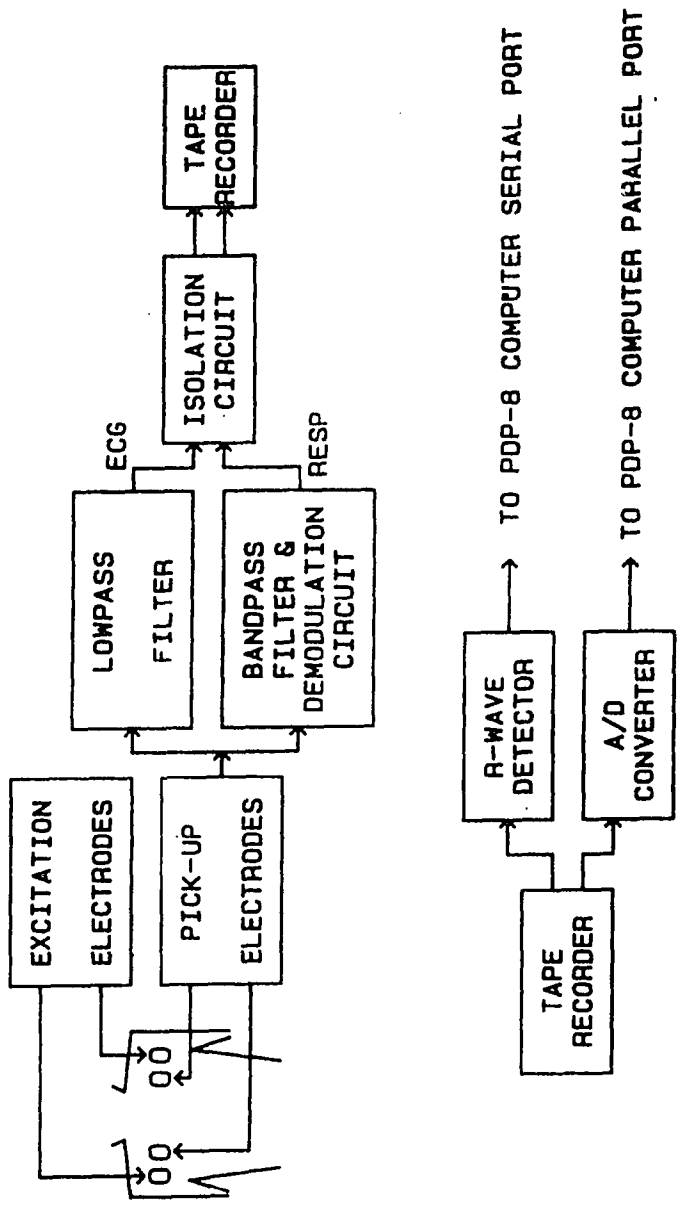

FIGURE 2.3 THE BLOCK DIAGRAM OF THE SIGNAL ACQUISITION SYSTEM.

which pick up both ECG and respiration signals. Since both signals are simultaneously picked up through the same electrodes, the two signals are separated in frequency in order to be usable. This is done by using a constant current 50k Hz source for the respiration measurement while the ECG is in the frequency range of 0 to 100 Hz.

The moderate current i(t) = 3mA at a 50K Hz frequency is not perceived or dangerous, and the inspiration and expiration movement will change the chest skin impedance r(t). Therefore, the magnitude of the voltage v(t) across the pick-up electrodes changes with inspiration and expiration.

$$| v (t) | = i (t). r (t)$$

where r (t) is the impedance of chest skin in ohms

| v (t) | is the voltage across pick-up electrodes in mV

After these two signals are acquired, a lowpass filter recovers the ECG signal and a bandpass filter plus a demodulation circuit will recover the respiration signal.

We then passed these two signals into an isolation circuit before recording them on tape. In this part of the hardware, the SONY 8 channel tape recorder uses AC power. Without the isolation circuit, the AC power from the tape recorder might be fed back into the pick-up circuit and hurt

the subject.

2-4 R-WAVE DETECTOR AND A/D CONVERTER

The two signals of concern are the heart rate variability signal (HRV) and respiration signal. In order to derive the HRV signal from the ECG signal, the ECG signal was first passed from the tape through an adaptive R-wave detector (33) which detects the R-wave of each ECG cycle and correspondingly generates a pulse, Fig. 2.4 (a) and (b) illustrate the action of the R-wave detector. The variable threshold R-wave detector was designed so that it automatically adapts to a drifting baseline and changes in ECG morphology such as varying R wave amplitude and reduced R/T ratio. Therefore, this device provides a reliable automatic R wave detector even in recording situations that are substantially less than optimal. We then input this R-wave pulse train into a PDP-8 computer serial port to count the time duration from one pulse to the next. The values of those pulse-to-pulse durations are called interbeat intervals (IBI) and can be used to produce a non-interpolated type of heart rate variability signal as shown in Fig. 2.4 (c) in which the amplitude of the pulse is proportional to the IBI.

The respiration signal is fed into a 12-bit A/D converter with a 10 Hz sampling rate and then input into the PDP-8 computer parallel port. Figure 2.5 shows the block

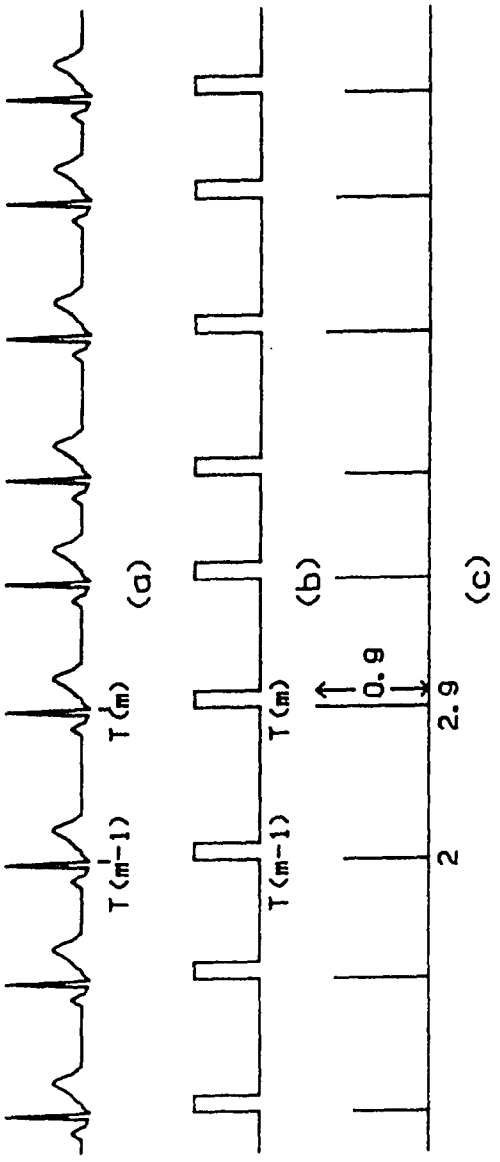

FIGURE 2.4 (a) THE ECG SIGNAL.

(b) THE R-WAVE PULSE TRAIN.

(c) THE IBI SAMPLES.

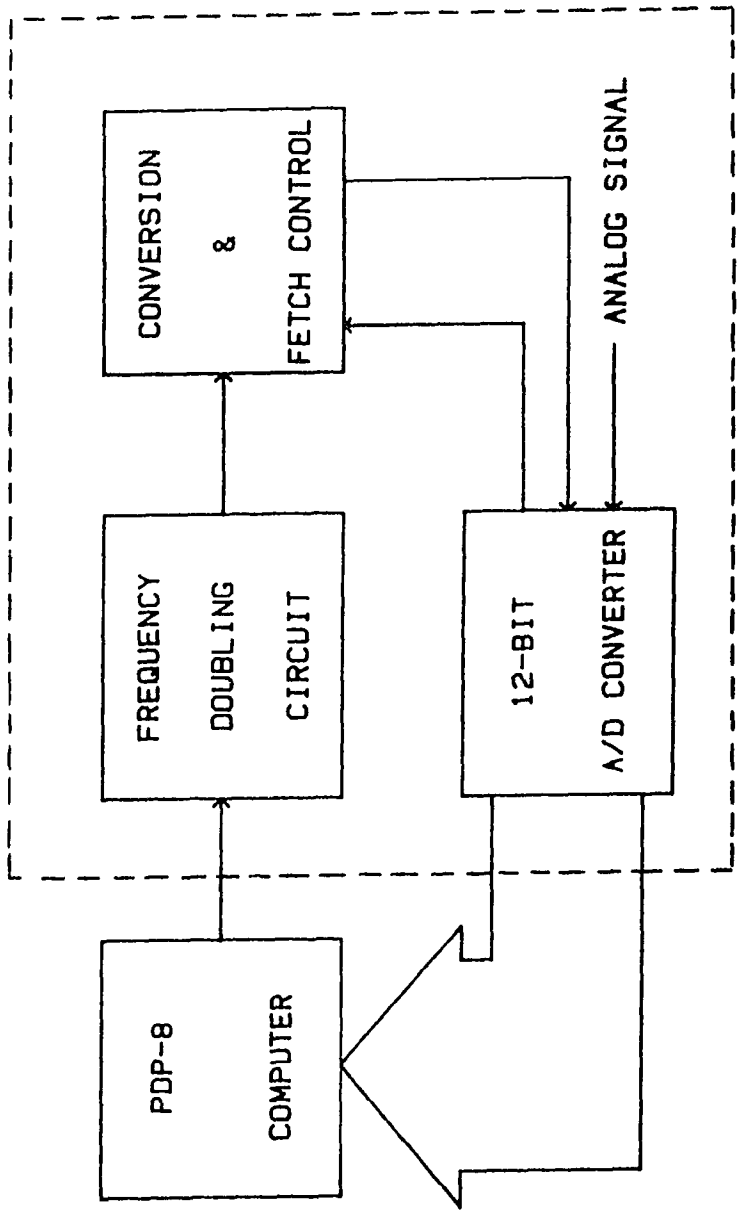

FIGURE 2.5 THE BLOCK DIAGRAM OF THE A/D CONVERTER.

diagram of this A/D converter. The circuitry of the 12-bit A/D converter and the description of this circuit is in Appendix A. The A/D converter was so designed that the first conversion will occur when the first R-wave is detected from the serial port of the PDP-8 computer. Therefore, the IBI values are the values of time from the previous R-wave to the present one and the respiration samples are derived from the respiration signal sampled every 0.1 second.

2-5 TRANSFERRING DATA TO THE VAX 11/750

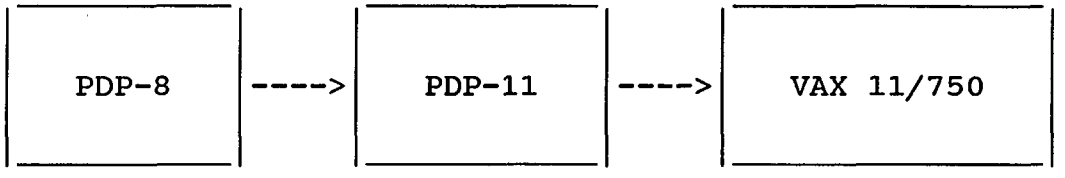

FIGURE 2.6 Data transferred from the PDP-8 to the VAX 11/750

A VAX 11/750 computer was used to analyze the signals. However, it was not convenient to set up the hardware for acquiring the R-wave pulse train from the ECG and quantized respiration values from the analog respiration signal directly by the VAX 11/750 computer in our lab. Therefore, we used the PDP-8 computer to acquire the signals and

transfered them first to the PDP-11 computer, then from the PDP-11 computer to the VAX 11/750 computer for processing. Figure 2.6 shows the block diagram of the signal transformation. The reason that we transferred data through the PDP-11 to the VAX 11/750 is that there is no direct access from the PDP-8 computer to the VAX 11/750.

The data transferred between computers was by means of a file transfer protocol called " Kermit " (10).

Kermit embodies a set of rules for transferring files reliably between two computers. It provides a way of ensuring that the transmitted data has been received correctly and completely in spite of such factors as noise interference, timing asynchronism, and intermittent failures of the transmission line.

In order for the Kermit protocol to function, a Kermit program must be running on each end of the communication line- one on the transmitting computer, and one on the receiving computer. A cable links the serial ports of the computers. The procedure and commands used to transfer data files from the PDP-8 to the VAX 11/750 are listed in Appendix B.

Once the data were transferred to the VAX 11/750, they were stored with the following format:

1	1983	1	1963	1	2050
1	1975	1	1984	1	2077
1	1964	1	2000	1	2048
1	1965	2	86	.	.
1	1984	1	2026	.	.

Each four-digit numeral has a code number in front of it. " 1 " indicates that the value following is the respiration value in quantized form, and " 2 " indicates that the value following is the IBI value in centi-second (10^{-2}).

CHAPTER III

SIGNAL PROCESSING

3-1 INTRODUCTION

The data which were transfered to the VAX 11/750 computer contained IBI values and the sampled respiration signal combined as shown in section 2-5. Before processing, those two signals needed to be separated from each other. In addition, the IBI signal had to be interpolated to produce equally spaced samples along the real time axis. Finally, the signals had to be detrended to take out the very low frequency component. This low frequency component is usually caused by an artifact and it smears the low frequency response produced by spectral analysis and complex demodulation. The main component of this signal processing is the complex demodulation accompanied by the technique of zero-phase-shift lowpass filtering.

Figure 3.1 shows the flow chart for the software used to acquire the respiration signal from the combined IBI and respiration signals. First, the 17 fortran input-output units on the VAX 11/750 computer have to be surveyed to see if one of these units is available to us. If not, we need to run the program at another time. If one of the input-output units is available, then we can open the file that we want to read, read a code number and the subsequent four-digit numeral, and check the code number. If the code number is 1,

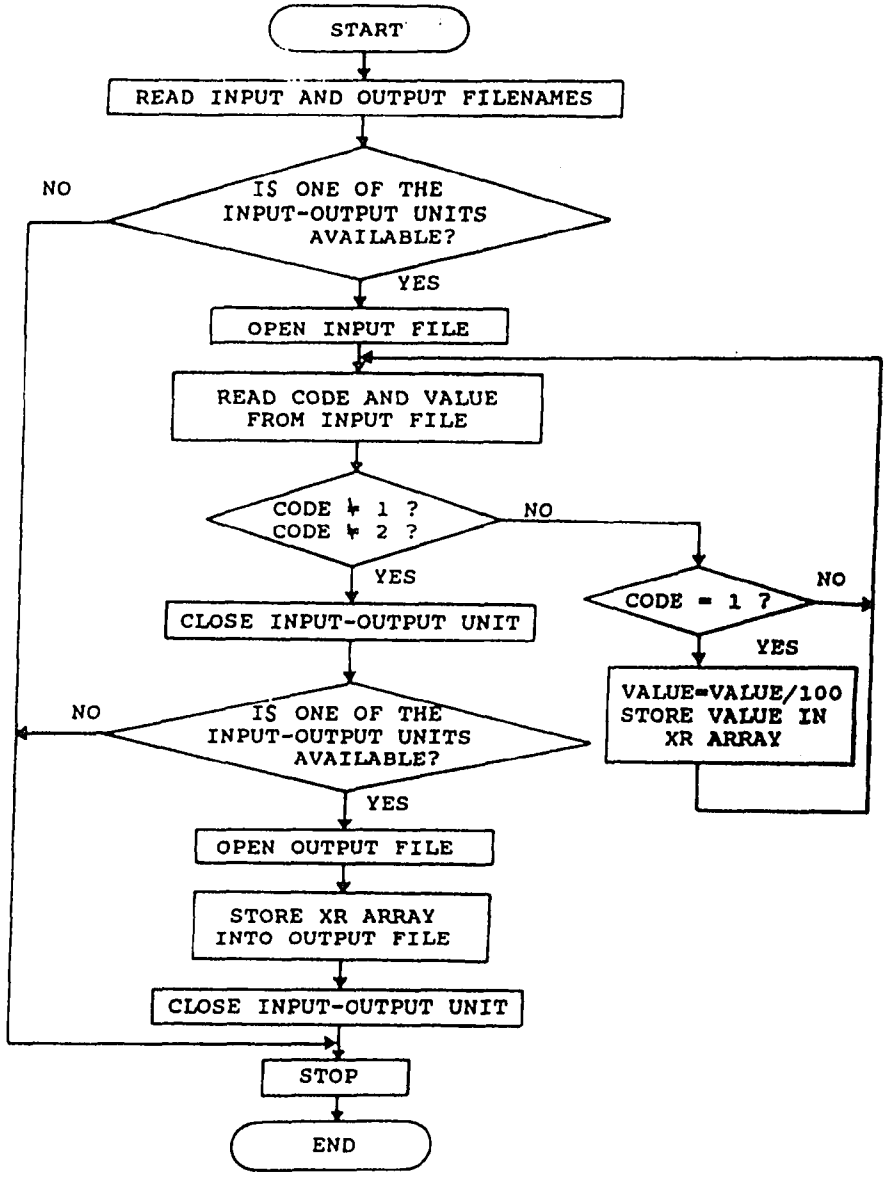

FIGURE 3.1 THE FLOW CHART TO ACQUIRE THE RESPIRATION SIGNAL FROM THE COMBINED IBI AND RESPIRATION VALUES.

the subsequent four-digit numeral is a respiration value; we take that value, divide it by 100 and store the result. Then the program reads the next code and the subsequent four-digit numeral. if the code number is 2, then the subsequent four-digit numeral is an IBI, and the program just ignores it and reads the next code. If the code number is neither 1 nor 2, the program has reached the end of the data file, then we write the respiration values into a separate data file for later processing.

Figure 3.2 shows the software flow chart to acquire the IBI signal from the combined IBI and respiration signals, and interpolate it so that every value is 0.1 second apart. Basically, this flow chart is similar to the flow chart mentioned above to acquire the respiration signal, except for the addition of two features. First, if the IBI value is less than 0.1 second, it can not be a real IBI value because the corresponding heart rate would be above 600 beats/minute. Such small values are usually caused by the noise spikes in the ECG signal train and detected by the R-wave detector. These artifacts typically have a particular structure such that the short artifact can be added to the next IBI value and the resulting IBI fits into the rest of the IBI sequence. Second, after all the IBI values are acquired, a 0.1 second interpolation is performed based on the existing IBI values before furthering processing. The interpolation method will be discussed in the next section.

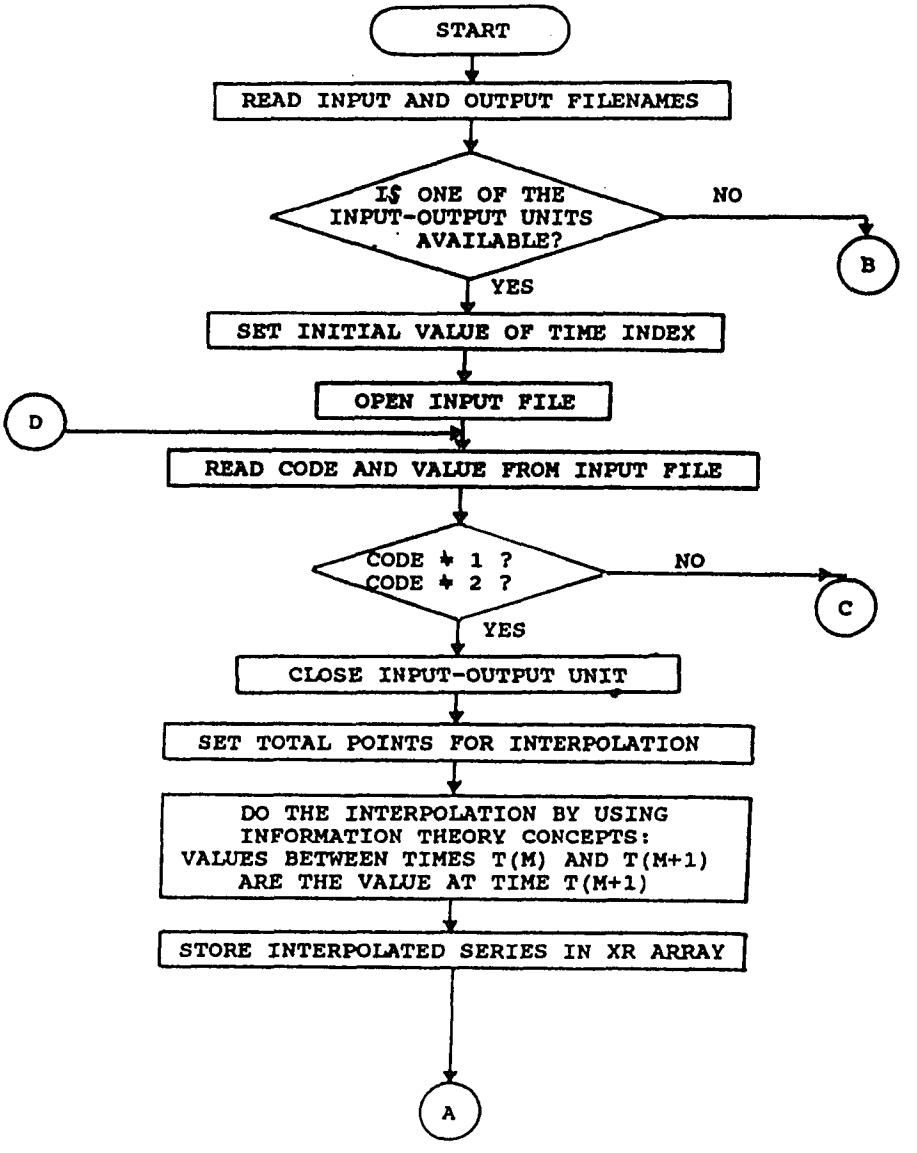

FIGURE 3.2 THE FLOW CHART TO ACQUIRE THE IBI SIGNAL AND INTERPOLATE IT FROM THE COMBINED IBI AND RESPIRATION VALUES.

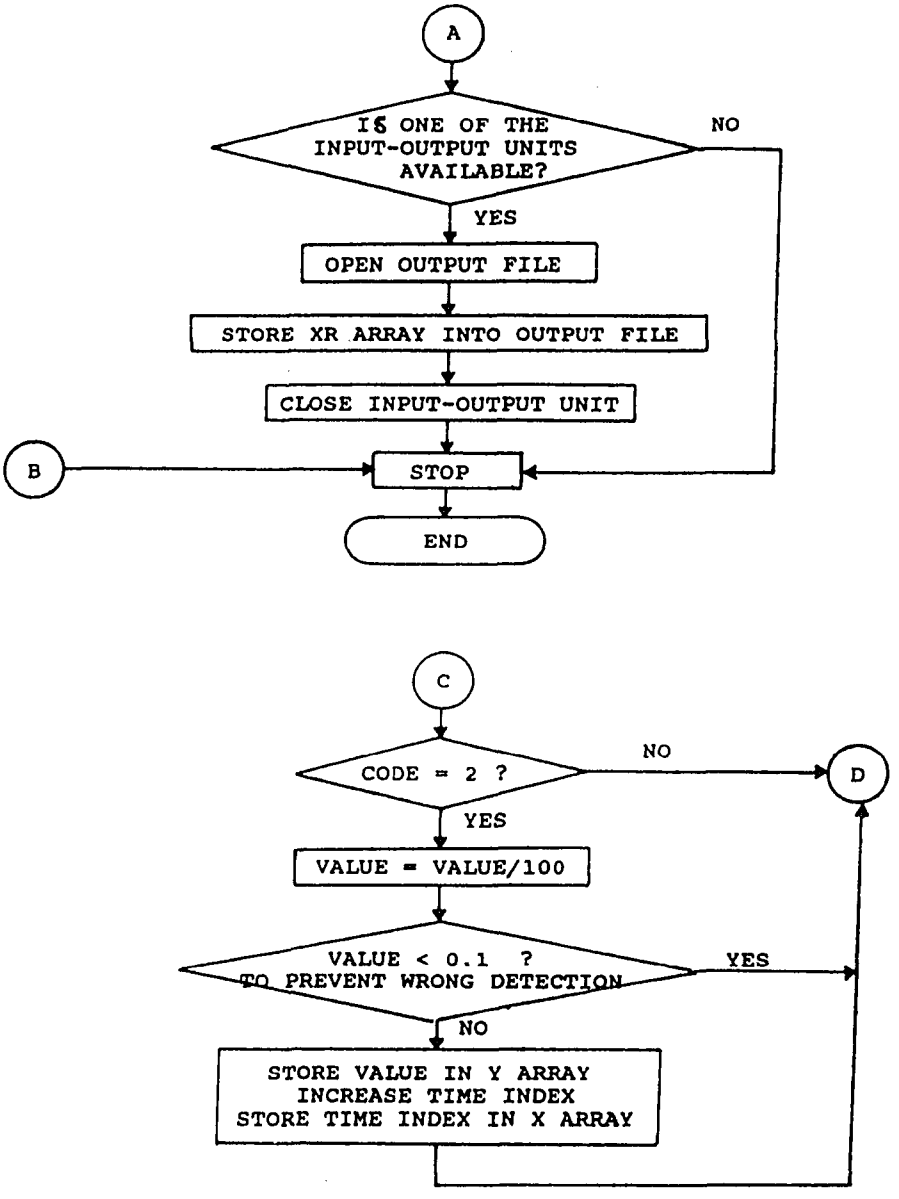

FIGURE 3.2 THE FLOW CHART TO ACQUIRE THE IBI SIGNAL AND INTERPOLATE IT FROM THE COMBINED IBI AND RESPIRATION VALUES.

3-2 INTERPOLATION

The samples of the respiration signal are equidistant in time (0.1 sec. apart). However, the IBI samples are not equidistant along the real time axis, since they occured whenever an R-wave was detected and represent the time intervals between R waves. In order to produce time-equidistant IBI samples suitable for analysis and synchronized with the respiration signal, interpolation is needed. We tried several different interpolation methods like cubic spline interpolation (5) which interpolates based on a polynomial, linear interpolation (5) which interpolates by connecting the start value and the end value with a straight line, and an interpolation scheme based on Information Theory concepts (28) which interpolates between beats. Figure 3.3 shows those different interpolation methods, where (a) is a set of IBI values, (b) is an interpolation scheme based on Information Theory concepts, (c) is a linear interpolation scheme, (d) is a cubic spline interpolation scheme. Comparing the power spectra from the interpolated IBI signal and respiration signal under the non-drug control condition showed that the different interpolation methods gave very similar results. They all showed respiratory frequency peak in the power spectrum of the interpolated IBI signal as shown in Figure 3.4.1, 3.4.2 and 3.4.3. Figure 3.4.1 (a) and (b) are 60-second

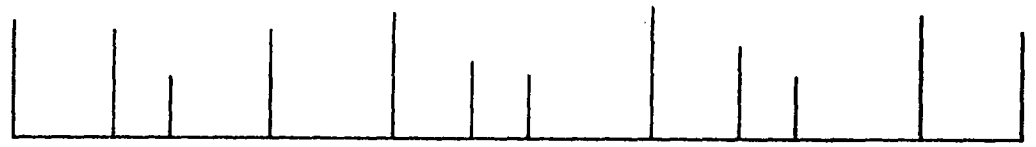

(a)

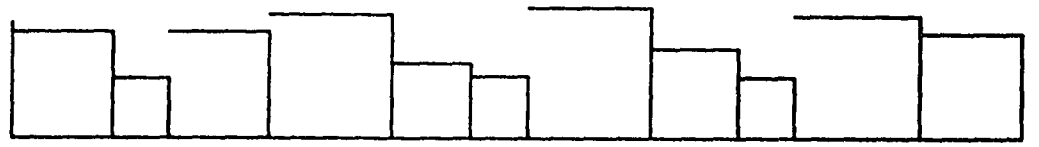

(b)

FIGURE 3.3 (a) A SET OF IBI VALUES.
(b) AN INTERPOLATION SCHEME BASED ON INFORMATION THEORY CONCEPTS.

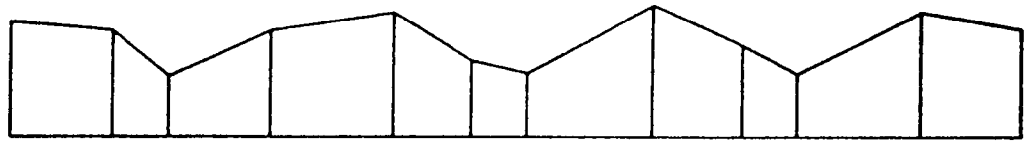

(c)

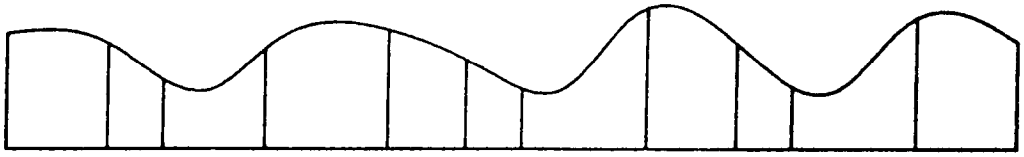

(d)

FIGURE 3.3 (c) A LINEAR INTERPOLATION SCHEME.

(d) A CUBIC SPLINE INTERPOLATION SCHEME.

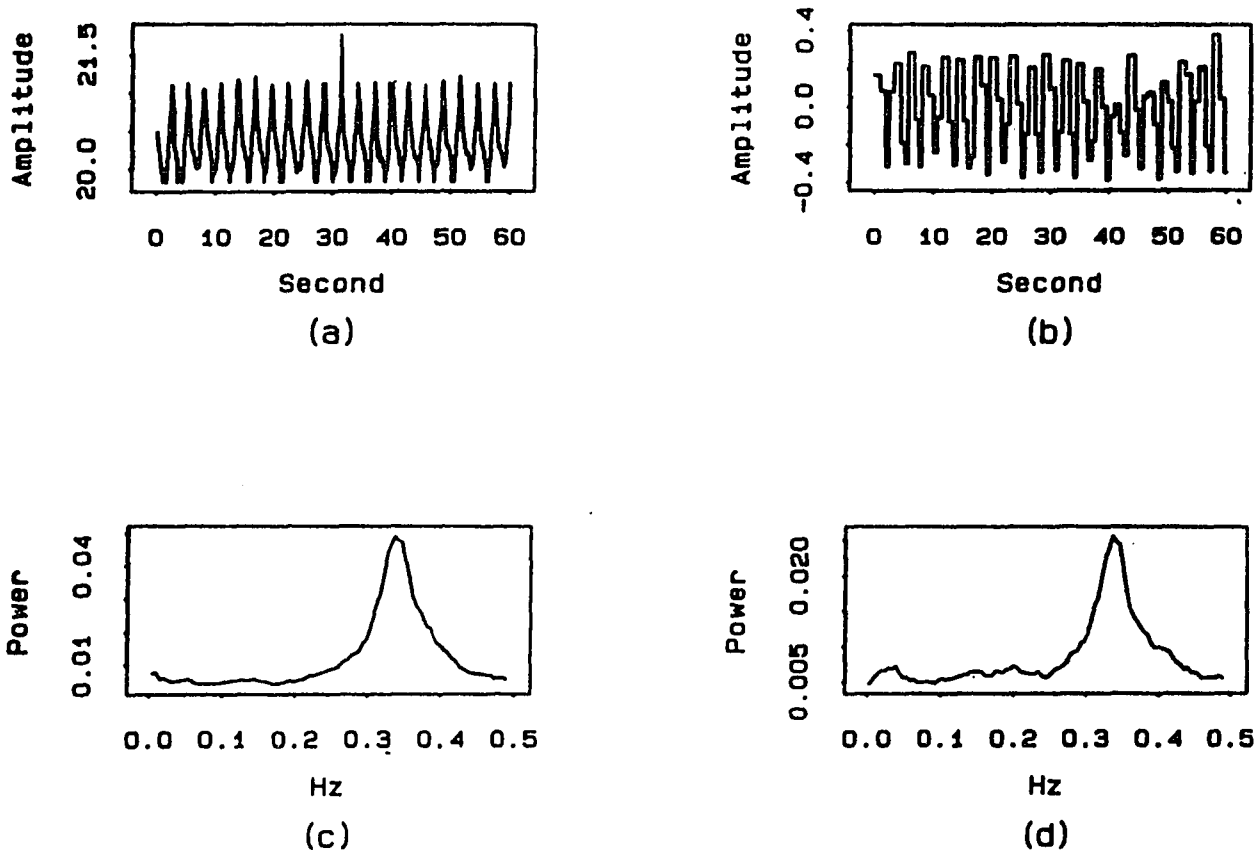

FIGURE 3.4.1 (a) A 60-SECOND RESPIRATION SIGNAL.

(b) A CORRESPONDING INTERPOLATED IBI SIGNAL USING THE SCHEME FROM INFORMATION THEORY CONCEPTS.

(c) THE POWER SPECTRUM OF (a).

(d) THE POWER SPECTRUM OF (b).

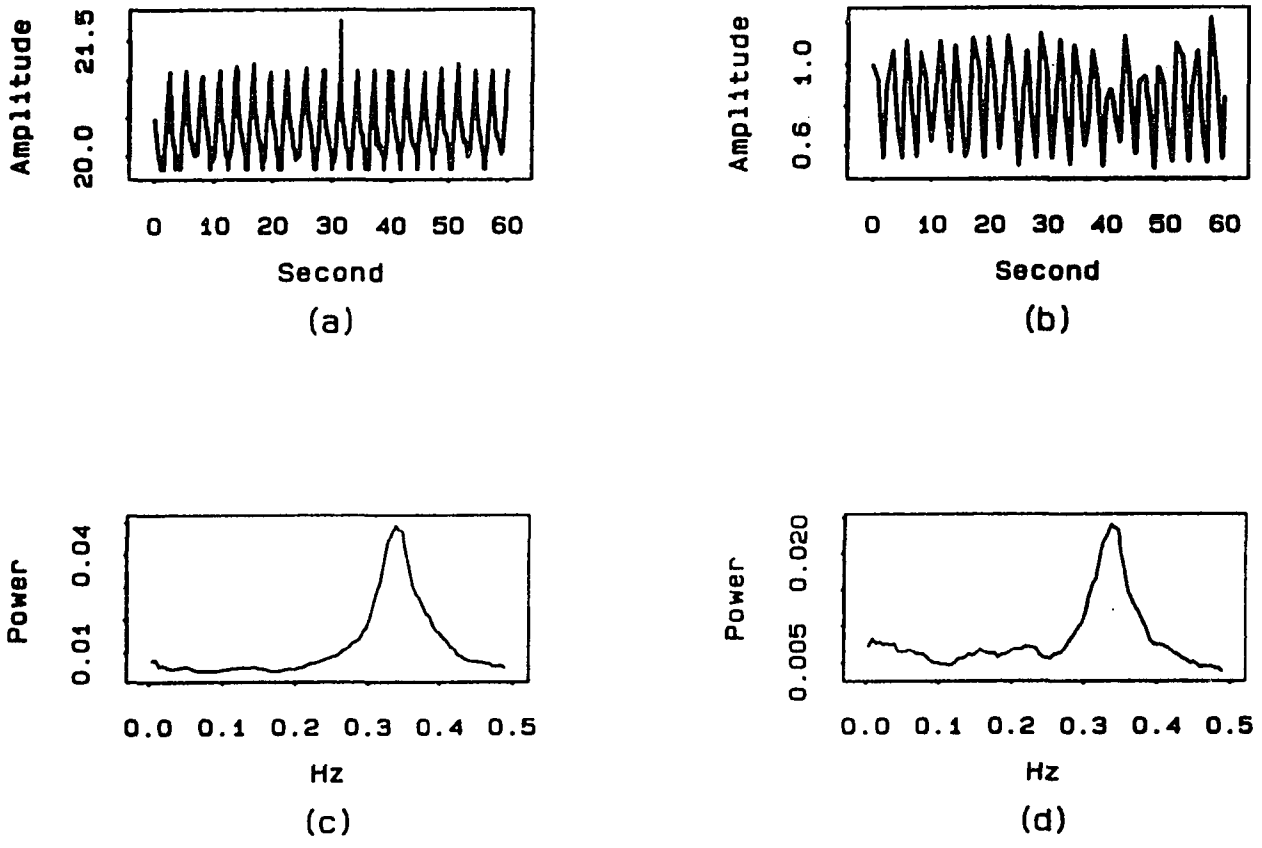

FIGURE 3.4.2 (a) A 60-SECOND RESPIRATION SIGNAL.

(b) A CORRESPONDING INTERPOLATED IBI SIGNAL USING THE LINEAR INTERPOLATION SCHEME.

(c) THE POWER SPECTRUM OF (a).

(d) THE POWER SPECTRUM OF (b).

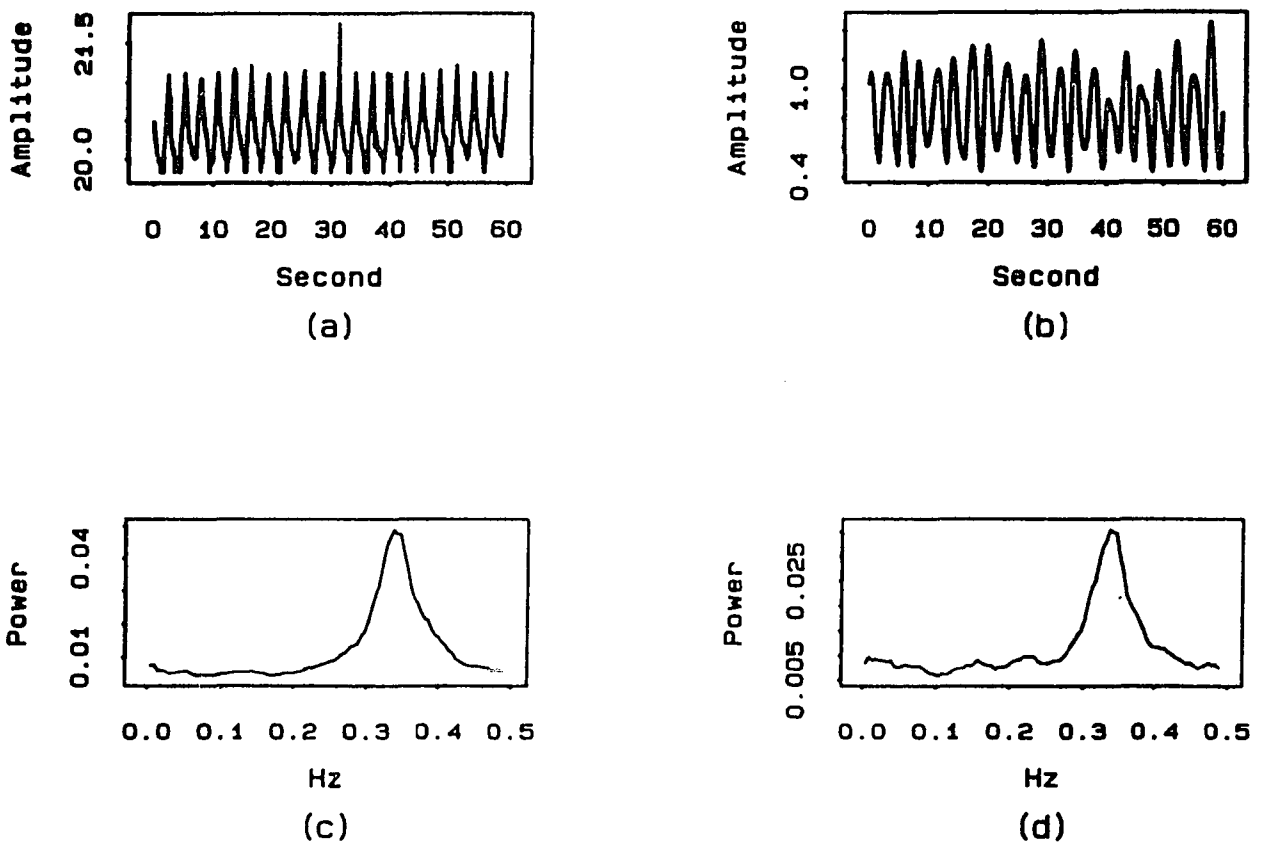

FIGURE 3.4.3 (a) A 60-SECOND RESPIRATION SIGNAL.

(b) A CORRESPONDING INTERPOLATED IBI SIGNAL USING THE CUBIC SPLINE INTERPOLATION SCHEME.

(c) THE POWER SPECTRUM OF (a).

(d) THE POWER SPECTRUM OF (b).

respiration signal and corresponding interpolated IBI signal using the scheme from Information Theory concepts, (c) and (d) are the power spectrum of (a) and (b), Figure 3.4.2 (a) and (b) are 60-second respiration signal and corresponding interpolated IBI signal using the linear interpolation scheme, (c) and (d) are the power spectrum of (a) and (b), and Figure 3.4.3 (a) and (b) are 60-second respiration signal and corresponding interpolated IBI signal using the cubic spline interpolation scheme, (c) and (d) are the power spectrum of (a) and (b). The scheme chosen is the above-mentioned scheme based on Information Theory concepts, which not only clearly showed the respiratory frequency peak in the power spectrum of the interpolated IBI signal but also is the easiest scheme to be implemented in software.

The interpolation using Information Theory concepts is based on the following argument: no new information about the course of the time series is available until the next value has occurred. Therefore, the interpolated values between the time T(m-1) and T(m) can be constant at the level of value T(m)-T(m-1) as shown in Figure 3.5.

3-3 DETRENDING

The very low frequency components contained in a signal (frequencies in the range 0 to 0.00244 Hz) are sometimes an artifact caused either by the instruments used to acquire the signal or by such effects as the movement of the dog

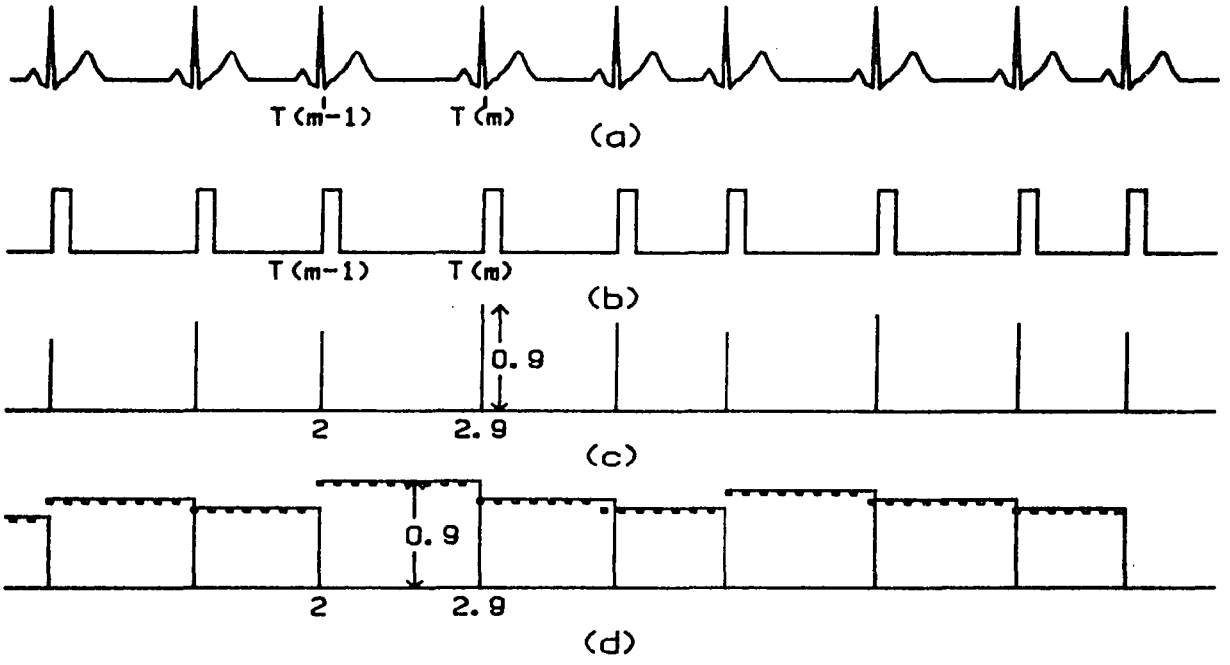

FIGURE 3.5 (a) THE ECG SIGNAL.

(b) THE R-WAVE PULSE TRAIN.

(c) THE IBI VALUES.

(d) THE INTERPOLATED IBI SIGNAL.

shifting the respiration signal up and down. Those very low frequency components smear the power spectrum of the signal at low frequencies (38). They also smear the result of the processing of the low frequency components by techniques such as complex demodulation. Figure 3.6 (a) shows a signal without the very low frequency components, (b) shows the signal with these low frequency components, and (c) and (d) are the power spectra of (a) and (b) respectively. From these figures, we can see the difference which exists between the two spectra at low frequencies. These very low frequency trends can dominate the spectrum even though the frequency of the component is too low to be characterized by the sample. Therefore, the very low frequency component in the signal was removed (detrended) before the signal was complex demodulated.

The interpolated IBI data series was detrended by using a locally weighted robust regression procedure. According to Cleveland (7), the locally weighted robust regression procedure is defined as follows:

Let W be a weight function:

$$W(x) = (1 - |x|^3)^3 \quad , \text{ for } |x| < 1 \qquad (3\text{-}1)$$

$$= 0 \ , \qquad \text{for } |x| \geq 1. \qquad (3\text{-}2)$$

Let f be a fraction of 1 ($0 < f \leq 1$) and r be f*n rounded to the nearest integer, where n is the total number of the

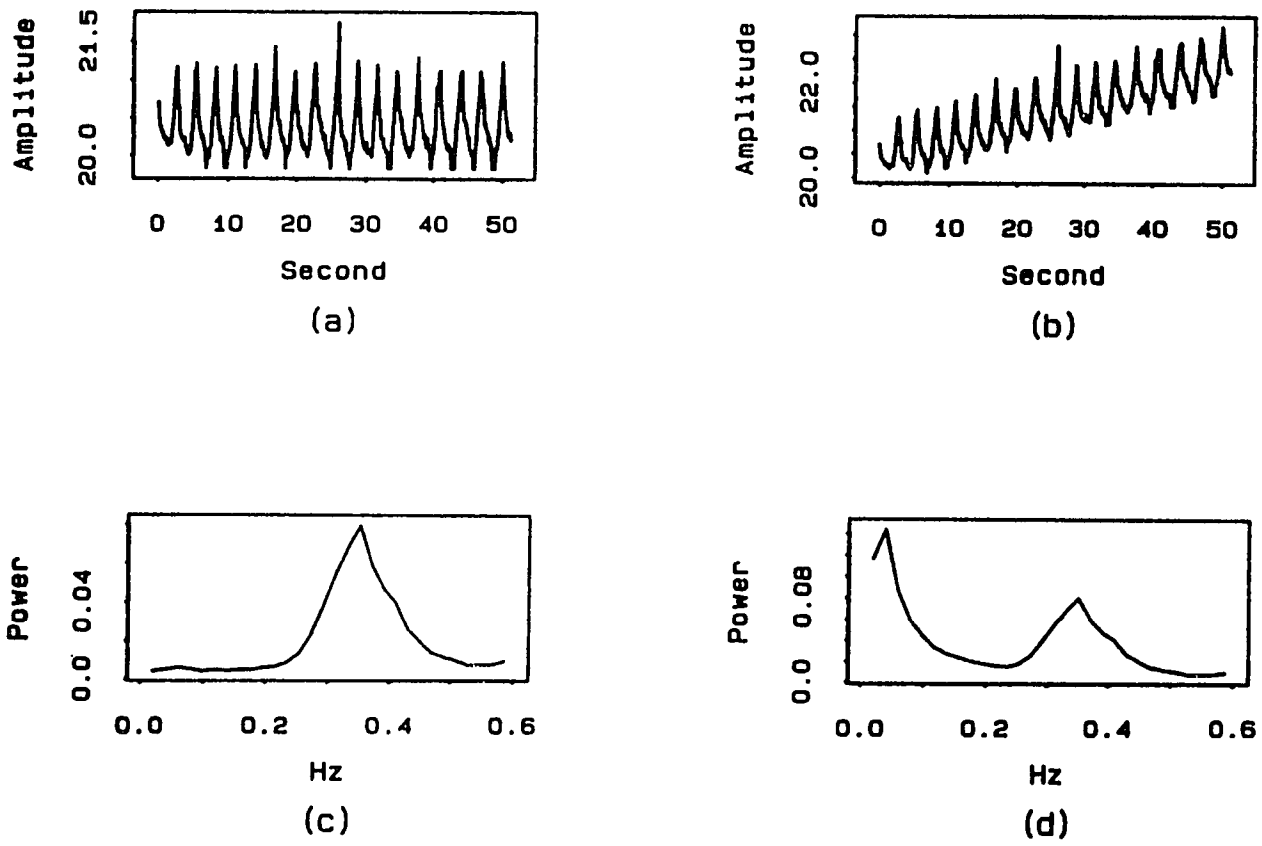

FIGURE 3.6 (a) A SIGNAL WITHOUT THE VERY LOW FREQUENCY COMPONENTS.

(b) THE SIGNAL WITH THESE LOW FREQUENCY COMPONENTS.

(c) THE POWER SPECTRUM OF (a).

(d) THE POWER SPECRRUM OF (b).

data points to be processed. For a set of points (x_i, y_i), where i=1,....., n, weights $w_k(x_i)$ are defined for all k, k=1,....., n, using the weight function W as follows:

$$w_k(x_i) = W(h_i^{-1}(x_k - x_i)) \qquad (3\text{-}3)$$

where h_i is the rth smallest number among $|x_i - x_k|$ for $j = 1, \ldots\ldots\ldots, n$

We can see that the point at which W first becomes zero is at the rth nearest neighbor of x_i. The initial fitted value, $\bar{y}_i$, at each x_i is the fitted value of a dth degree polynomial fit to the data using weighted least squares with weights $w_k(x_i)$,

$$\bar{y}_i = \sum_{j=0}^{d} \bar{c}_j(x_i) * x_i^j \qquad (3\text{-}4)$$

where $\bar{c}_j(x_i)$ are the values of c_j that minimize

$$\sum_{k=1}^{n} w_k(x_i) * (y_k - c_0 - c_1 x_k - \ldots - c_d x_k^d)^2 \qquad (3\text{-}5)$$

This procedure for computing the initial fitted values is referred to as locally weighted regression. A different set of weights, g_i, is now defined for each (x_i, y_i) based on the size of the residual $y_i - \bar{y}_i$.

If $e_i = y_i - \bar{y}_i$, and $s = |e_i| / 2$

then $g_k = B (e_k / 6s)$ (3-6)

$$\text{where } B(x) = (1 - x^2)^2 \quad \text{for } |x| < 1$$
$$= 0 \quad \text{for } |x| \geq 1$$

Large residuals result in small weights and small residuals result in large weights. New fitted values are now computed as before but with $w_k(x_i)$ replaced by $g_i w_k(x_i)$. The effect of this adjustment is to downweight the influence of extremely deviated points (outlier points) that produce large residuals. The computation of new weights and new fitted values is now repeated several times. (Usually two times will give good result and we repeated two times.) The entire procedure, including the initial computation and the iteration, is referred to as robust locally weighted regression.

The robust locally weighted regression process was invented for getting the smoothed points (a regression line) of a data set. This process also guards against extremely deviated points of the data set distorting the smoothed points.

From the frequency domain point of view, the robust locally weighted regression process acts like a lowpass filter, and the passband of this lowpass filter can be chosen from f (a fraction of the length of the data set). If f is chosen to be 0.2 for a data series of 15 minutes sampled at 10 Hz, then $\bar{y}_i$ would give the components approximately down to 0.0056 Hz. The detrended data can be

obtained by $y_i - \bar{y}_i$.

3-4 COMPLEX DEMODULATION

Complex demodulation is a method of producing a low frequency response around a given frequency of a time series (4). Unlike power spectral analysis which gives the overall frequency response during the duration of the time series, complex demodulation gives results in the time domain. It shows the variation of the amplitude and phase of the signal at given frequency along the time axis. The variation of amplitude indicates the intensity of the signal around that given frequency, whereas the variation of phase indicates the relative frequency deviation from the center frequency of the complex demodulation.

Suppose a time series X(t) has the following representation:

$$X(t) = R(t) * \cos [2\pi f_0 t + @(t)] \qquad (3-7)$$

where R(t) is a slowly changing amplitude
and @(t) is a slowly changing phase

Then R(t) and @(t) can be extracted if we know the frequency f_0 by using complex demodulation as follows:

Let us first use the Euler equation to replace equation 3-7

$$X(t) = R(t)*[EXP(i\{2\pi f_0 t+@(t)\})+EXP(-i\{2\pi f_0 t+@(t)\})]/2 \quad (3\text{-}8)$$

If

$$Y(t) = X(t) * 2 * EXP(-i2\pi f_0 t)$$

then

$$Y(t)= R(t)*[EXP(i@(t)) + EXP(-i\{2* 2\pi f_0 t+@(t)\})] \quad (3\text{-}9)$$

If $\overline{Y}(t)$ is the complex signal when Y(t) is passed through a lowpass filter, then

$$\overline{Y}(t) = R(t) * EXP[i@(t)] \quad (3\text{-}10)$$

Therefore, R(t) and @(t) can be recovered as follows:

$$R(t) = | \overline{Y}(t) | \quad (3\text{-}11)$$

$$@(t)=COS^{-1}\{REAL(Z)/SQRT[(REAL(Z))^2+(IMAG(Z))^2]\} \quad (3\text{-}12)$$

$$\text{where } Z = \overline{Y}(t) / | \overline{Y}(t) |$$

From the frequency domain point of view, each frequency band of interest is shifted to zero frequency. This frequency shift enables us to recover variations in the

frequency of interest by using a lowpass filter. The amplitude variation R(t) of the complex demodulation indicates the intensity of the signal around the frequency f_0 and the phase variation @(t) indicates the relative frequency deviation from the frequency f_0.

Let us examine two examples of the application of complex demodulation, Figure 3.7 (a) shows a signal with 10 Hz sampling and consists of a 0.073 Hz cosine waveform in the first half and a 0.317 Hz cosine waveform in the second half. Figure 3.7 (b) shows the resulting magnitude variations when the signal from (a) was complex demodulated at 0.073 Hz with a lowpass filter cutoff frequency 0.122 Hz. In other words, the complex demodulation was centered at 0.073 Hz and only allowed signals in the band from 0.073-0.122=-0.049 Hz to 0.073+0.122=0.195 Hz to pass. Since the signal from (a) contains a 0.073 Hz component in the first half and this frequency component is within the passband, the output magnitude shows a constant high value for the first half and a low value for the second half. Note that the second half of the signal from (a) contains a 0.317 Hz component which is out of the passband. If we check the corresponding phase response which is shown in (e), we find that the first half of the phase response is zero because the centered demodulation frequency is the same as the signal frequency component in this region, which is 0.073 Hz. The second part of the phase response from (e)

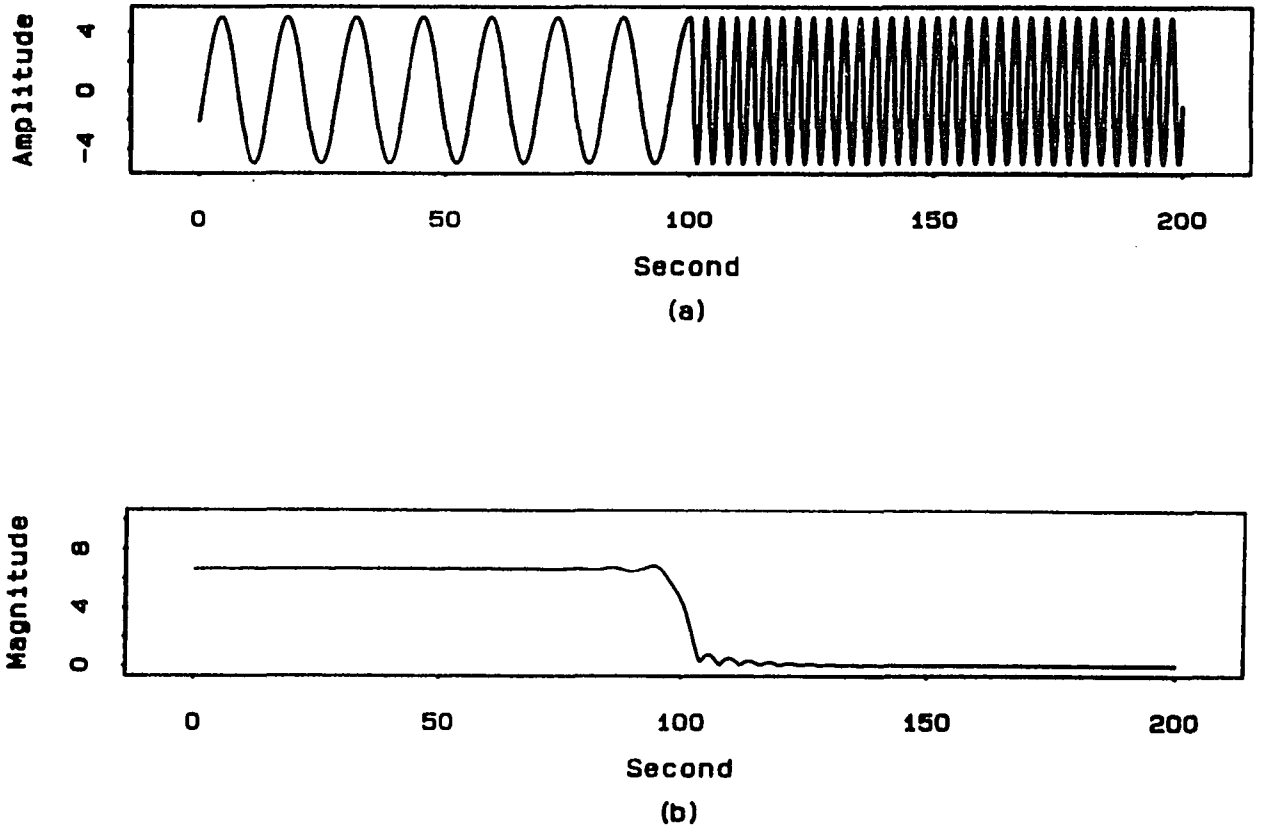

FIGURE 3.7 (a) A SIGNAL WITH 0.073 HZ FREQUENCY IN THE FIRST HALF AND 0.317 HZ FREQUENCY IN THE SECOND HALF.

(b) THE MAGNITUDE RESULT WHEN (a) WAS COMPLEX DEMODULATED AT 0.073 HZ WITH LOWPASS FILTER CUTOFF FREQUENCY 0.122 HZ.

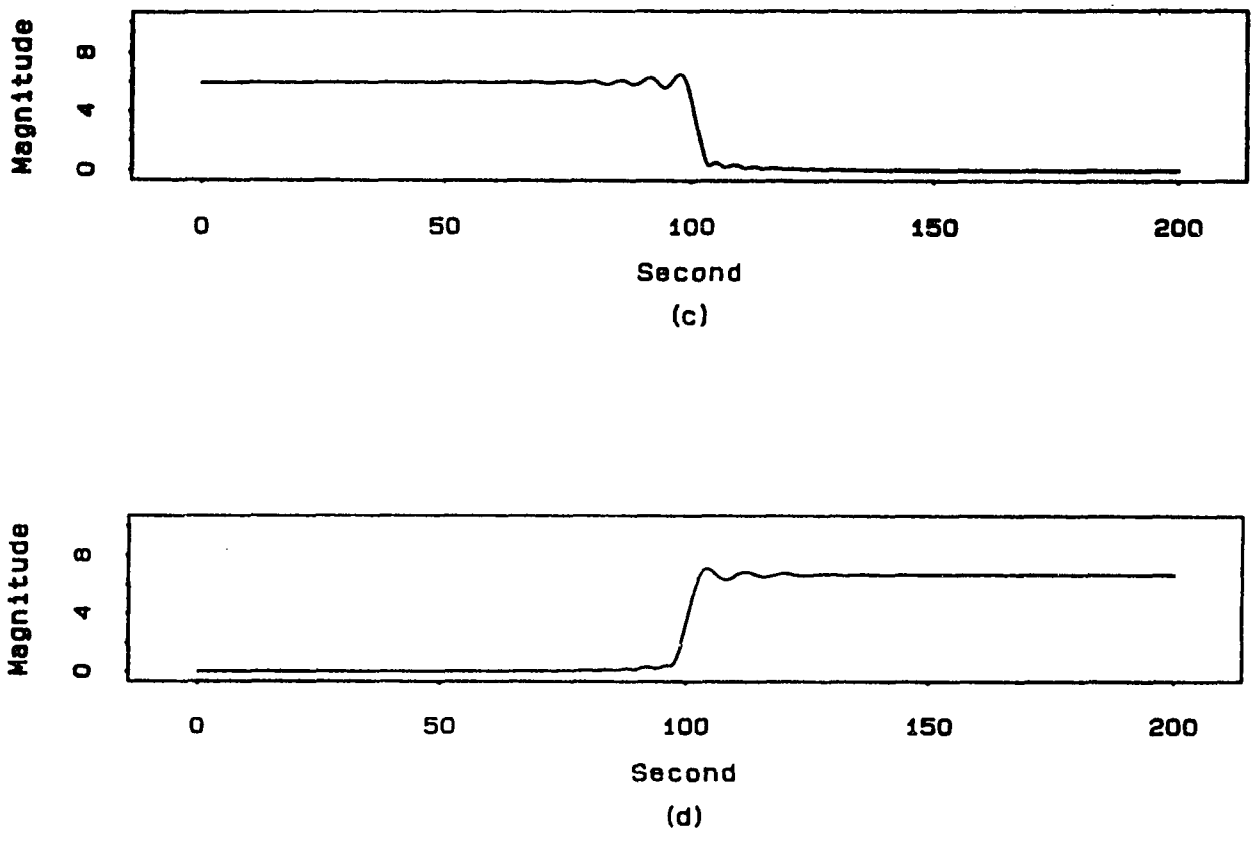

FIGURE 3.7 (c) THE MAGNITUDE RESULT WHEN (a) WAS COMPLEX DEMODULATED AT 0.122 HZ WITH LOWPASS FILTER CUTOFF FREQUENCY 0.122 HZ.

(d) THE MAGNITUDE RESULT WHEN (a) WAS COMPLEX DEMODULATED AT 0.317 HZ WITH LOWPASS FILTER CUTOFF FREQUENCY 0.122 HZ.

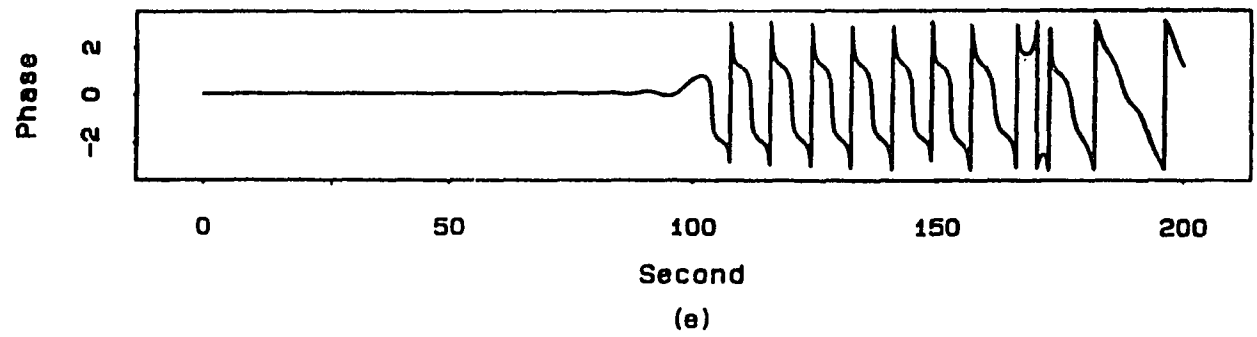

(e)

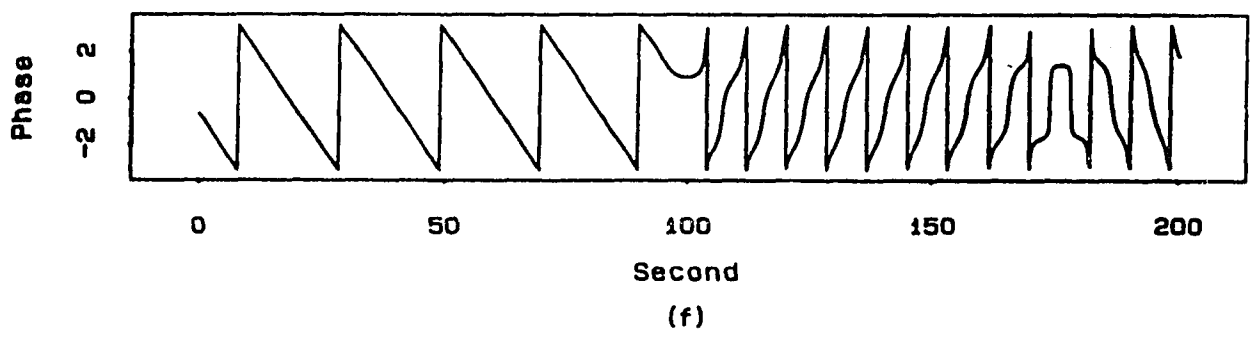

(f)

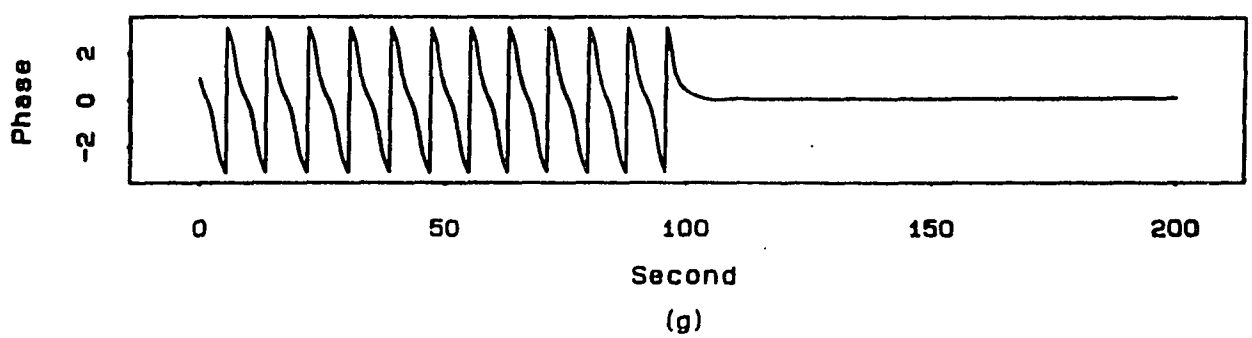

(g)

FIGURE 3.7 (e) THE PHASE RESULT CORRESPONDING TO (b).

(f) THE PHASE RESULT CORRESPONDING TO (c).

(g) THE PHASE RESULT CORRESPONDING TO (d).

fluctuates because the complex demodulation frequency bandwidth does not include the 0.317 Hz component. Let us examine what happens if we move the centered frequency from 0.073 Hz to 0.122 Hz with the same lowpass filter cutoff frequency of 0.122 Hz. The resulting magnitude response is shown in (c) and the phase response in (f). We can see that (c) has a very similar response to (b), because the pass band ranges becomes from 0 Hz to 0.244 Hz which still includes 0.073 Hz, but the phase result in (f) is different from that in (e), and shows a frequency deviation in the first half, because the centered frequency has been shifted from 0.073 Hz to 0.122 Hz. Figure 3.7 (d) and (g) are the resulting magnitude variation and phase variation when (a) was complex demodulated at 0.317 Hz (which is the frequency component of the second half of (a)) with lowpass filter cutoff frequency 0.122 Hz. (d) shows a low value for the first half of the result and a constant high value for the second half of the result; (g) shows a constant phase response in the second half and phase fluctuates in the first half. This example also shows us that from the fluctuation of the phase, we may approximately calculate the slope and determine how far the true frequency component in the signal is from the frequency at which we complex demodulated. For example, if the phase @(t) from the phase result when we complex demodulated the signal at f_0 is a linear function of time, and can be expressed as

$@(t) = a + bt$ where a and b are constants.

Then equation (3-7) becomes

$$X(t) = R(t) * \cos [2\pi f_0 t + @(t)]$$

$$= R(t) * \cos [2\pi f_0 t + (a + bt)]$$

$$= R(t) * \cos [2\pi f_0 t + bt + a]$$

$$= R(t) * \cos [(2\pi f_0 + b)t + a]$$

$$= R(t) * \cos [2\pi f_1 t + a]$$

where $f_1 = f_0 + b/2\pi$

and $b/2\pi$ is the frequency deviation from the true frequency f_1.

As in Fig. 3.7, if we assume that we didn't know that the first part of the signal has a frequency component of 0.073 Hz and we complex demodulated with a 0.122 Hz cutoff lowpass filter and obtained the magnitude and phase results in (c) and (f), the magnitude result looks as if we had complex demodulated at the right frequency, but the phase result tells us that we are off from the right frequency because the phase result is not a constant value in the first half. We could then approximately calculate the slope of the phase in the first part of the phase result, which is around -0.29, and therefore we were about $0.29/2\pi$ Hz

greater than the correct peak frequency, and the correct peak frequency is approximately equal to 0.122 - $0.29/2\pi$ = 0.076 Hz.

Figure 3.8 (a) shows a signal with 10 Hz sampling rate consisting of frequency components from 0.064 Hz to 0.083 Hz and from 0.308 Hz to 0.327 Hz. Fig. 3.8 (b) and (c) show the magnitude variation of the signal when it is complex demodulated at 0.073 Hz and 0.122 Hz respectively with the same lowpass filter cutoff frequency 0.122 Hz, (d) and (e) show the magnitude variation when the signal is complex demodulated at 0.317 Hz and 0.366 Hz respectively with lowpass filter cutoff frequency 0.122 Hz, (f) and (g) show the phase variation when it is complex demodulated at 0.073 Hz and 0.122 Hz respectively with lowpass filter cutoff frequency 0.122 Hz, (h) and (i) show the phase variation when it is complex demodulated at 0.317 Hz and 0.366 Hz respectively with the same lowpass filter cutoff frequency 0.122 Hz. This example shows that even though the signal was complex demodulated at different frequencies but the lowpass filter (0.122 Hz) covered all of the demodulation frequencies, the amplitude variation would be the same but the phase variation would be different. In other words, if we are only interested in whether the signal has a frequency component in the band of frequencies over which the complex demodulation was performed, the magnitude result becomes more important than the phase result.

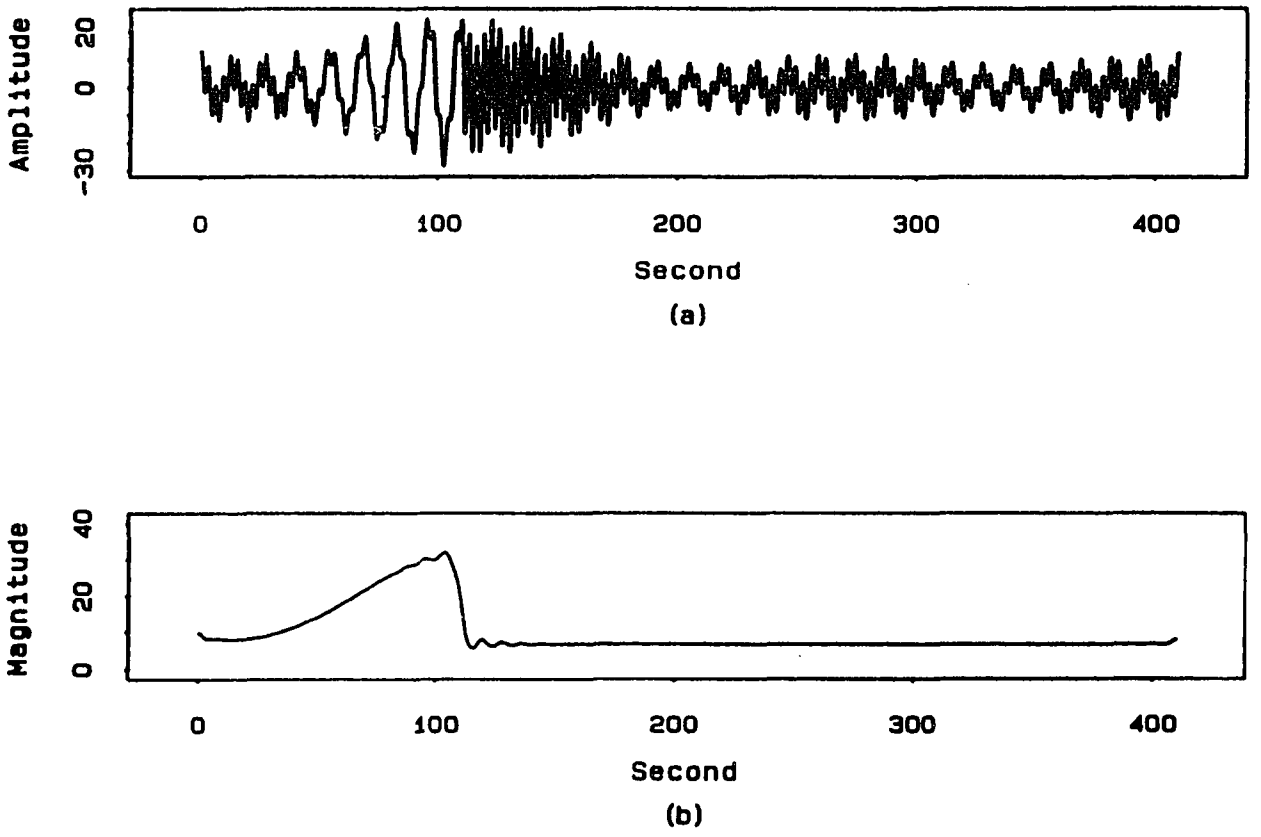

FIGURE 3.8 (a) A SIGNAL WITH THE FREQUENCY COMPONENTS FORM 0.064 HZ TO 0.083 HZ AND FROM 0.308 HZ TO 0.327 HZ.

(b) THE MAGNITUDE RESULT WHEN SIGNAL FROM (a) WAS COMPLEX DEMODULATED AT 0.073 HZ WITH LOWPASS FILTER CUTOFF FREQUENCY 0.122 HZ.

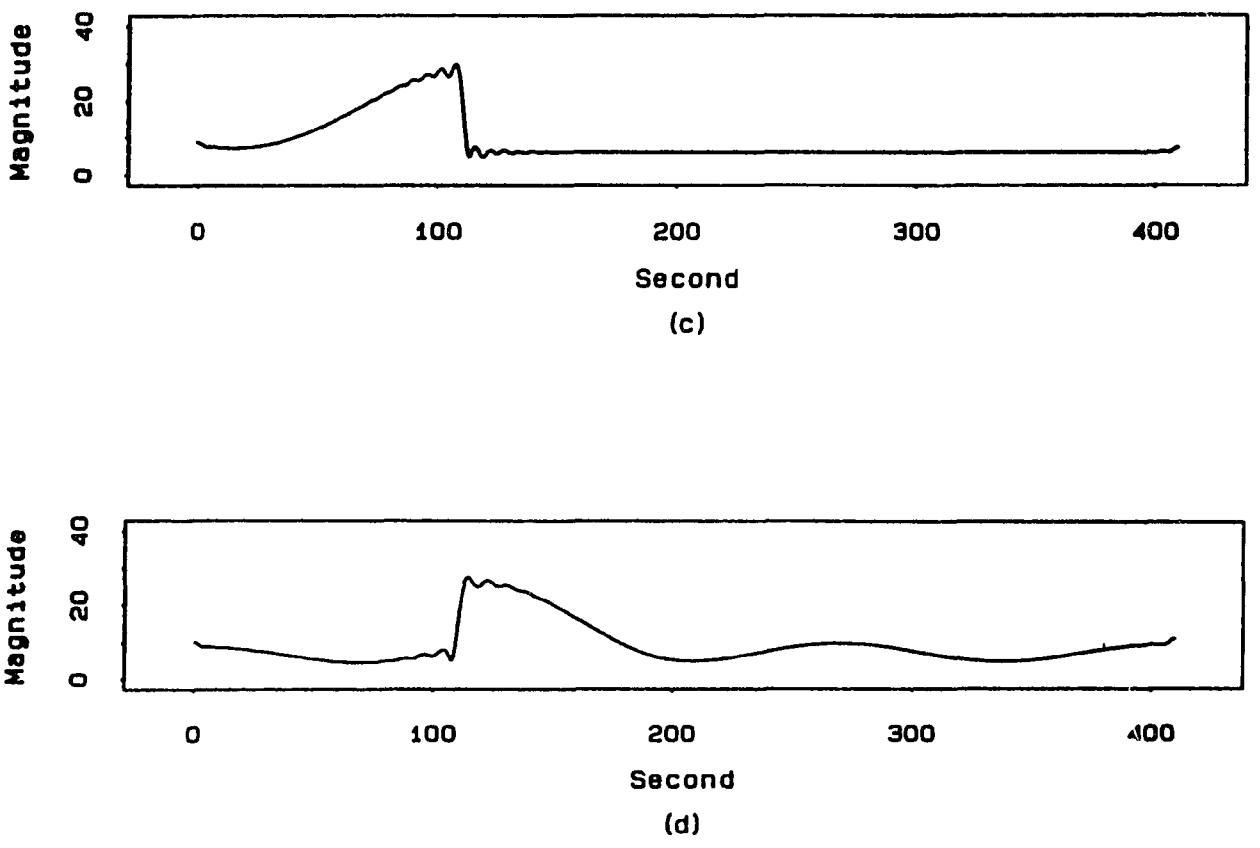

FIGURE 3.8 (c) THE MAGNITUDE RESULT WHEN SIGNAL FROM (a) WAS COMPLEX DEMODULATED AT 0.122 HZ WITH LOWPASS FILTER CUTOFF FREQUENCY 0.122 HZ.

(d) THE MAGNITUDE RESULT WHEN SIGNAL FROM (a) WAS COMPLEX DEMODULATED AT 0.317 HZ WITH LOWPASS FILTER CUTOFF FREQUENCY 0.122 HZ.

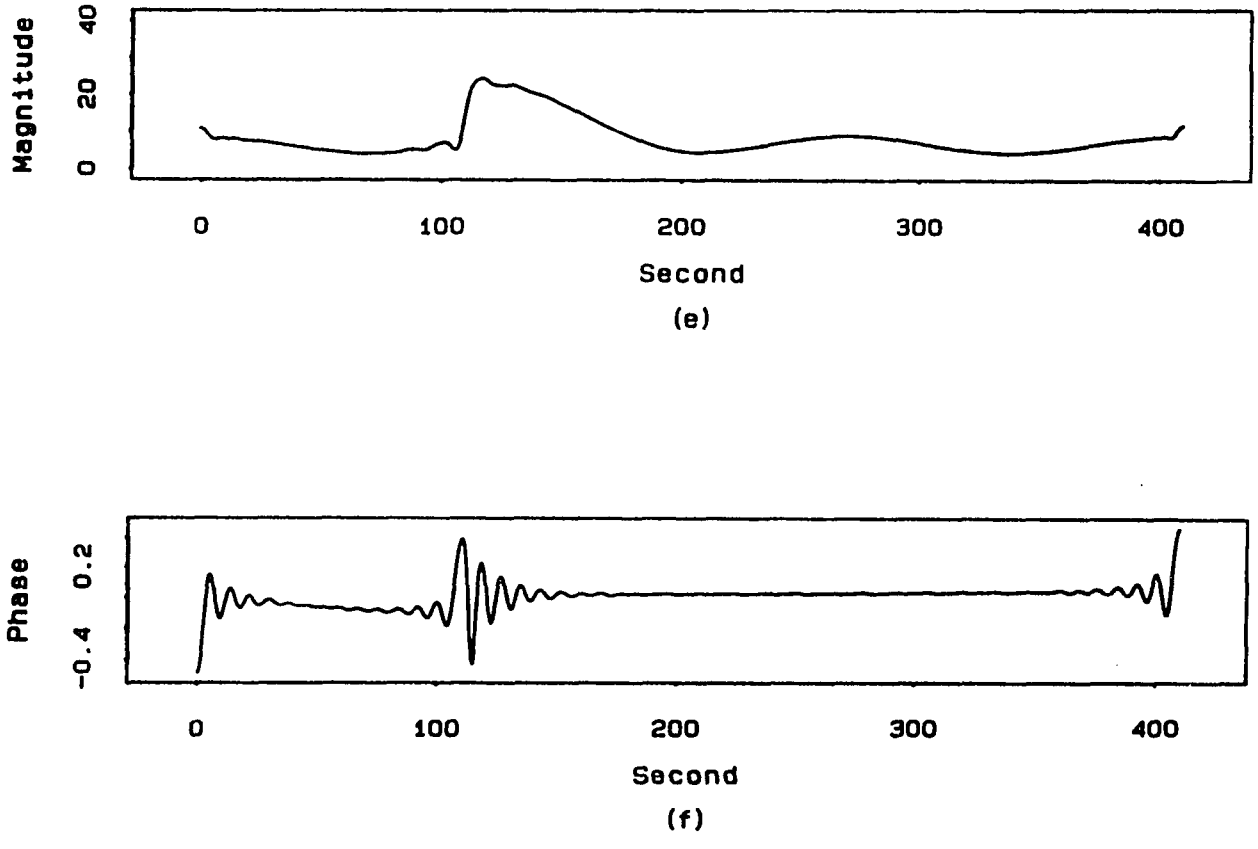

FIGURE 3.8 (e) THE MAGNITUDE RESULT WHEN SIGNAL FROM (a) WAS COMPLEX DEMODULATED AT 0.366 HZ WITH LOWPASS FILTER CUTOFF FREQUENCY 0.122 HZ.
(f) THE PHASE RESULT CORRESPONDING TO (b).

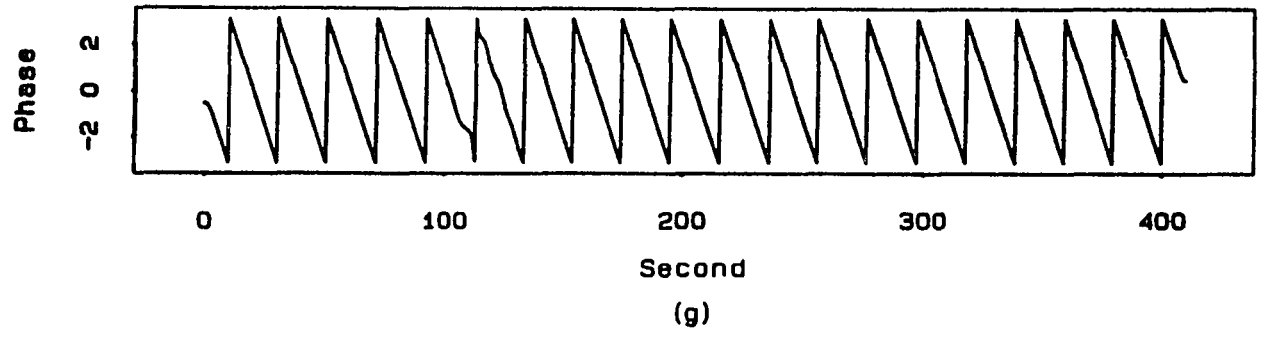

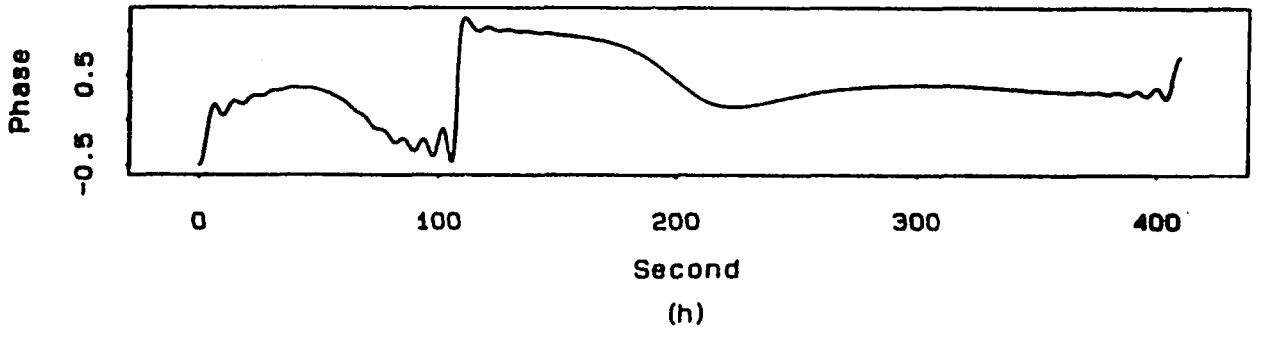

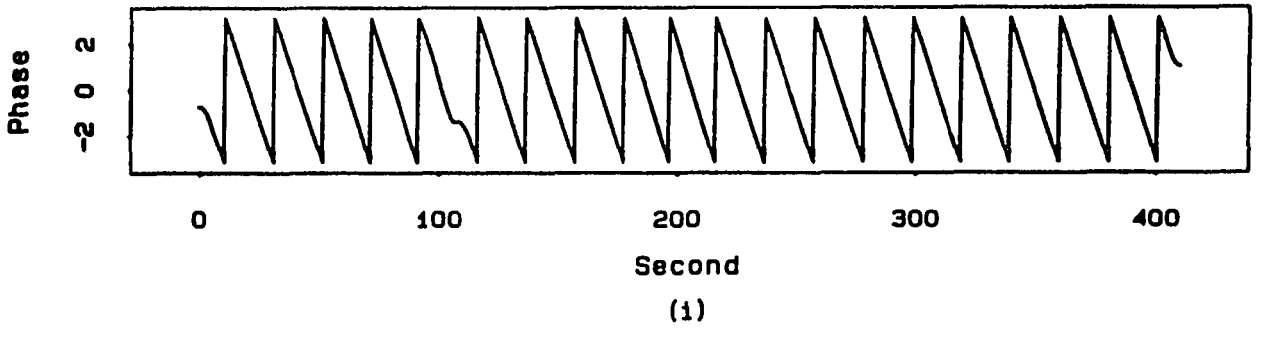

FIGURE 3.8 (g) THE PHASE RESULT CORRESPONDING TO (c).
(h) THE PHASE RESULT CORRESPONDING TO (d).
(i) THE PHASE RESULT CORRESPONDING TO (e).

We can also prove the above mathematically as shown in the following:

From equation 3-7

$$X(t) = R(t) * \cos [\, 2\pi f_0 t + @(t) \,]$$

R(t) and @(t) can be extracted by using complex demodulation at frequency f_0 accompanied by a lowpass filter whose bandwidth is less than $2f_0$. Now if X(t) is complex demodulated at frequency f_1 and $f_1 = f_0 + f$,

then

$$f_0 = f_1 - f$$

equation 3-7 becomes

$$X(t) = R(t) * \cos [2\pi f_1 t - 2\pi f t + @(t) \,]$$
$$= R(t) * \cos [2\pi f_1 t + \varnothing(t) \,] \qquad (3\text{-}13)$$

where $\varnothing(t) = - 2\pi f t + @(t)$

Therefore, if X(t) is complex demodulated at frequency f_1 with the proper lowpass filter, the magnitude variation would be R(t) as if it were complex demodulated at f_0, but the phase variation would be $\varnothing(t)$ where $\varnothing(t) = - 2\pi f t + @(t)$

Since the parasympathetic and sympathetic nervous systems make specific contributions to the HRV spectrum (the parasympathetic nervous system modulates the mid- and respiration frequency peaks of the HRV spectrum and both

sympathetic and parasympathetic nervous systems modulate the low frequency peak of the HRV spectrum), we can separate the HRV spectrum into two parts: the low frequency part with bandwidth from 0 to 0.124 Hz is the contribution from both divisions of the autonomic nervous system, and the respiration frequency part with bandwidth from 0.171 Hz to 0.537 Hz is the contribution from the parasympathetic division. Therefore, when HRV signals are complex demodulated according to the above two different bandwidths, the results of magnitude variation represent the intensity of the activity of the two divisions of the autonomic nervous system, and the results of phase variation represent the frequency deviation from the frequency at which the signal was complex demodulated. Since proper lowpass filter bandwidths were chosen to cover the frequency areas for demodulation at low and at respiration frequencies, phase results become meaningless and only magnitude results were considered to show the intensity of the two divisions of the autonomic nervous system.

3-5 ZERO-PHASE-SHIFT LOWPASS FILTERING

The need for tracking the exact time sequence is very important in dealing with the result of the complex demodulation. However, IIR (infinite impulse response) filters cause phase-shifts which results in time delays in the time domain, and transient responses at the beginning of

the filtered data series. This would cause the whole time series to be shifted and some points at both ends of the data series to be lost. Figure 3.9 (a) shows a 0.0733 Hz cosine waveform, (b) shows that cosine waveform passed through a Butterworth lowpass filter with cutoff frequency 0.122 Hz, (we can see that points are lost at the beginning and at the end of the record.) (c) shows no loss of points and no phase shift when we use a zero-phase-shift lowpass filter to filter the same cosine waveform. Since our data series are time-locked during different trials, the results after filtering must have the same time periods as before filtering. To reduce these end effects and eliminate the phase shift, we first extended the data series before lowpass filtering by repeating points in reverse order at each end, and then passed the data through a zero-phase-shift lowpass filter.

The theoretical zero-phase-shift lowpass filter is as follows:

Suppose that x(n) is the input and g(n) is the output of a lowpass filter which has the impulse response h(n) as shown in Fig 3.10, with Fourier transform pairs:

$x(n) <=> X(e^{jw})$ $\quad g(n) <=> G(e^{jw})$ $\quad h(n) <=> H(e^{jw})$

We then have

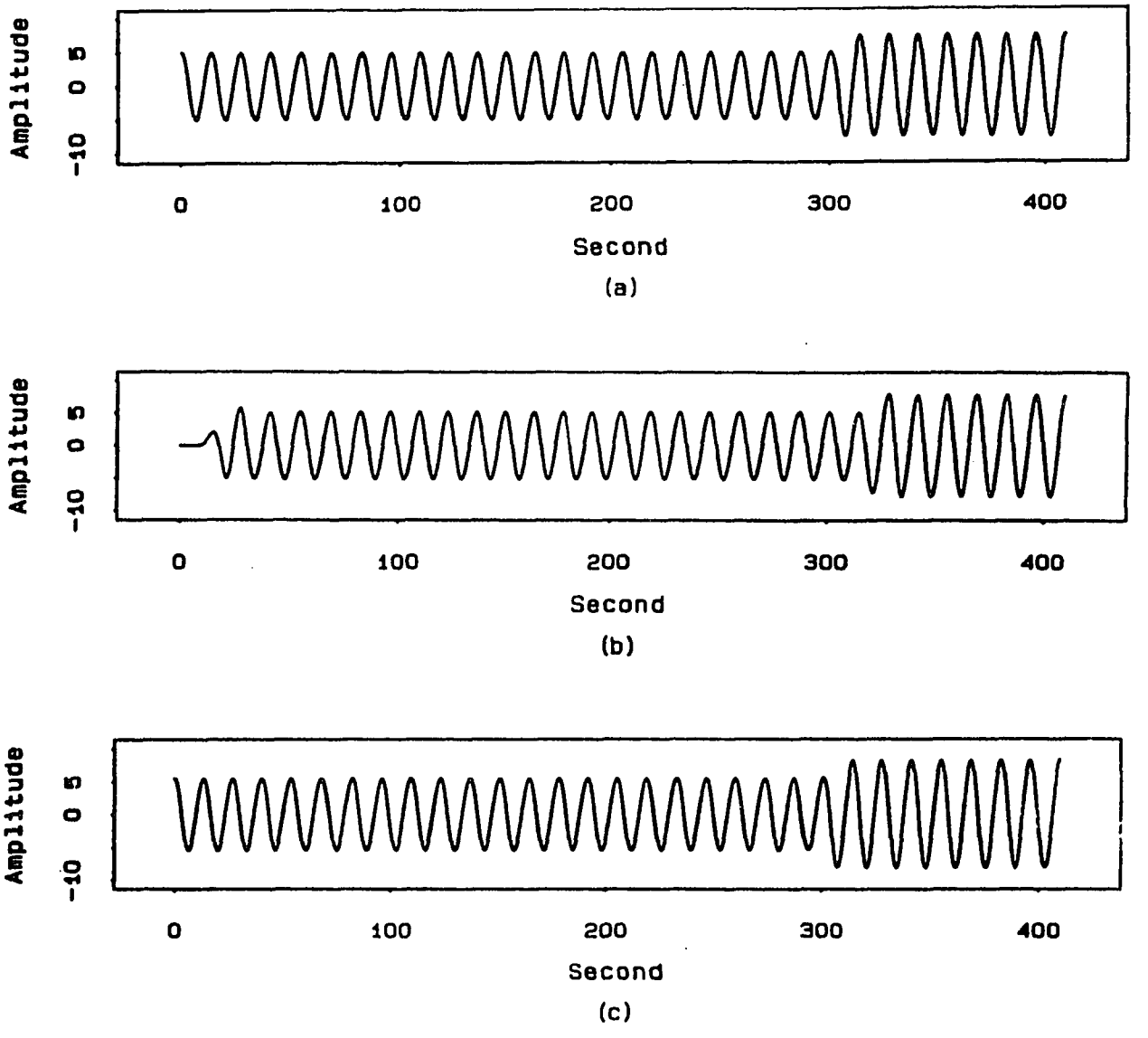

FIGURE 3.9 (a) A 0.0733 HZ COSINE WAVEFORM.

(b) THE SIGNAL FROM (a) WAS FILTERED BY USING A BUTTERWORTH LOWPASS FILTER WITH CUTOFF FREQUENCY 0.122 HZ.

(c) THE SIGNAL FROM (a) WAS FILTERED BY USING A ZERO-PHASE-SHIFT LOWPASS FILTER.

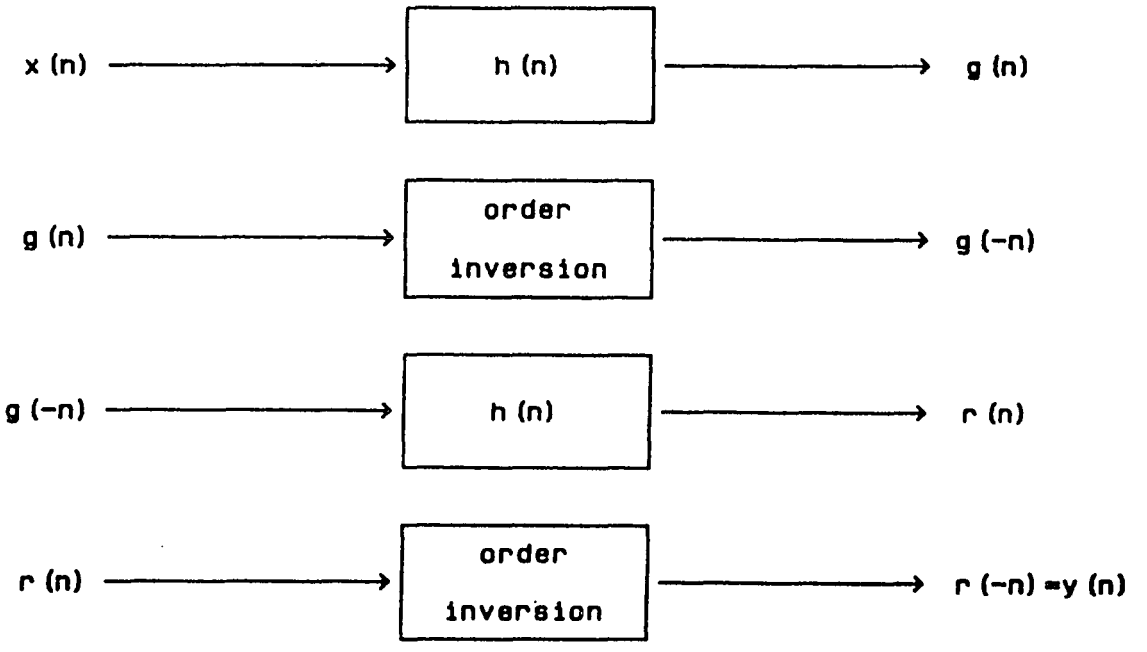

FIGURE 3.10 THE BLOCK DIAGRAM OF PERFORMING THE ZERO-PHASE-SHIFT LOWPASS FILTERING.

$$G(e^{jW}) = X(e^{jW}) \cdot H(e^{jW}) \qquad (3\text{-}14)$$

We then pass g(n) backward into the same lowpass filter. In other words, take g(-n) as input into the same lowpass filter, and take the output as r(n). y(n) is obtained if we reverse the order of r(n), that is,

$$y(n) = r(-n)$$

Their Fourier transform pairs are:

$$g(-n) \Leftrightarrow G^*(e^{jW}) \qquad r(n) \Leftrightarrow R(e^{jW}) \qquad r(-n) \Leftrightarrow R^*(e^{jW})$$

Therefore

$$R(e^{jW}) = G^*(e^{jW}) \cdot H(e^{jW}) \qquad (3\text{-}15)$$

From equation 3-14, we can derive

$$G^*(e^{jW}) = [\, X(e^{jW}) \cdot H(e^{jW}) \,]^*$$

$$= X^*(e^{jW}) \cdot H^*(e^{jW}) \qquad (3\text{-}16)$$

Substitute equation 3-16 into equation 3-15;

$$R(e^{jW}) = X^*(e^{jW}) \cdot H^*(e^{jW}) \cdot H(e^{jW})$$

$$= X^*(e^{jW}) \cdot |\, H(e^{jW}) \,|^2 \qquad (3\text{-}17)$$

If we let r(-n) = y(n), we can get $Y(e^{jW})$ as

$$Y(e^{jw}) = R^*(e^{jw})$$

$$= [\ X^*(e^{jw}) \ . \ |\ H(e^{jw})\ |^2\ ]^*$$

$$= X(e^{jw}) \ . \ |\ H(e^{jw})\ |^2 \qquad (3\text{-}18)$$

Therefore we have a lowpass filter transfer fuction $|H(e^{jw})|^2$ with zero-phase-shift characteristic.

The lowpass filter used here is a 16-pole, Butterworth lowpass filter designed by Dr. Arthur T. Johnson (23).

Figure 3-11 shows the software flow chart for complex demodulation and zero-phase-shifting lowpass filtering.

The complex demodulation main program consists of several subroutines, which are: the input subroutine, the complex demodulation subroutine, the flip-over subroutine, the polar subroutine, and the output subroutine. The input subroutine checks the input-output unit, reads data from a data file and also calculates the mean of the input data series. The complex demodulation subroutine calculates the demodulated real part and imaginary part of the input data series. The flip-over subroutine adds repeating points at the two ends of the data series and uses another subroutine called lowpass filtering subroutine to filter the data series forward and backward and then output the right region of the data series. The polar subroutine calculates the magnitude and phase from the filtered real part and

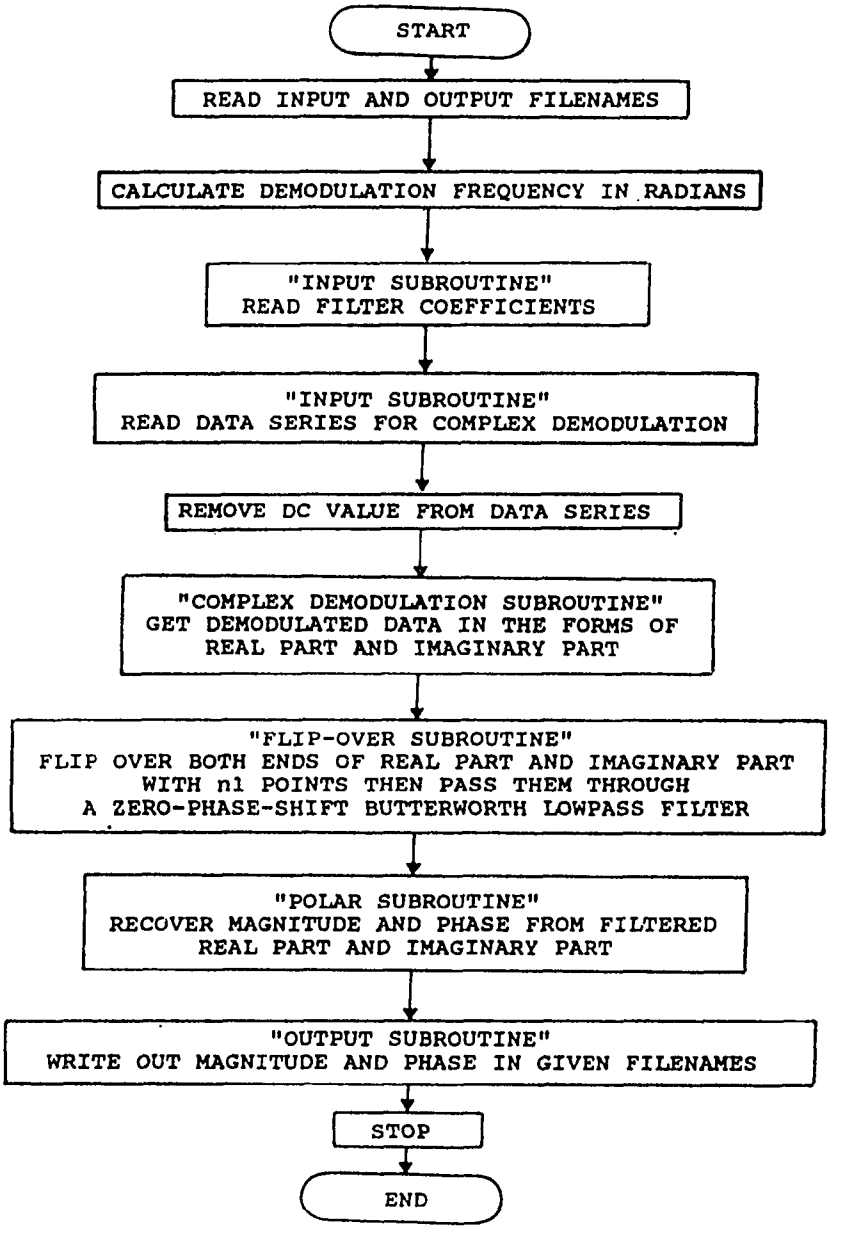

(a)

FIGURE 3.11 (a) THE FLOW CHART OF THE MAIN PROGRAM OF THE COMPLEX DEMODULATION.

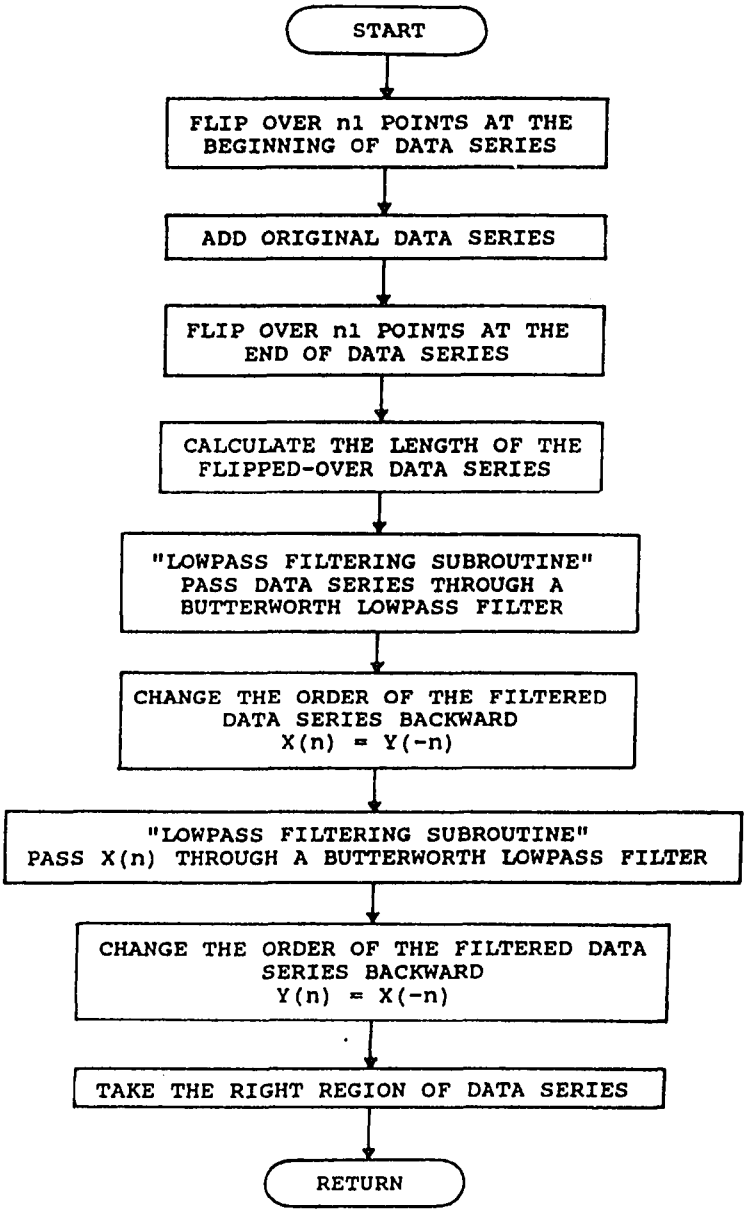

(b)

FIGURE 3.11 (b) THE FLOW CHART OF THE FLIP-OVER SUBROUTINE.

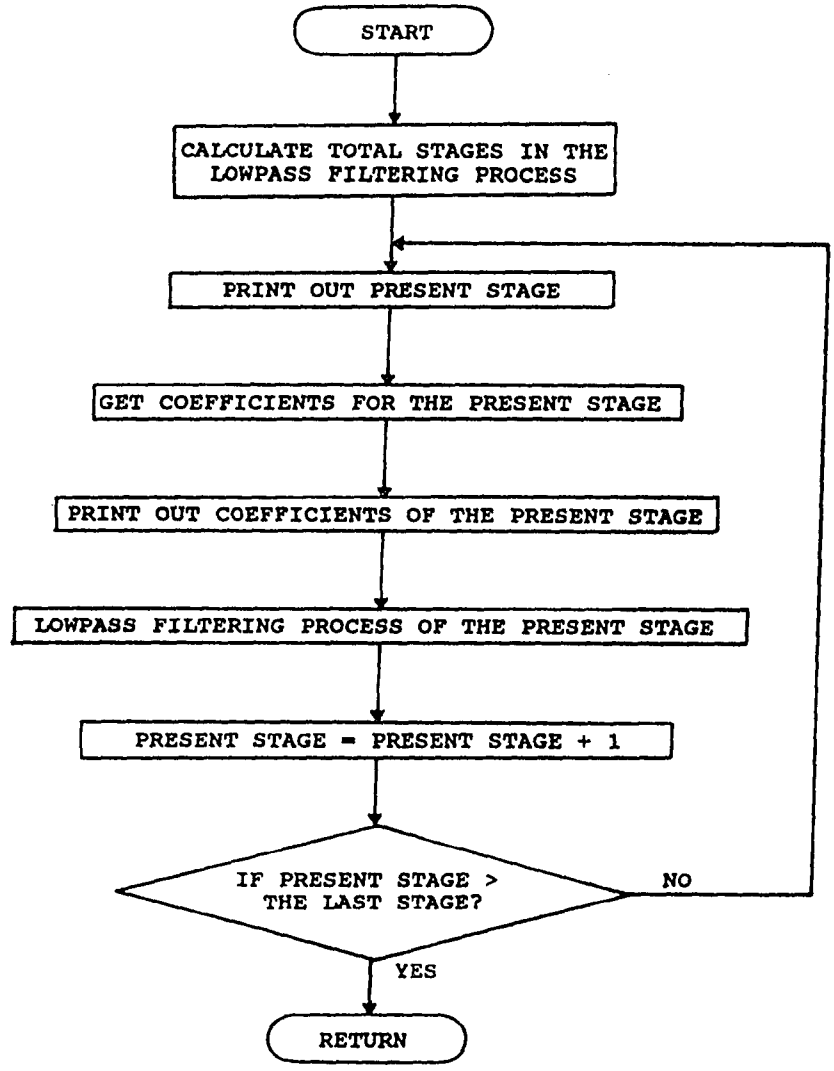

(c)

FIGURE 3.11 (c) THE FLOW CHART OF LOWPASS FILTERING SUBROUTINE.

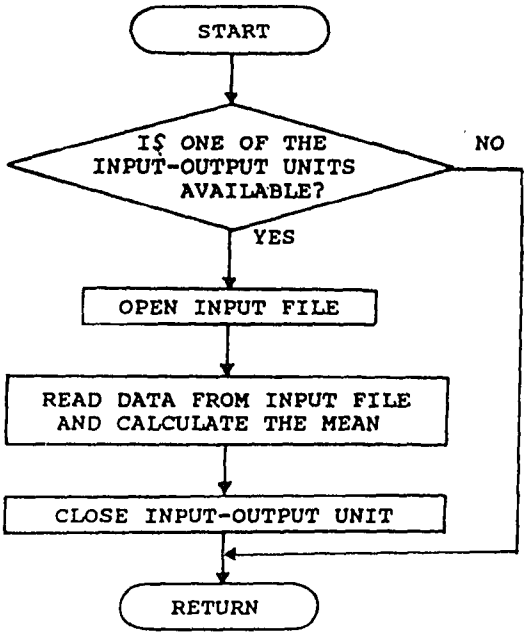

(d)

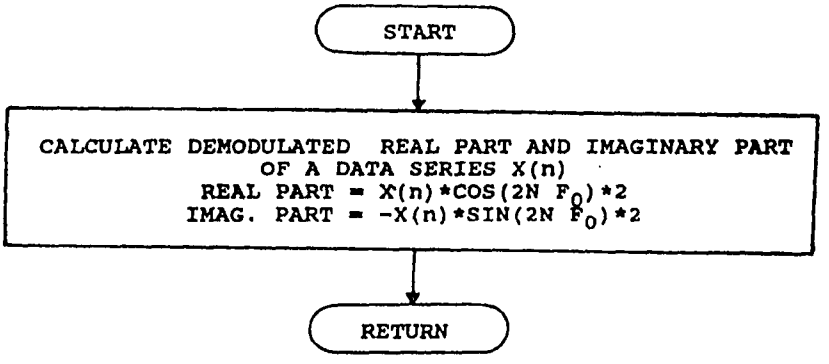

(e)

FIGURE 3.11 (d) THE FLOW CHART OF INPUT SUBROUTINE.

(e) THE FLOW CHART OF COMPLEX DEMODULATION SUBROUTINE.

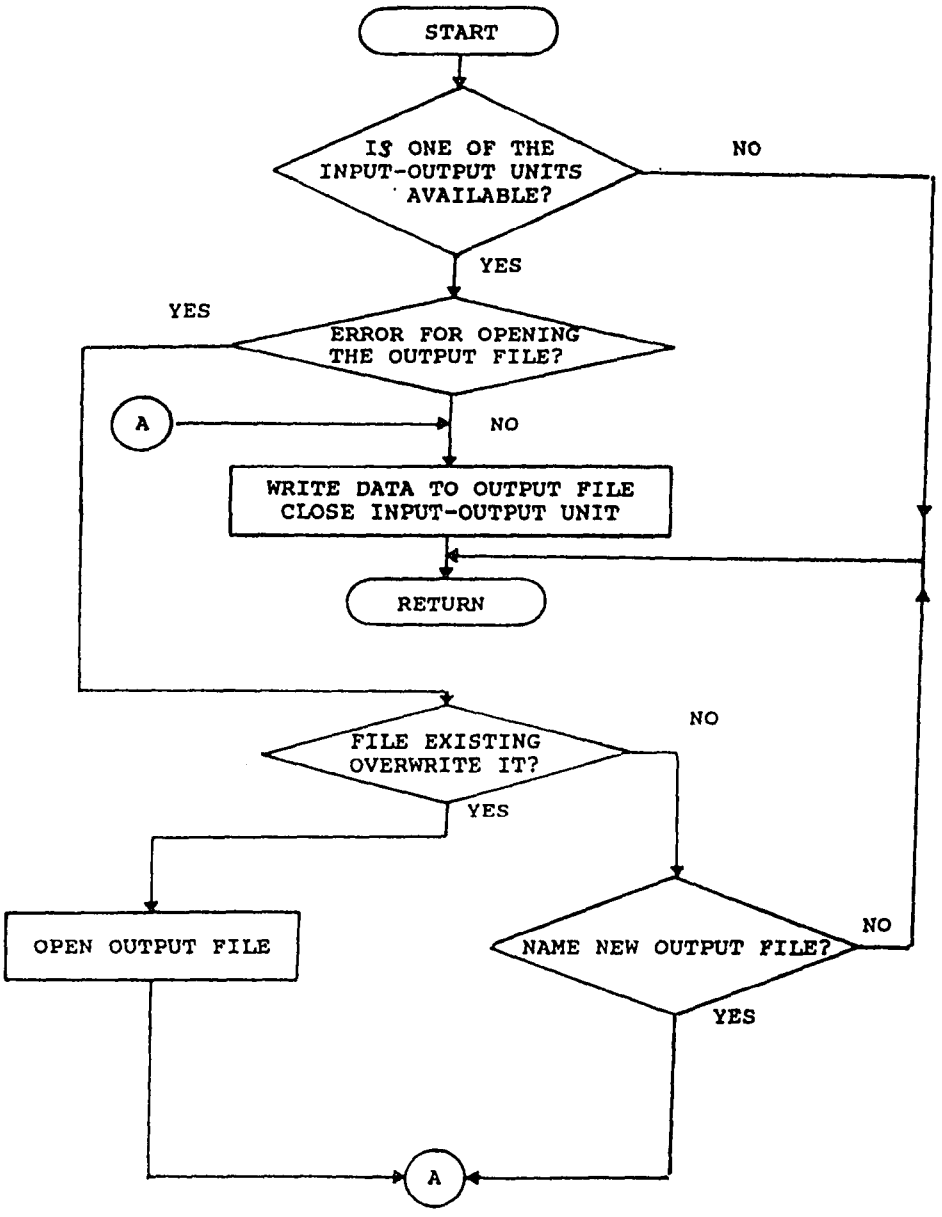

(f)

FIGURE 3.11 (f) THE FLOW CHART OF OUTPUT SUBROUTINE.

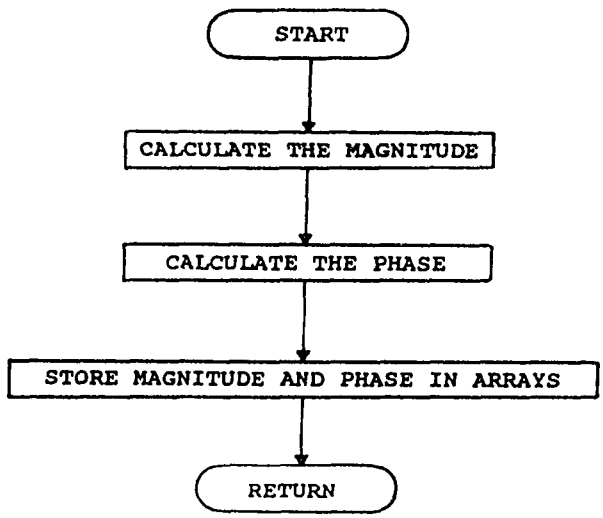

(g)

FIGURE 3.11 (g) THE FLOW CHART OF POLAR SUBROUTINE.

imaginary part. The output subroutine stores the magnitude and phase into two different data files.

CHAPTER IV

RESULTS AND DISCUSSION

4-1 INTRODUCTION

The investigation of the effect of the autonomic nervous system on heart rate has been studied for many years. When studied with classical conditioning of the heart rate response, it reveals some information about the response of the autonomic nervous system to external stimuli. However, the traditional way to assess the effect of the autonomic regulation of heart rate is to block one division of the autonomic nervous system by either peripheral nerve ablation or pharmacological blockade. This may cause some drawbacks as discussed earlier, since, blocking one of the divisions of the autonomic nervous system may bias the whole system.

In this work, we applied a method called complex demodulation to the heart rate variability signal to extract information about the activity of the autonomic nervous system from specific frequency bands of interest without using any pharmacological blockade or peripheral nerve ablation.

The heart rate variability signal is obtained by first passing the ECG signal through an R-wave detector and then calculating the interval between two adjacent R-wave pulses (IBI). An interpolation method is then used to interpolate

the IBI signal. After that, a robust regression procedure is used to remove very low frequency components. When complex demodulation is performed on the HRV signal, zero-phase-shift lowpass filtering is also used to keep the time series from shifting or delaying.

4-2 RESULTS

The magnitude results of the complex demodulation will now be considered. The low frequency response is the result of complex demodulation centered at 0.00244 Hz with the passband from -0.12 Hz to 0.124 Hz; the respiration frequency response is the result of complex demodulation centered at 0.345 Hz with the passband from 0.162 Hz to 0.528 Hz. Successive five second (50 points) averages are taken from the magnitude results to represent the respiration frequency response and the low frequency response. This averaging results in a smoother curve without losing the important features. Fig. 4.1 shows an example of a 50 point average taken from a magnitude curve, where (a) is a 90 second interpolated IBI signal, (b) is the respiration frequency response from the complex demodulation processing of (a), and (c) is the successive five second averages of (b).

In order to draw inferences from the data, we developed confidence intervals based on the t-distribution at the appropriate degrees of freedom (21). Since we made 18

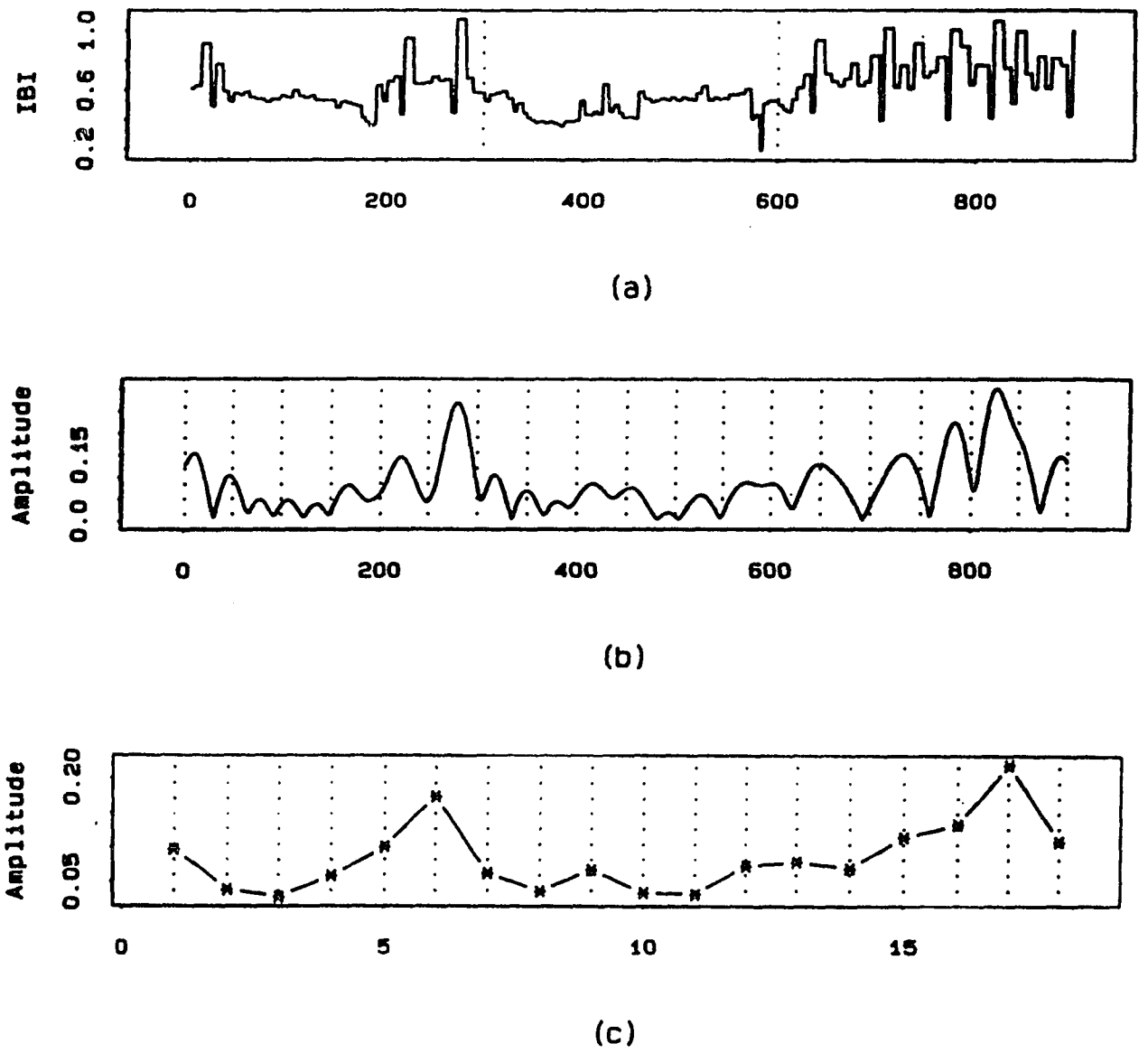

FIGURE 4.1 (a) A 900 POINT (5 SEC.) IBI SIGNAL.
(b) THE RESPIRATION FREQUENCY RESULT FROM COMPLEX DEMODULATION PROCESS.
(c) THE SUCCESSIVE FIVE-SECOND (50 POINTS) AVERAGE OF (b).

comparisons (90 seconds) based on this confidence interval, we set our alpha level of significance to be .05/18 instead of 0.05 so that we could maintain at least 95% confidence over all 18 comparisons. For example, the confidence interval we used in our experiment is as follows:

Let qt(p,df)*SEM = C

where qt(p,df) is the confidence interval coefficient,

p = 1 - 0.05/18 = 0.99722, % of confidence,

df = 5, degree of freedom, which is the total number of sampling data set - 1,

so, qt(0.99722,5) = 4.65443 obtained from t-statistic table,

SEM is the standard error of the mean and is defined as follows:

$$SEM = SQRT\{[SIGMA(X-\overline{X})^2]/(N-1)\}/SQRT(N)$$

where $\overline{X}$ is the mean of the sampling data sets,

N = 6 is the total number of sampling data sets from 30 second data before pre-CSs trials.

Then

$$\overline{X} - C \leq \text{95\% confidence interval} \leq \overline{X} + C$$

If the data is within this 95% confidence interval, we have 95% confidence to conclude that this data is not

increasing or decreasing. On the other hand, if the data is above or below this 95% confidence interval, the hypothesis that the data is not increasing or decreasing, is not true any more. By observing the plot of the data and whether the data fall above or below the 95% confidence interval, we then can decide whether the data is increasing or decreasing. Each magnitude result, the average magnitude result and the successive five second average magnitude result will now be presented for one COND dog and one NCOND dog for each type of conditioning trial. Other dogs' results are shown in Appendix D. Also, the average magnitude results of different dogs under the same type of conditioning trial will be compared.

Each graph consists of three periods, which are the pre-CS period, CS period, and post-CS period.

CONDITIONED Dog, CS+ trial Figure 4.2 (a) to (c) show three CS+ trial runs of the respiration frequency responses of a single conditioned dog (dog 2). Figure 4.2 (d) is the average respiration frequency response of Fig. 4.2 (a) to (c). The solid vertical lines indicate the beginning of each of the different periods in the trial -- pre-CS+, CS+, and post-CS+. The dotted vertical lines serve as a time reference by dividing the record into 5 second epochs. Although these individual files show normal intertrial variability, careful inspection of the records shows a clear general pattern. In all 3 trials, activity is lowest during

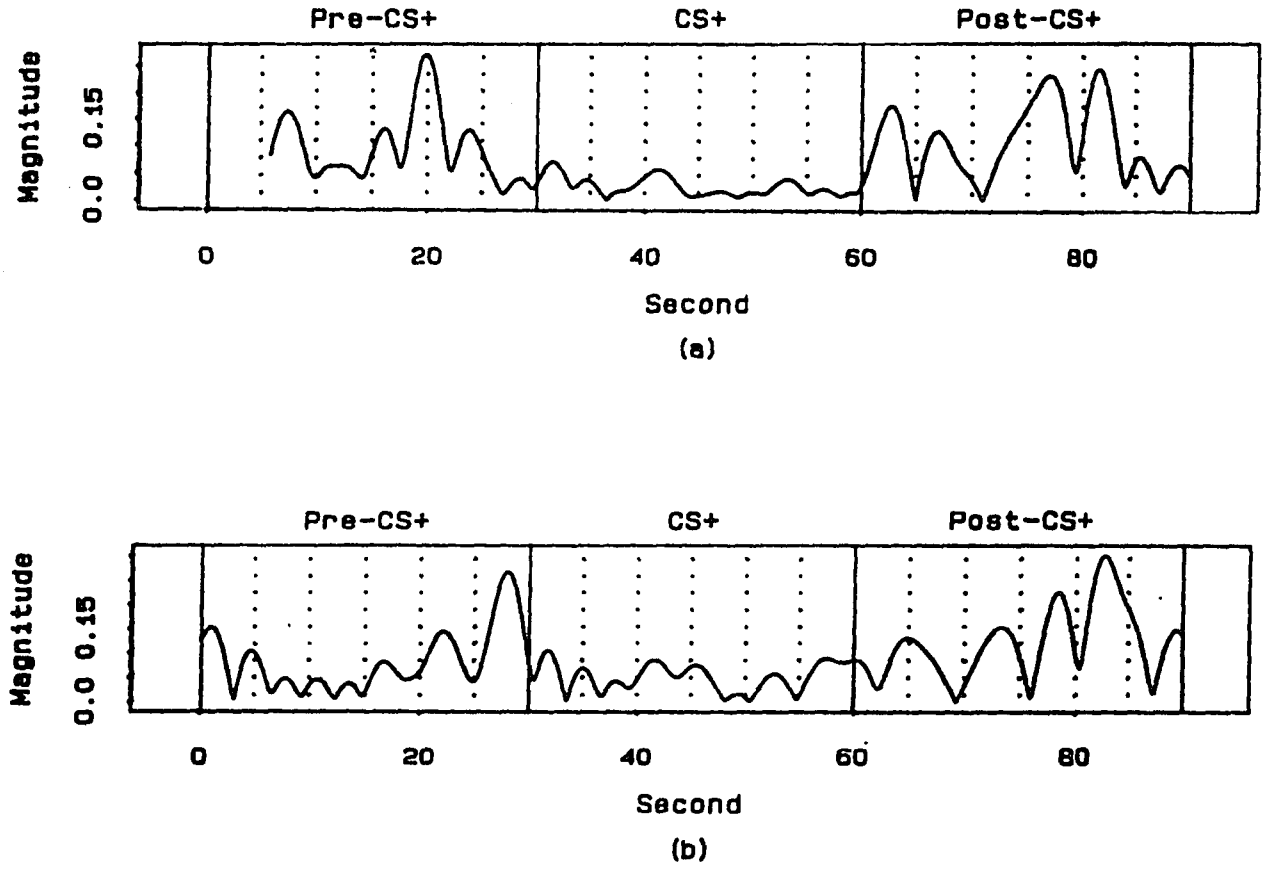

FIGURE 4.2 (a) THE RESPIRATION FREQUENCY MAGNITUDE RESULT OF DOG 2 UNDER CS+ TRIAL 1.

(b) THE RESPIRATION FREQUENCY MAGNITUDE RESULT OF DOG 2 UNDER CS+ TRIAL 2.

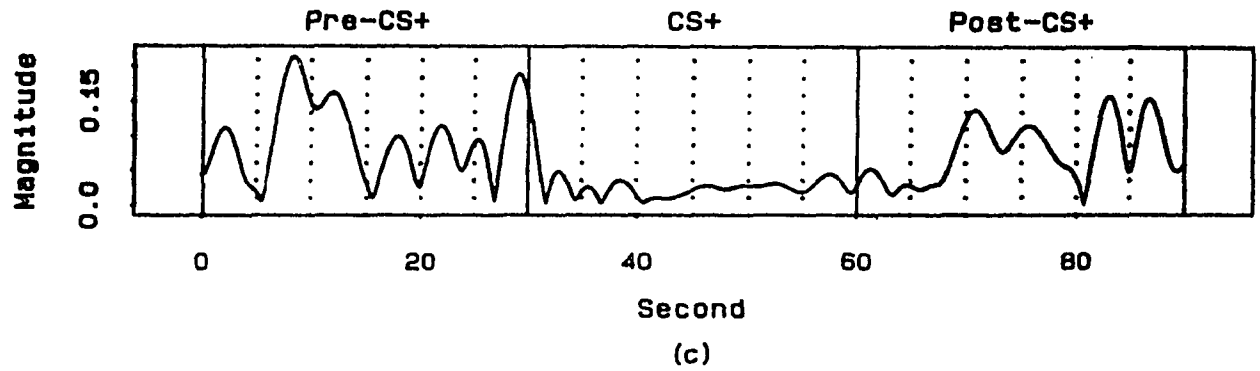

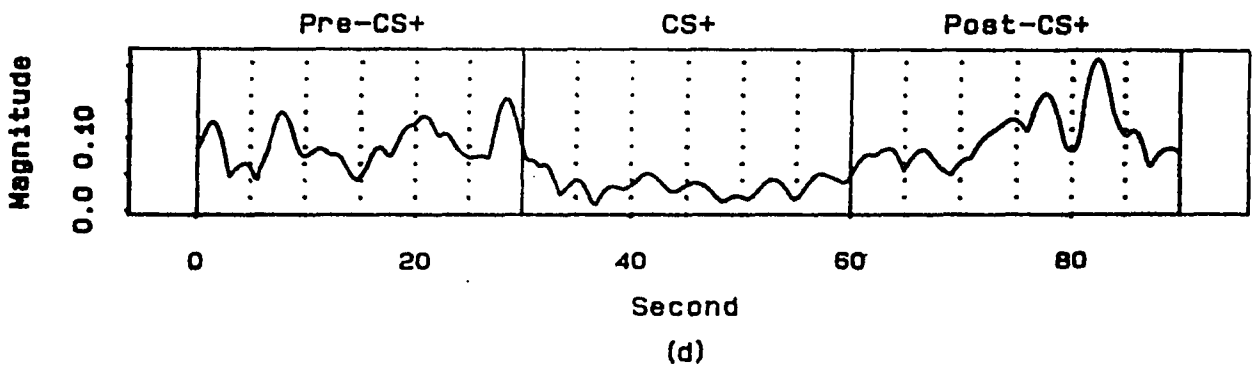

FIGURE 4.2 (c) THE RESPIRATION FREQUENCY MAGNITUDE RESULT OF DOG 2 UNDER CS+ TRIAL 3.

(d) THE AVERAGE FROM (a) TO (c).

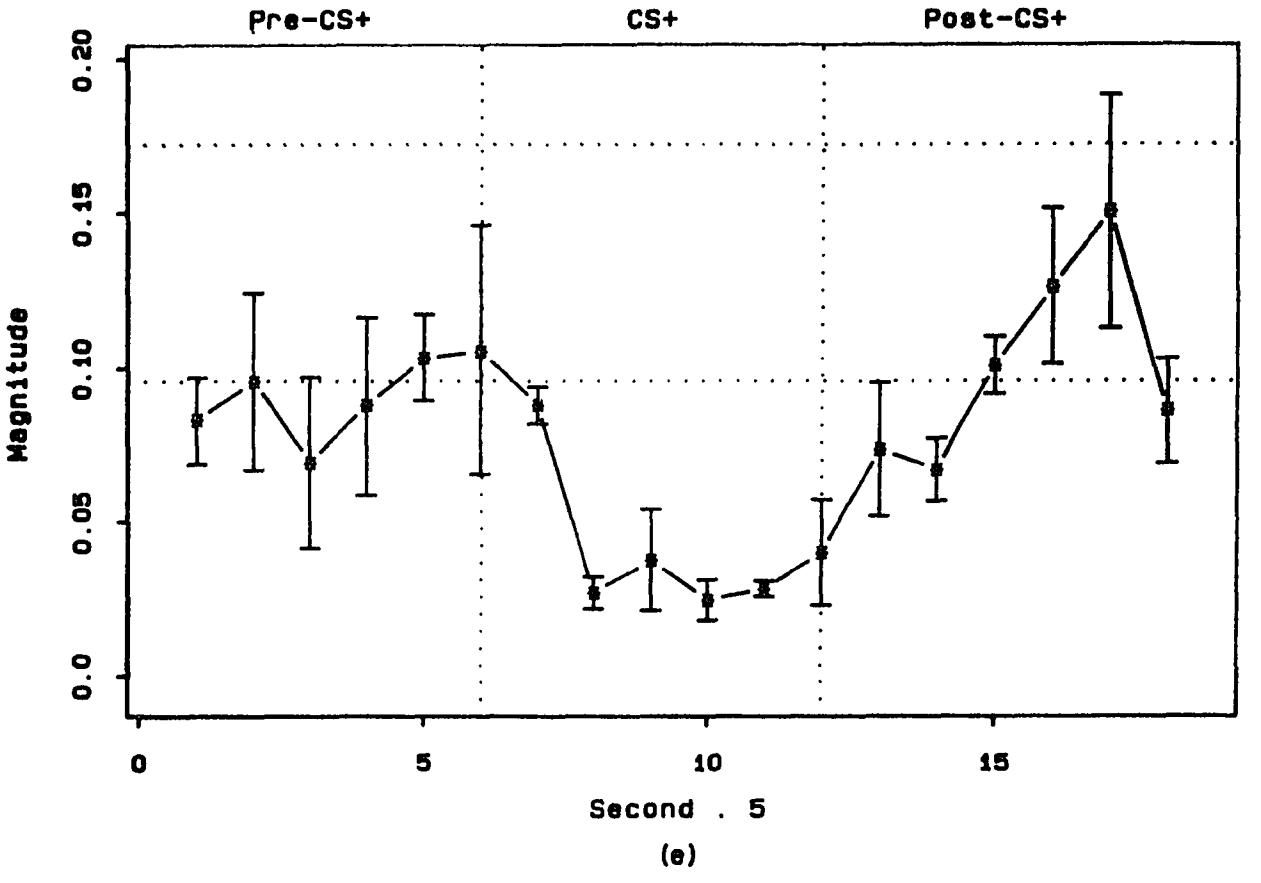

FIGURE 4.2 (e) THE 5-SECOND AVERAGE OF (d) WITH STANDARD ERROR AND 95% CONFIDENCE INTERVAL.

the middle section, at the time of the CS+ signal. Since the respiration frequency response reflects the parasympathetic activity, this phenomenon indicates that there is less parasympathetic activity during the CS+ period than during pre-CS+ and post-CS+ periods.

This pattern emerges very clearly in the plot of the averaged records shown in Fig. 4.2 (e). This plot shows the data averaged across 5 second epochs and across trials. The horizontal dotted lines in this plot show the 95% confidence interval for the 30 second baseline data prior to the pre-CS+ interval, while the vertical dotted lines indicate the divisions between pre-CS+, CS+, and post-CS+ portions of the trial. Also, the standard error of mean for each point was calculated and plotted.

The first thing that we see in Fig. 4.2 (e) is that the respiration frequency response is already diminished below baseline levels during the pre-CS+ interval. However, power at the respiration frequency drops even further during the CS+ interval. And finally, respiration frequency power recovers to baseline levels in the post-CS+ interval. This indicates that the parasympathetic activity decreased in the pre-CS+ interval, decreased more in the CS+ interval and then increased in the post-CS+ interval.

From Fig. 4.3 (a) to (c), we see that there is a major maximum in the low frequency response early in the CS+ interval. Since the low frequency response reflects the

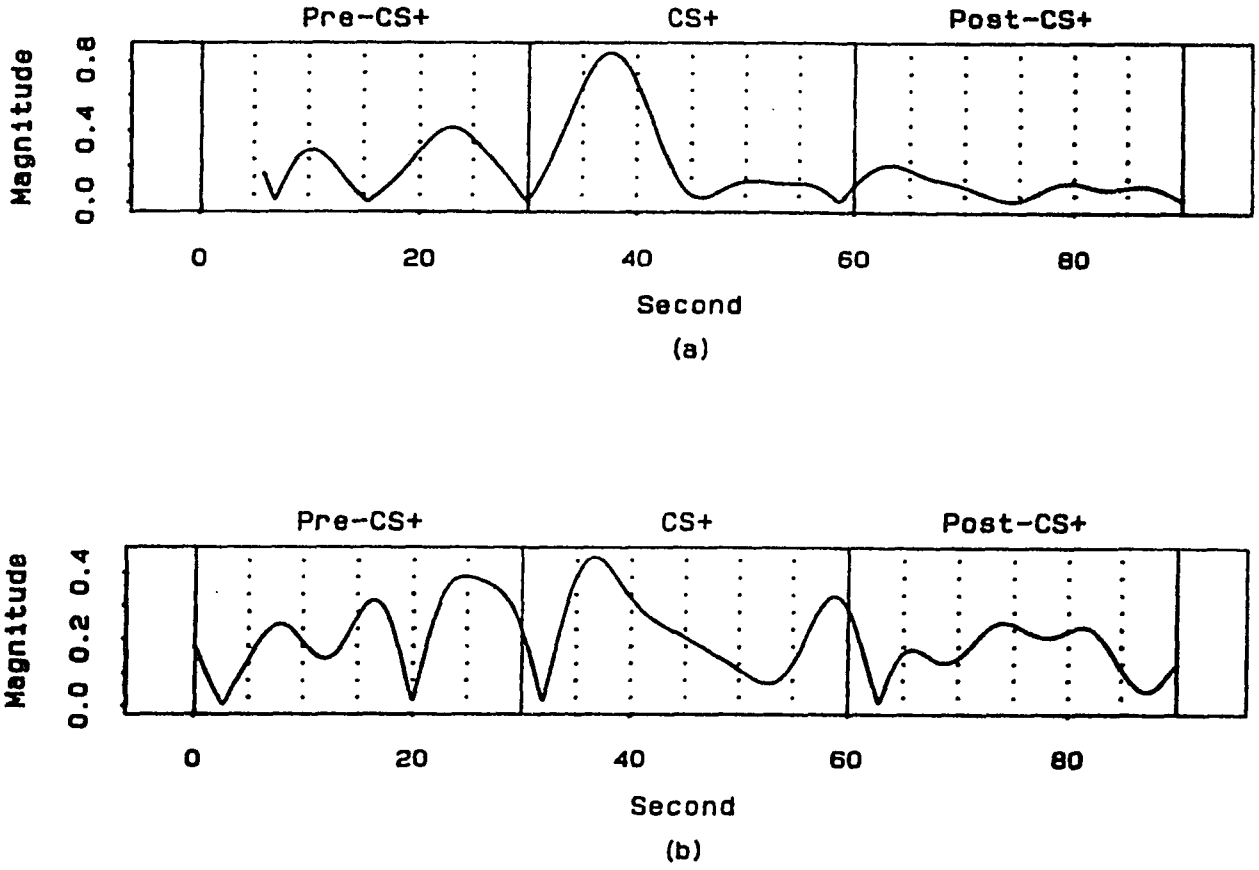

FIGURE 4.3 (a) THE LOW FREQUENCY MAGNITUDE RESULT OF DOG 2 UNDER CS+ TRIAL 1.

(b) THE LOW FREQUENCY MAGNITUDE RESULT OF DOG 2 UNDER CS+ TRIAL 2.

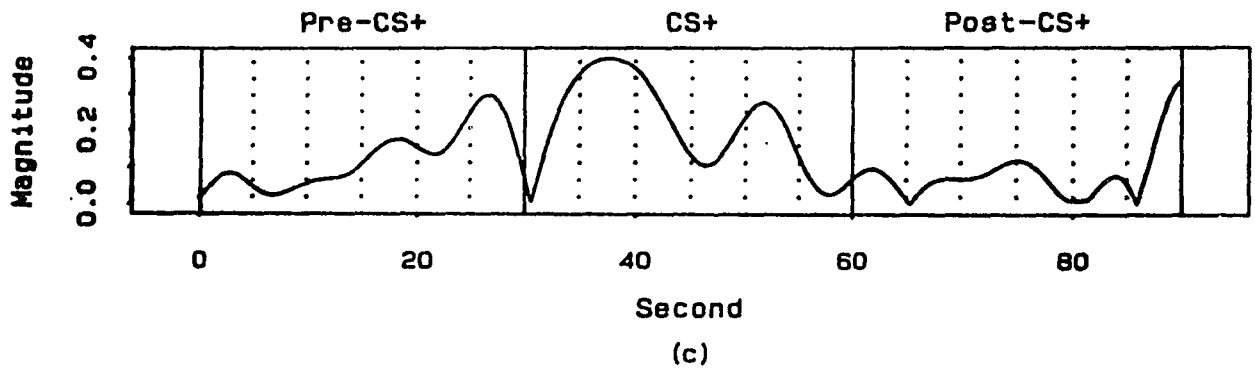

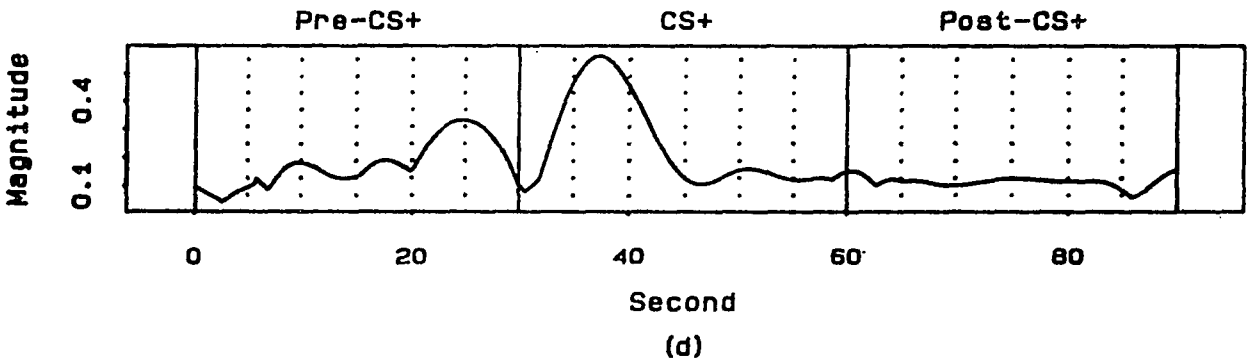

FIGURE 4.3 (c) THE LOW FREQUENCY MAGNITUDE RESULT OF DOG 2 UNDER CS+ TRIAL 3.
(d) THE AVERAGE FROM (a) TO (c).

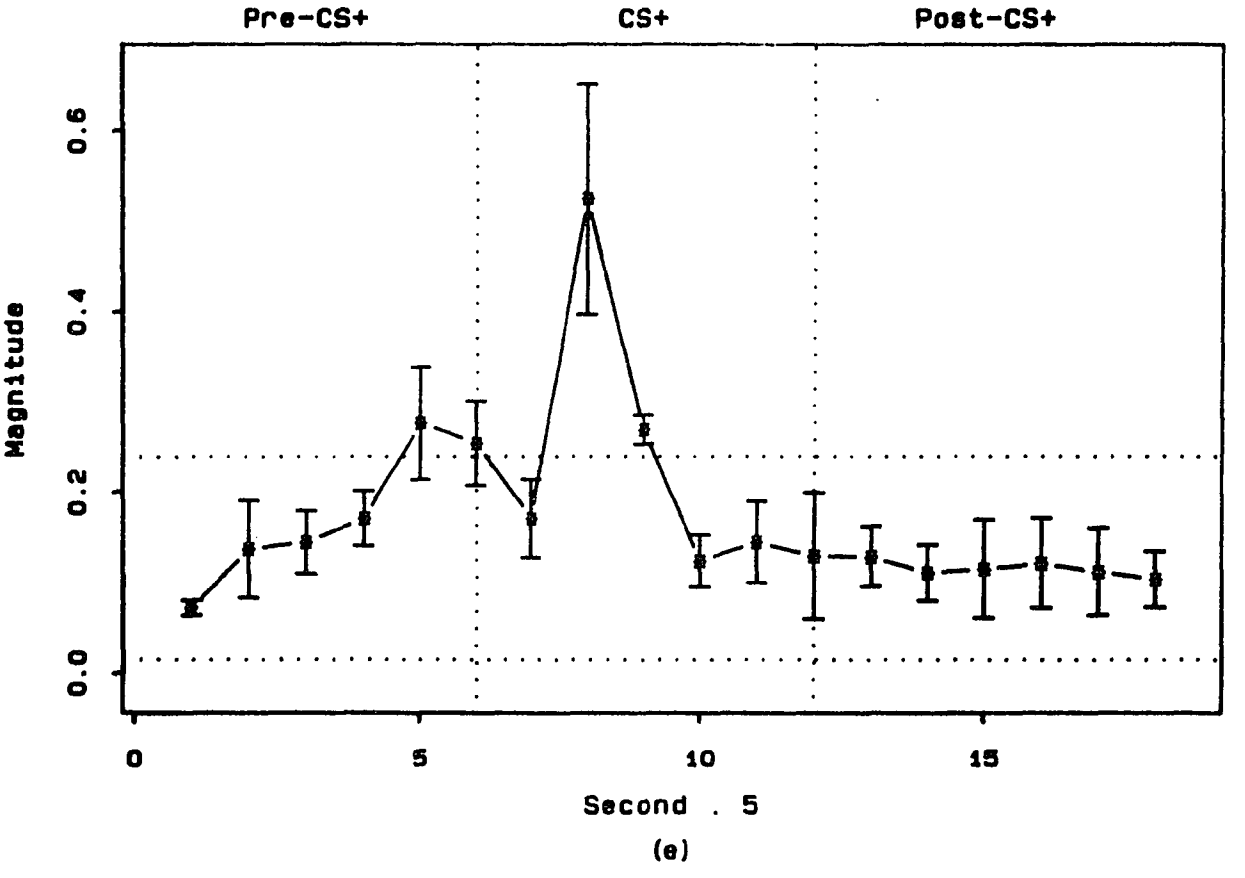

FIGURE 4.3 (e) THE 5-SECOND AVERAGE OF (d) WITH STANDARD ERROR AND 95% CONFIDENCE INTERVAL.

combined responses of the sympathetic and parasympathetic activities, and the respiration frequency responses from Fig. 4.2 decreased at the same time which indicates a decrease of the parasympathetic activity, we conclude that the sympathetic activity is increasing during the first portion of the CS+ periods.

CONDITIONED Dog, CS- trial From Fig. 4.4 (a) to (c), we see that the magnitude of the respiration frequency responses do not have large changes within the three periods. From the successive five second average result with 95% confidence interval shown in Fig. 4.4 (e), we can see that the magnitude decreased below the 95% confidence interval in the pre-CS- period, which indicates that the parasympathetic activity decreased during the pre-CS- period, and the remainder of the average data are either within or near the 95% confidence interval. If points are within the 95% interval, it indicates that there is no change in the parasympathetic activity; if they are above the confidence interval, the parasympathetic activity is considered to be increasing; if they are below the confidence interval, the parasympathetic activity is considered to be decreasing.

From Fig. 4.5 (a) to (c), the magnitude of the low frequency responses of CS- trials have high magnitude responses in the pre-CS- periods, but since the respiration frequency responses decreased during the same time shown in Fig. 4.4, we conclude that the sympathetic activity is

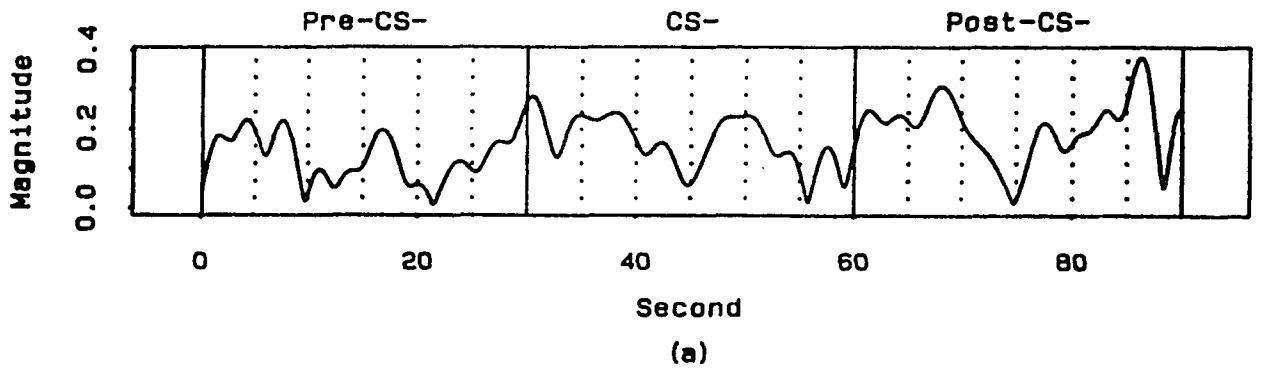

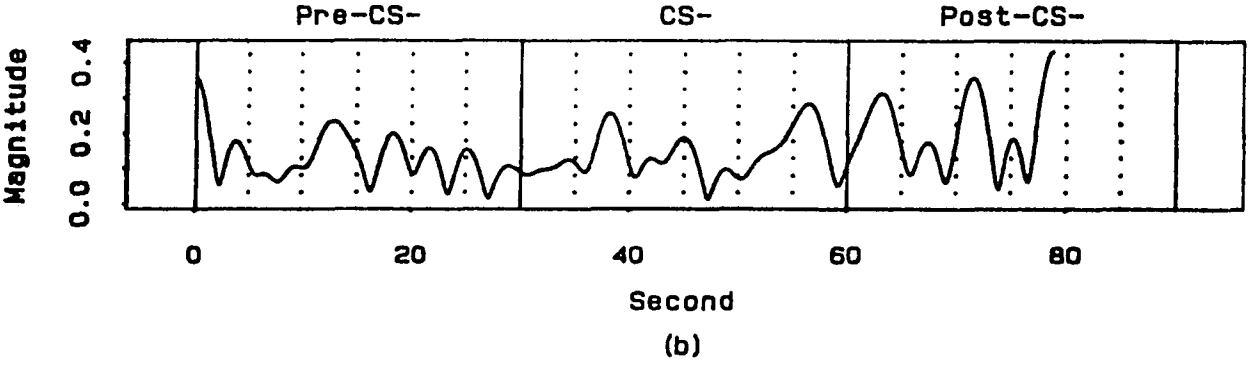

FIGURE 4.4 (a) THE RESPIRATION FREQUENCY MAGNITUDE RESULT OF DOG 2 UNDER CS- TRIAL 1.

(b) THE RESPIRATION FREQUENCY MAGNITUDE RESULT OF DOG 2 UNDER CS- TRIAL 2.

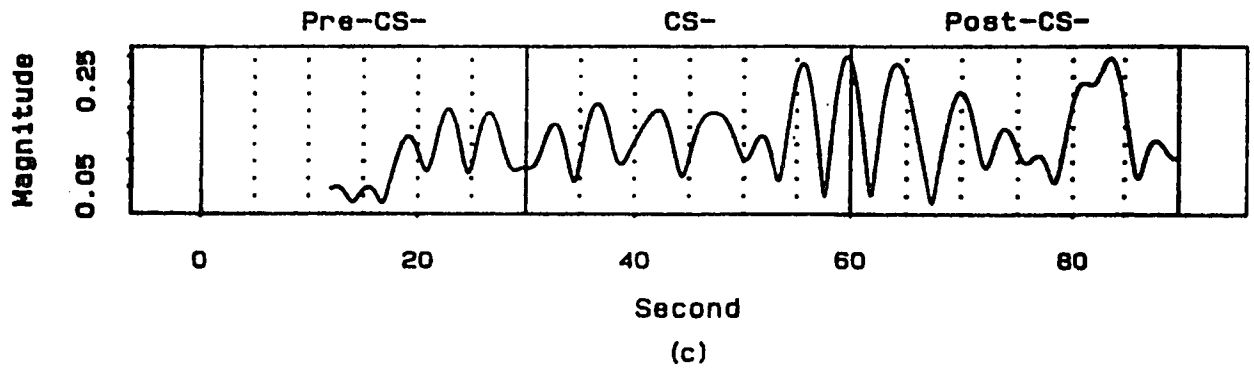

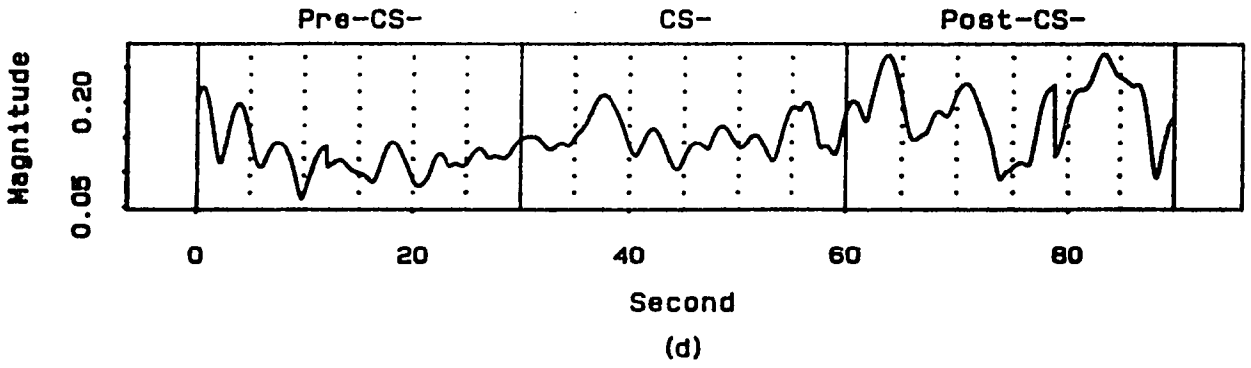

FIGURE 4.4 (c) THE RESPIRATION FREQUENCY MAGNITUDE RESULT OF DOG 2 UNDER CS- TRIAL 3.

(d) THE AVERAGE FROM (a) TO (c).

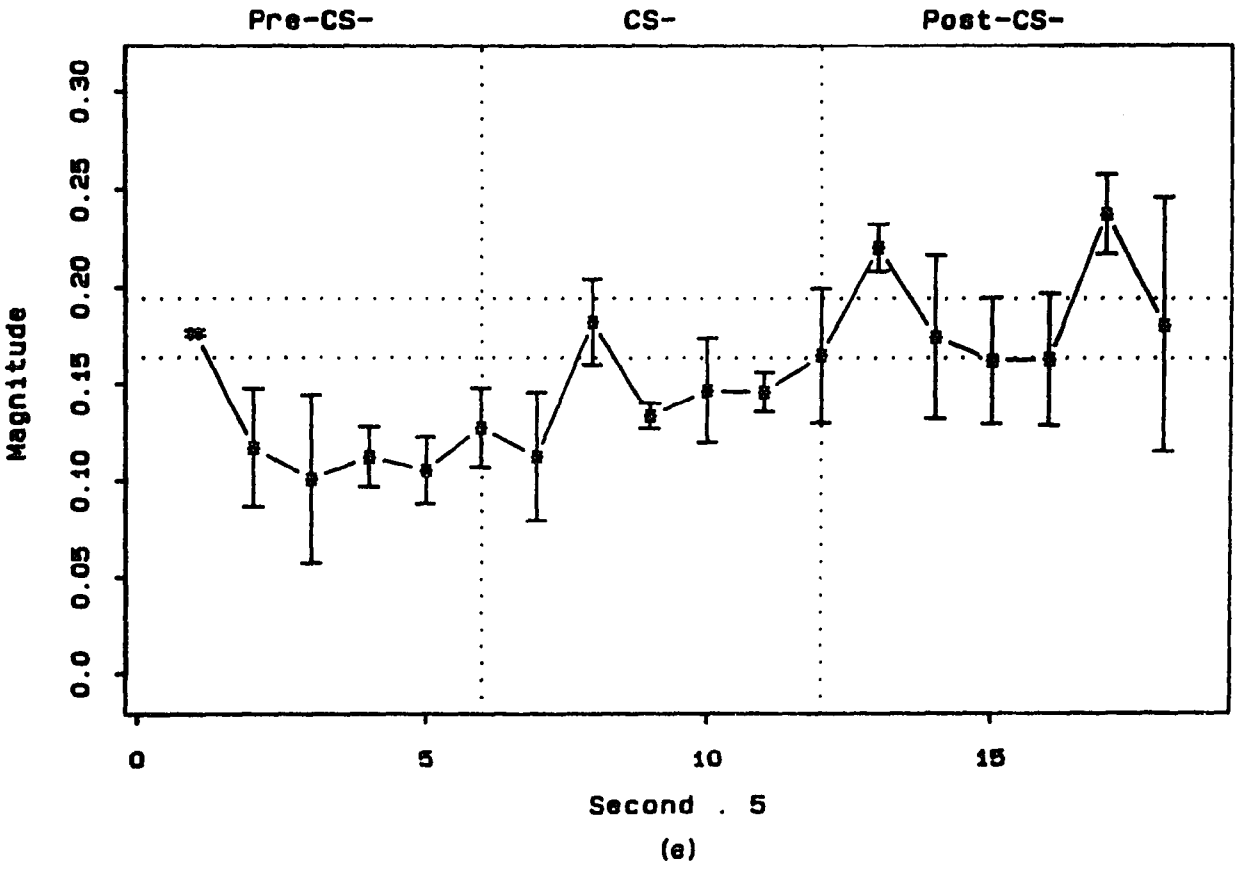

FIGURE 4.4 (e) THE 5-SECOND AVERAGE OF (d) WITH STANDARD ERROR AND 95% CONFIDENCE INTERVAL.

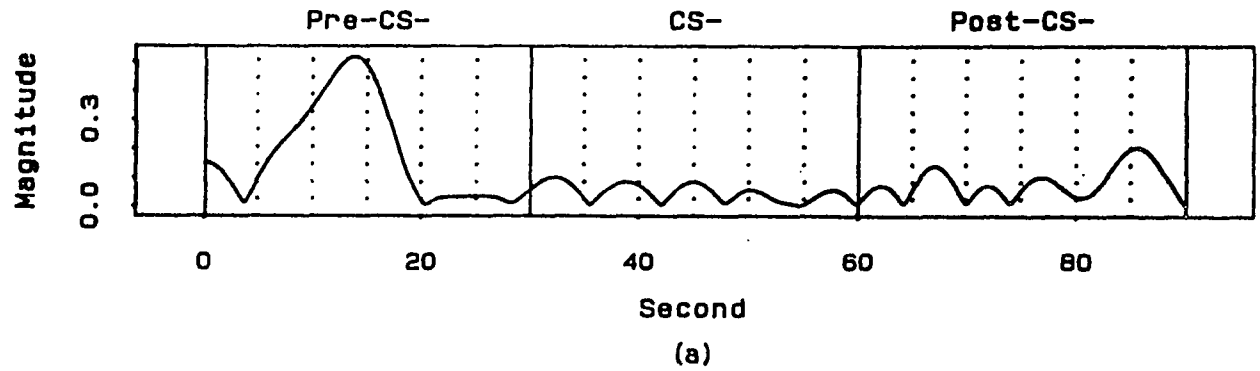

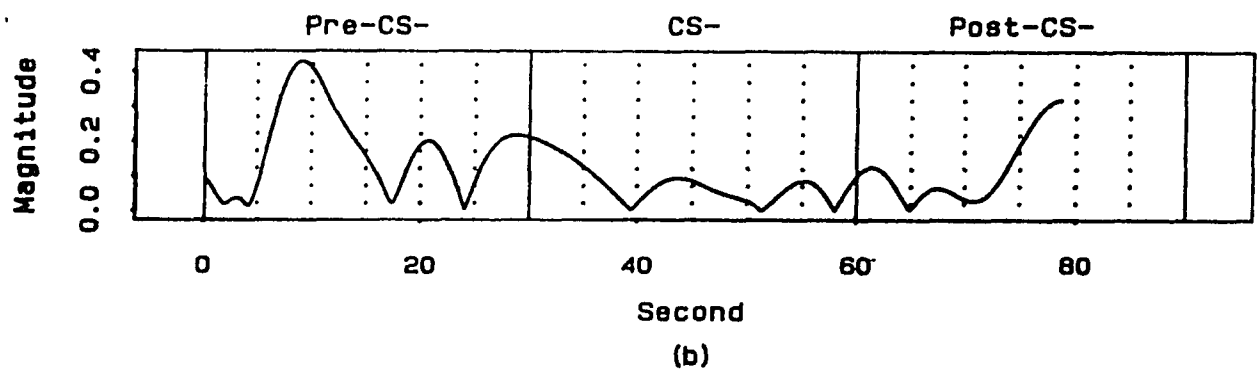

FIGURE 4.5 (a) THE LOW FREQUENCY MAGNITUDE RESULT OF DOG 2 UNDER CS- TRIAL 1.

(b) THE LOW FREQUENCY MAGNITUDE RESULT OF DOG 2 UNDER CS- TRIAL 2.

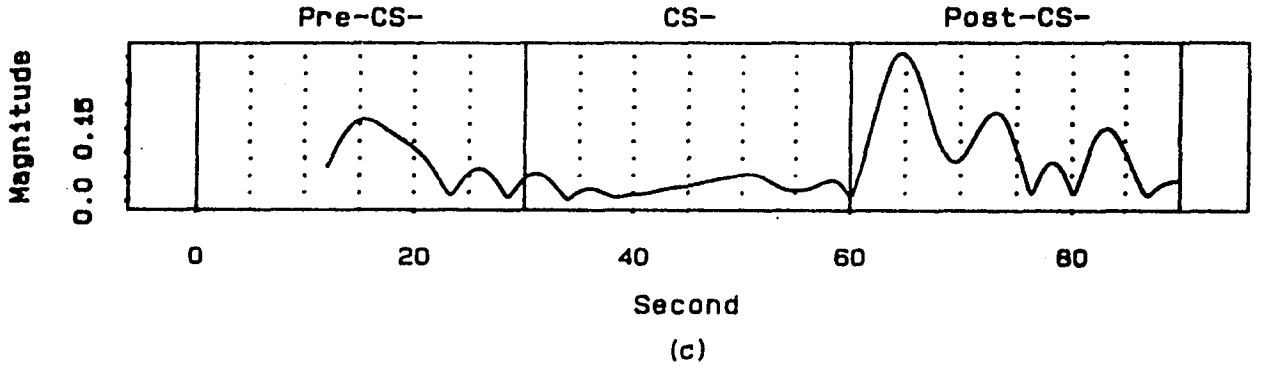

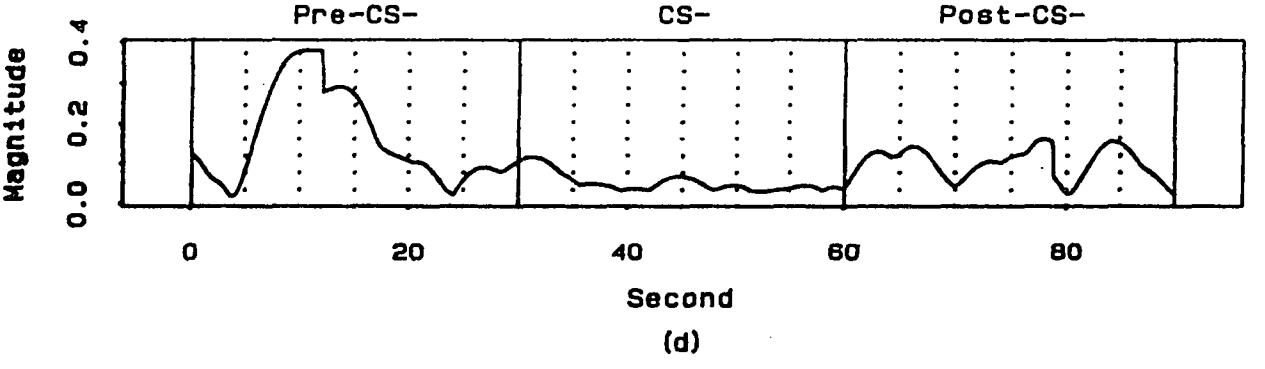

FIGURE 4.5 (c) THE LOW FREQUENCY MAGNITUDE RESULT OF DOG 2 UNDER CS- TRIAL 3.

(d) THE AVERAGE FROM (a) TO (c).

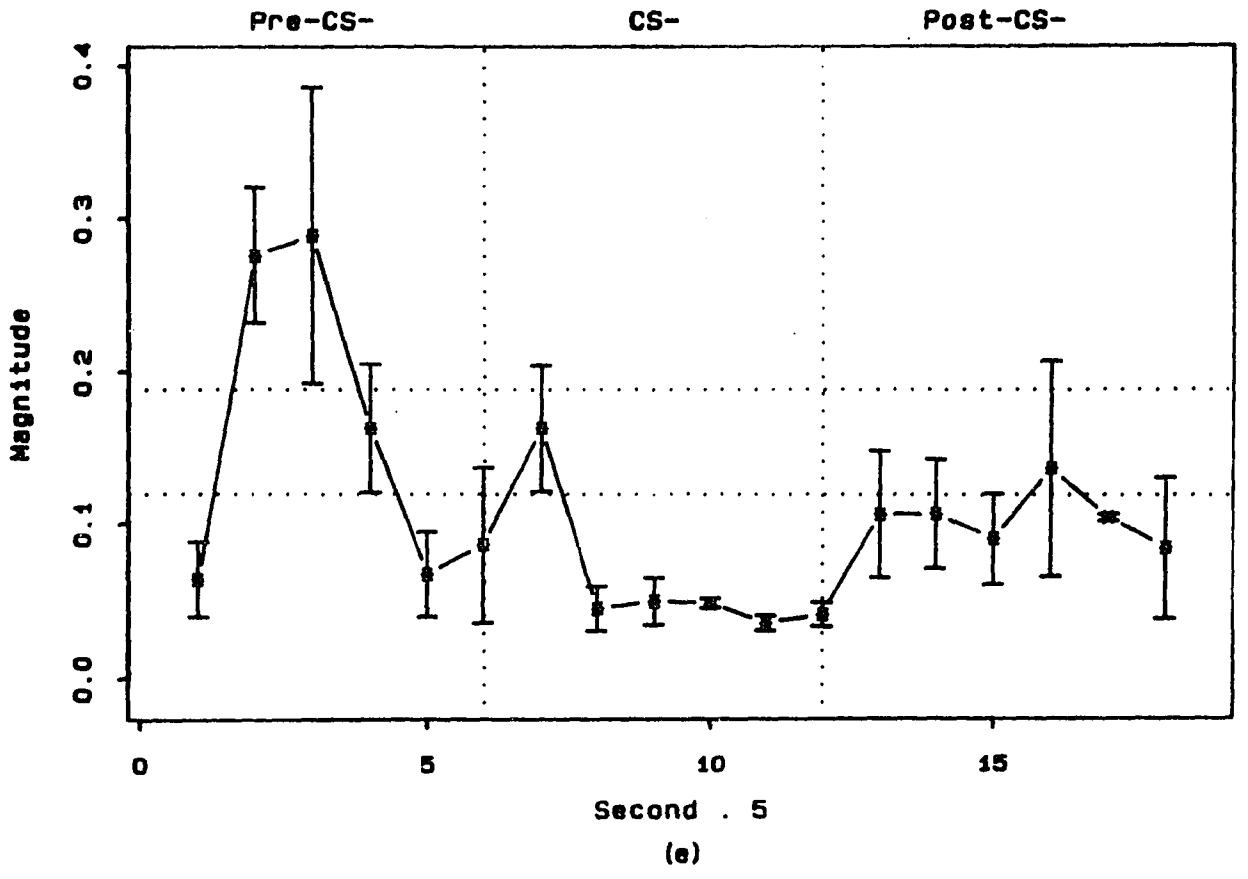

FIGURE 4.5 (e) THE 5-SECOND AVERAGE OF (d) WITH STANDARD ERROR AND 95% CONFIDENCE INTERVAL.

increasing in the pre-CS- period because the parasympathetic activity is decreasing.

NONCONDITIONED Dog, CS+ trial Figure 4.6 (a) to (c) show three CS+ trial runs of the respiration frequency responses of a single nonconditioned dog (dog3). The magnitude of the respiration frequency responses among different CS+ trials do not have consistent results. From Fig. 4.6 (e), the successive five second average result shows that some of the data are in the 95% confidence interval, and they can be treated as showing no parasympathetic activity change. Some data are above this 95% confidence interval, indicating that the parasympathetic activity increased.

The low frequency magnitude responses, Fig. 4.7 (a) to (c) show that the magnitude results are not consistent, and from the successive five second average result, we can see that all of the data are within the 95% confidence interval. From Fig. 4.6 (e) and Fig. 4.7 (e), we conclude that there is no change in the sympathetic and parasympathetic activities for most of the time in this trial but there are some changes of the parasympathetic activity observed from Fig. 4.6(e).

NONCONDITIONED Dog, CS- trial From Fig. 4.8 (a) to (c), the magnitude of the respiration frequency responses do not change significantly within each trial, and from Fig. 4.8 (e), the successive five second average data show that data

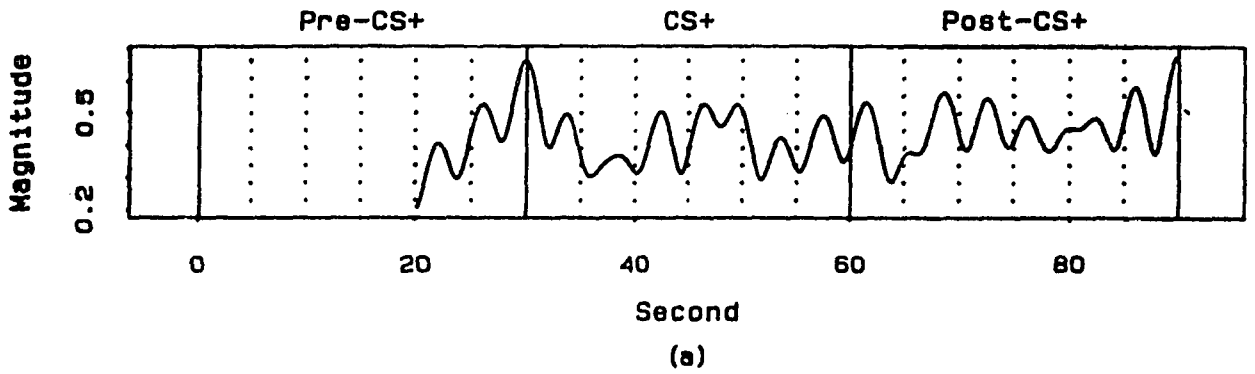

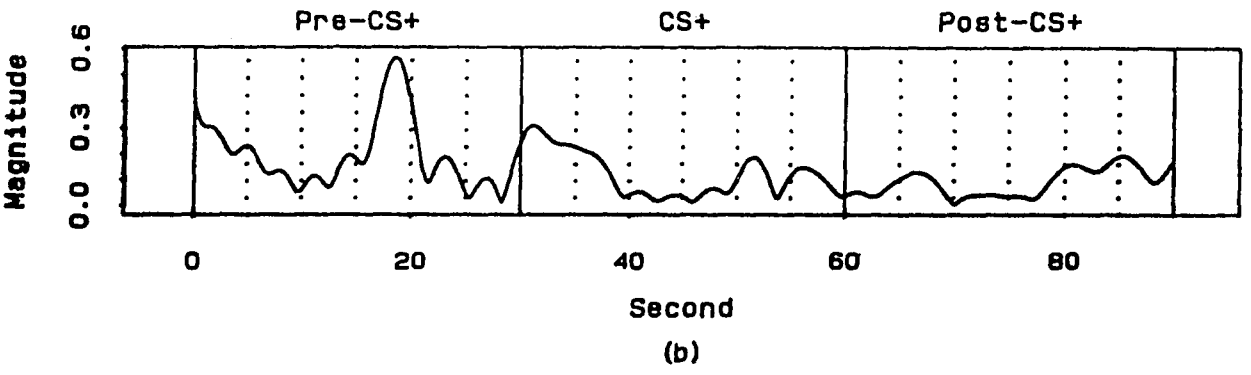

FIGURE 4.6 (a) THE RESPIRATION FREQUENCY MAGNITUDE RESULT OF DOG 3 UNDER CS+ TRIAL 1.

(b) THE RESPIRATION FREQUENCY MAGNITUDE RESULT OF DOG 3 UNDER CS+ TRIAL 2.

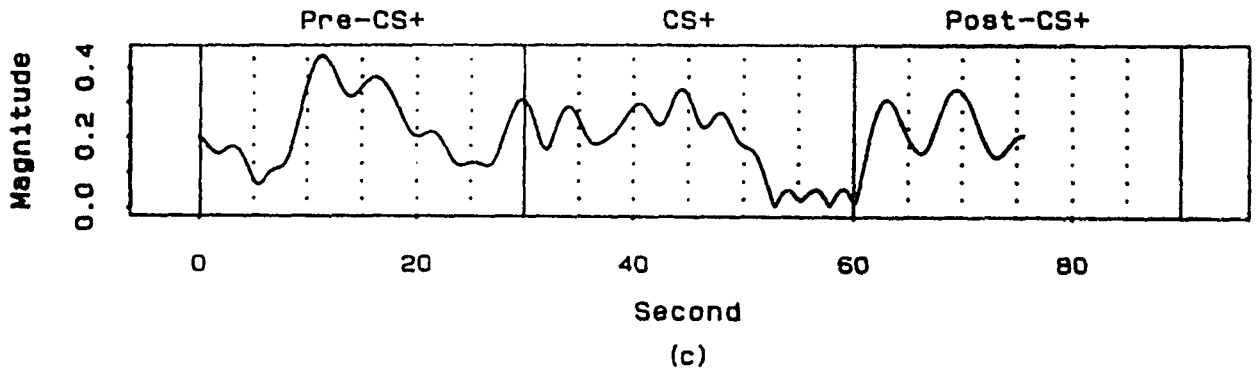

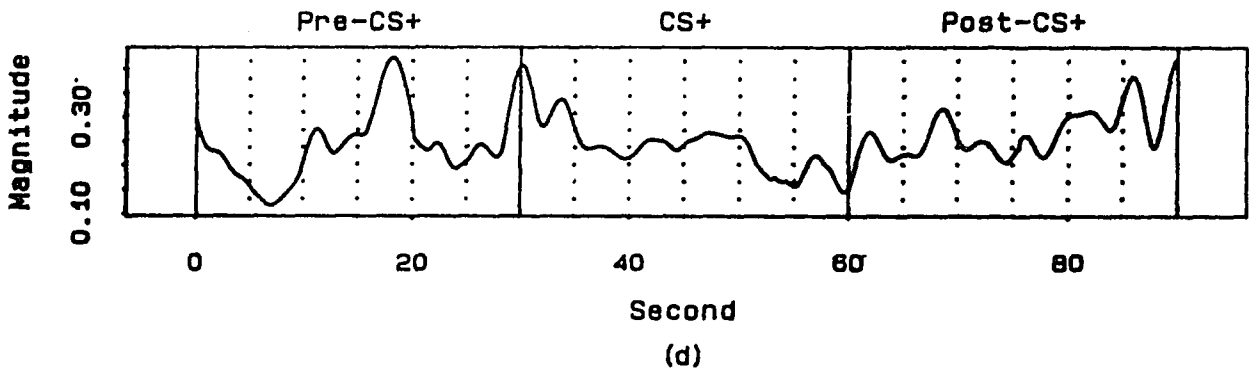

FIGURE 4.6 (c) THE RESPIRATION FREQUENCY MAGNITUDE RESULT OF DOG 3 UNDER CS+ TRIAL 3.

(d) THE AVERAGE FROM (a) TO (c).

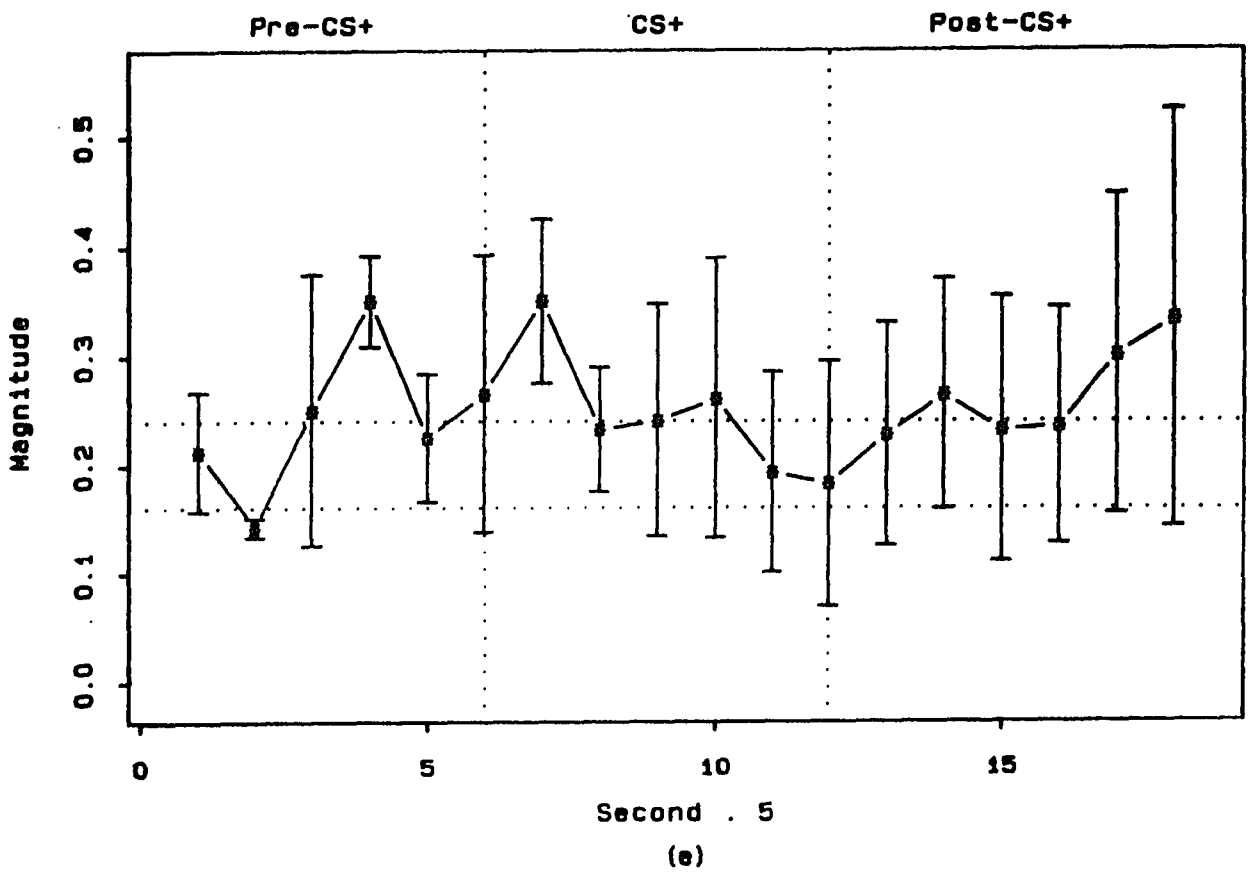

FIGURE 4.6 (e) THE 5-SECOND AVERAGE OF (d) WITH STANDARD ERROR AND 95% CONFIDENCE INTERVAL.

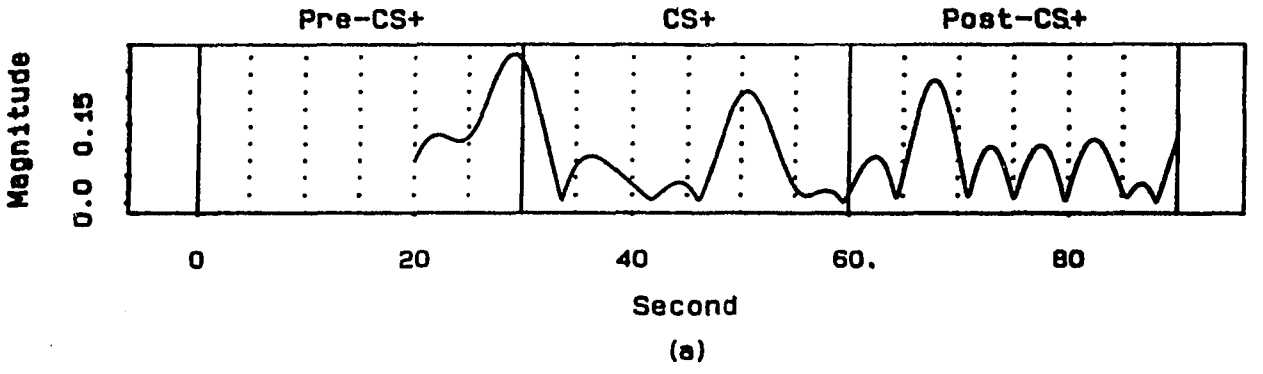

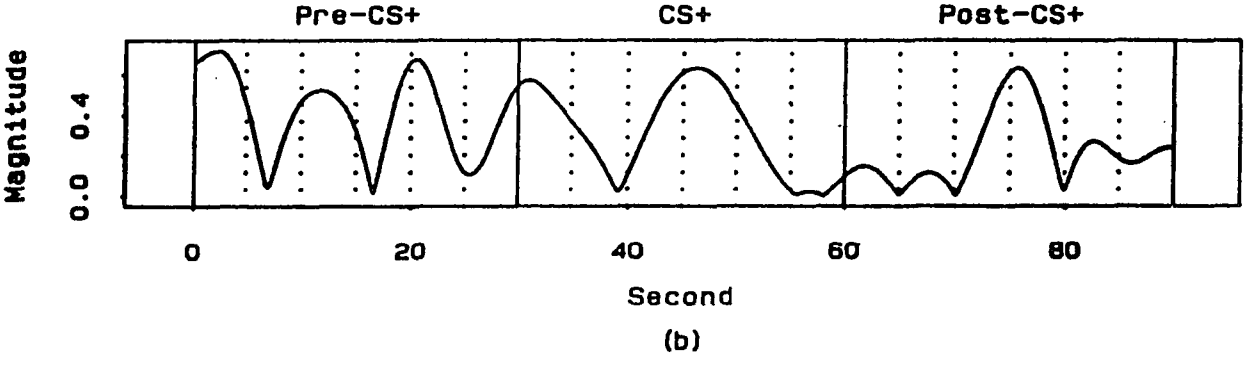

FIGURE 4.7 (a) THE LOW FREQUENCY MAGNITUDE RESULT OF DOG 3 UNDER CS+ TRIAL 1.

(b) THE LOW FREQUENCY MAGNITUDE RESULT OF DOG 3 UNDER CS+ TRIAL 2.

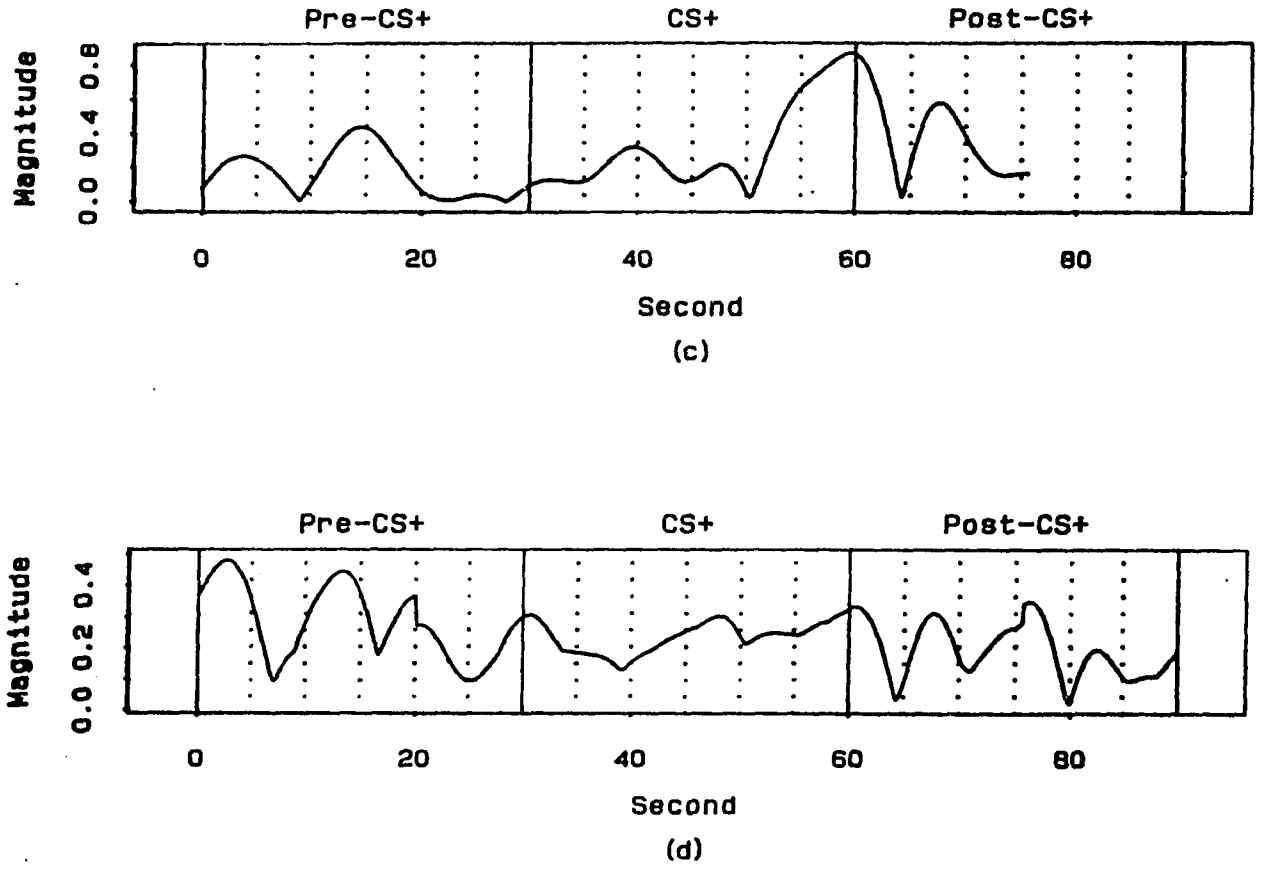

FIGURE 4.7 (c) THE LOW FREQUENCY MAGNITUDE RESULT OF DOG 3 UNDER CS+ TRIAL 3.

(d) THE AVERAGE FROM (a) TO (c).

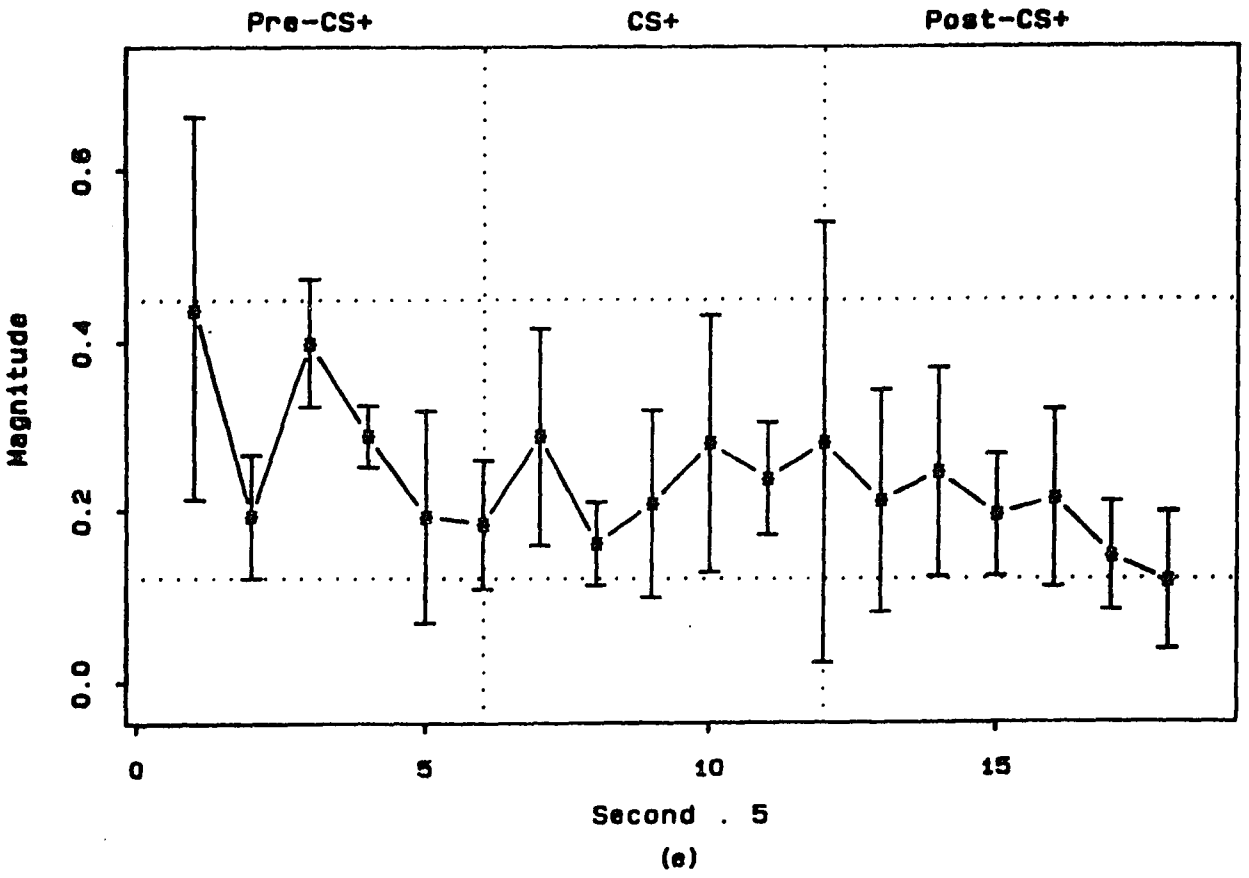

FIGURE 4.7 (e) THE 5-SECOND AVERAGE OF (d) WITH STANDARD ERROR AND 95% CONFIDENCE INTERVAL.

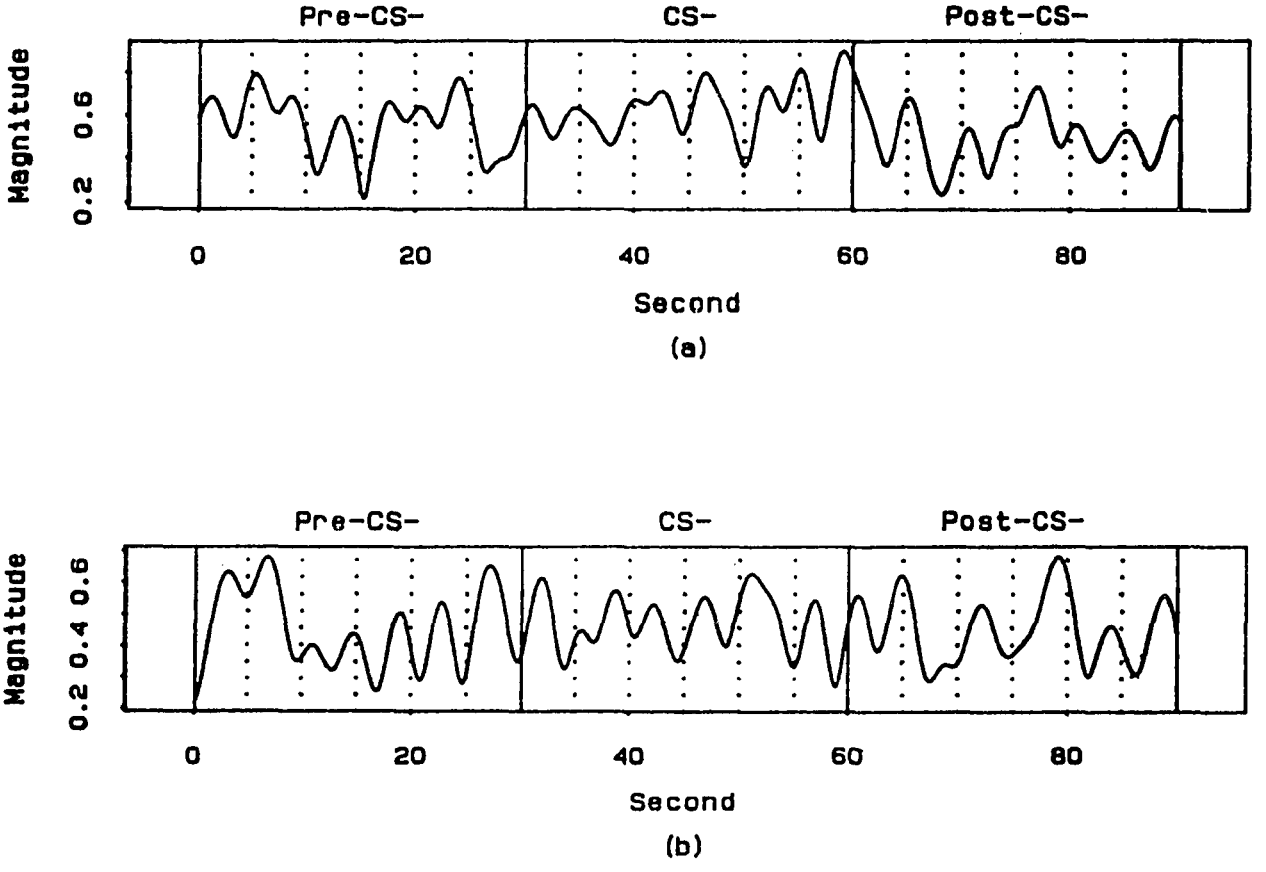

FIGURE 4.8 (a) THE RESPIRATION FREQUENCY MAGNITUDE RESULT OF DOG 3 UNDER CS- TRIAL 1.

(b) THE RESPIRATION FREQUENCY MAGNITUDE RESULT OF DOG 3 UNDER CS- TRIAL 2.

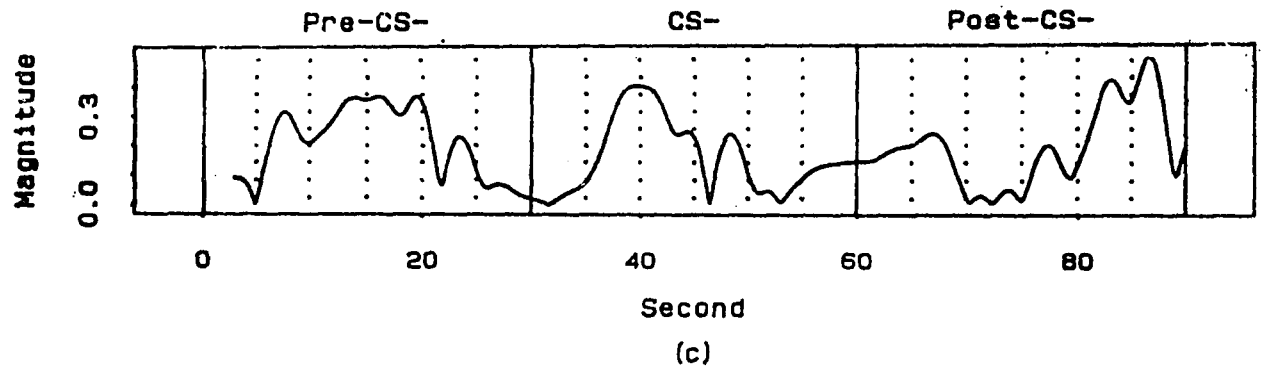

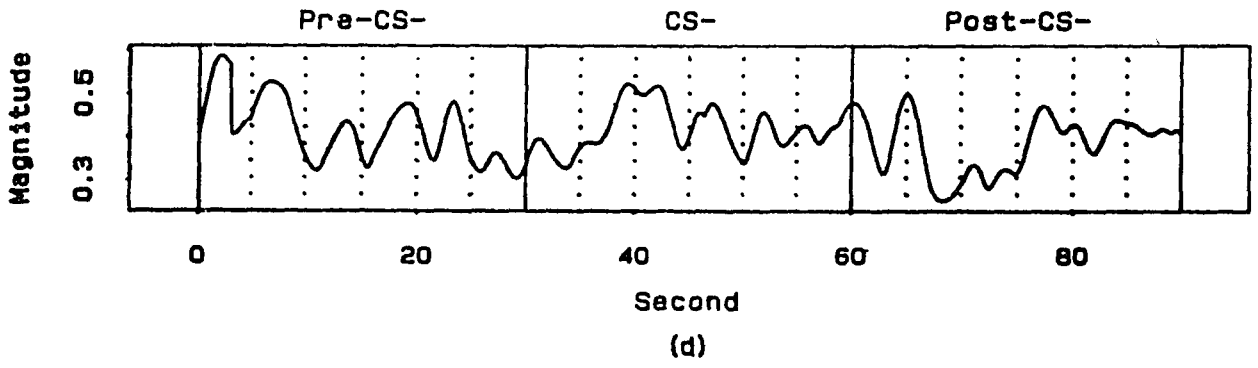

FIGURE 4.8 (c) THE RESPIRATION FREQUENCY MAGNITUDE RESULT OF DOG 3 UNDER CS- TRIAL 3.
(d) THE AVERAGE FROM (a) TO (c).

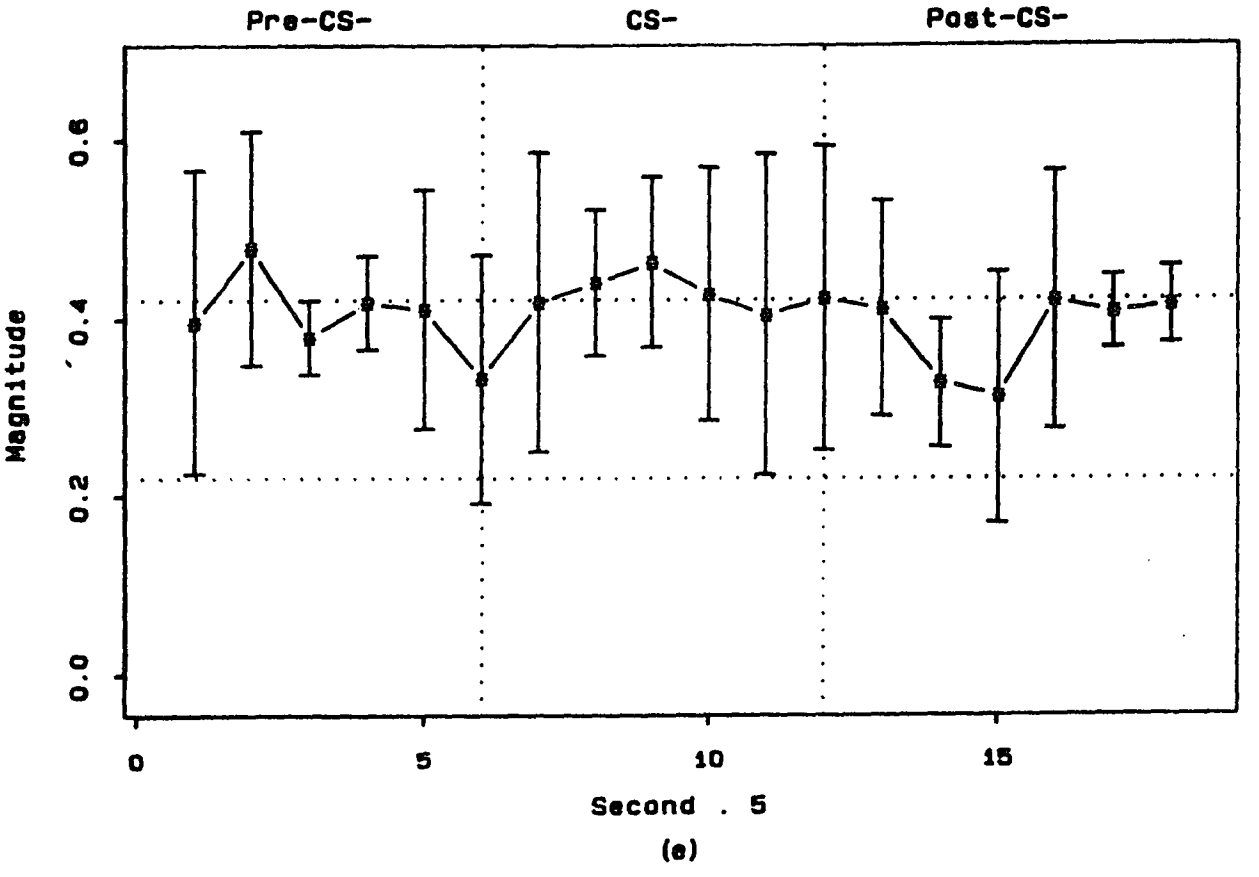

FIGURE 4.8 (e) THE 5-SECOND AVERAGE OF (d) WITH STANDARD ERROR AND 95% CONFIDENCE INTERVAL.

are within the 95% confidence interval or above it, which indicates that the parasympathetic activity can be deemed as either unchanged or increasing.

From Fig. 4.9 (a) to (c), we see that the low frequency magnitude responses of each trial show intertrial variability, and there is no specific pattern among these files. From Fig. 4.9 (e), the successive five second average shows that all of the data are in the 95% confidence interval so that we conclude that the sympathetic and parasympathetic activities do not change for most of this CS- trial and that there are some changes of the parasympathetic activity observed from Fig. 4.8 (e).

Since, as we expected, there are no large changes of the sympathetic and parasympathetic activities under CS+ and CS- trials for NCOND dogs, we can use the term "REF" to replace the CS+ and CS- for NCOND dogs. Fig. 4.10 shows the average magnitude results of different COND dogs under the same type of conditioning trials. Fig. 4.11 shows the average magnitude results of different NCOND dogs under the REF trials. The averages of the 30-second data before pre-CSs or pre-REF were plotted as horizontal reference dotted lines in each graph.

Comparing the graphs in Fig. 4.10, we can see that:
(i) For CS-, the low frequency response increased in the pre-CS- period, while the respiration frequency response decreased in this period. This strongly suggests an

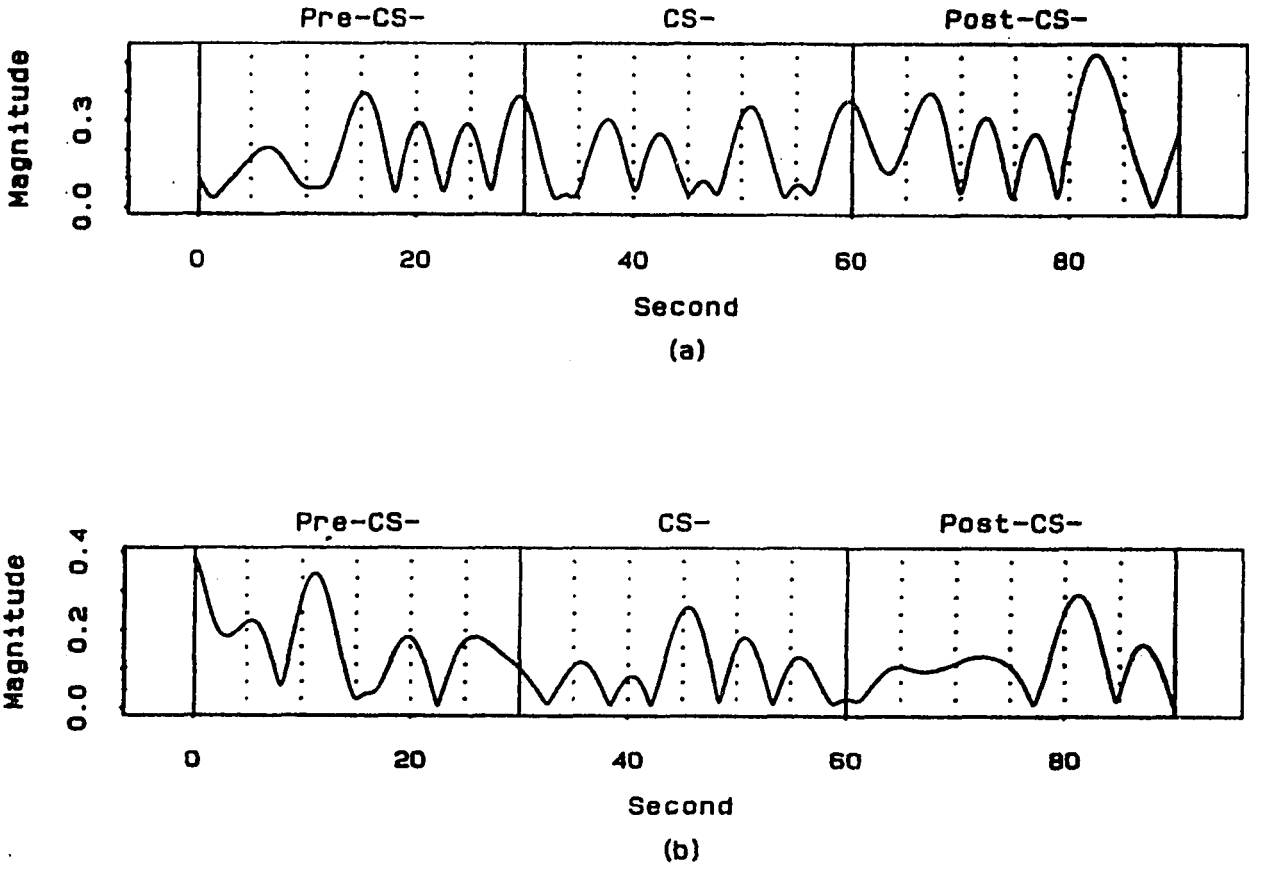

FIGURE 4.9 (a) THE LOW FREQUENCY MAGNITUDE RESULT OF DOG 3 UNDER CS- TRIAL 1.

(b) THE LOW FREQUENCY MAGNITUDE RESULT OF DOG 3 UNDER CS- TRIAL 2.

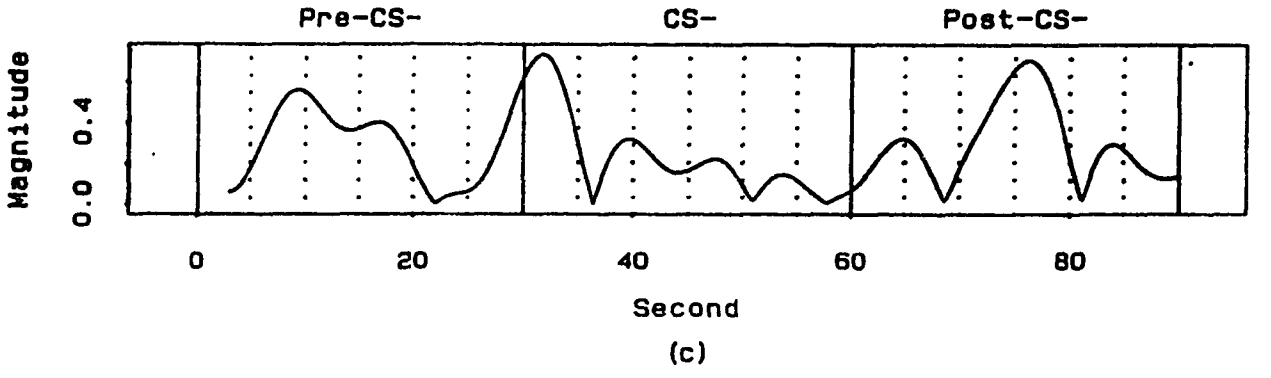

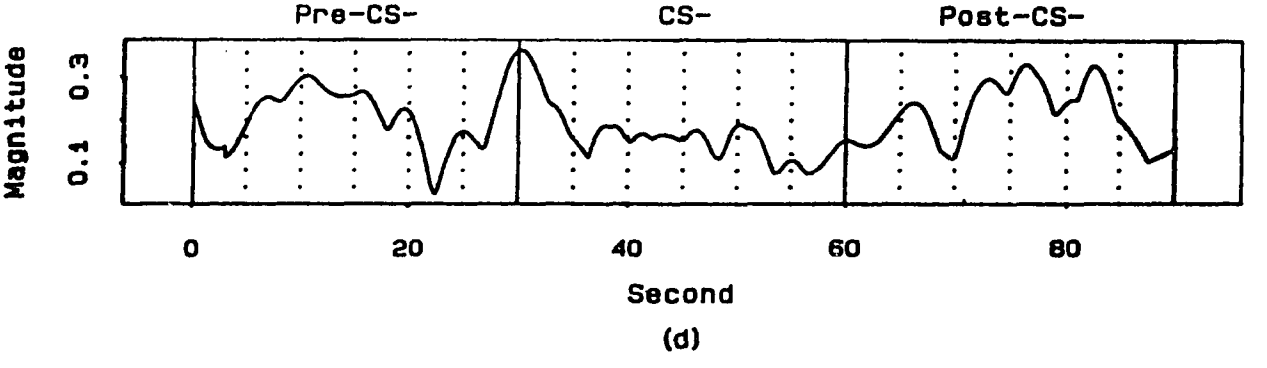

FIGURE 4.9 (c) THE LOW FREQUENCY MAGNITUDE RESULT OF DOG 3 UNDER CS- TRIAL 3.
(d) THE AVERAGE FROM (a) TO (c).

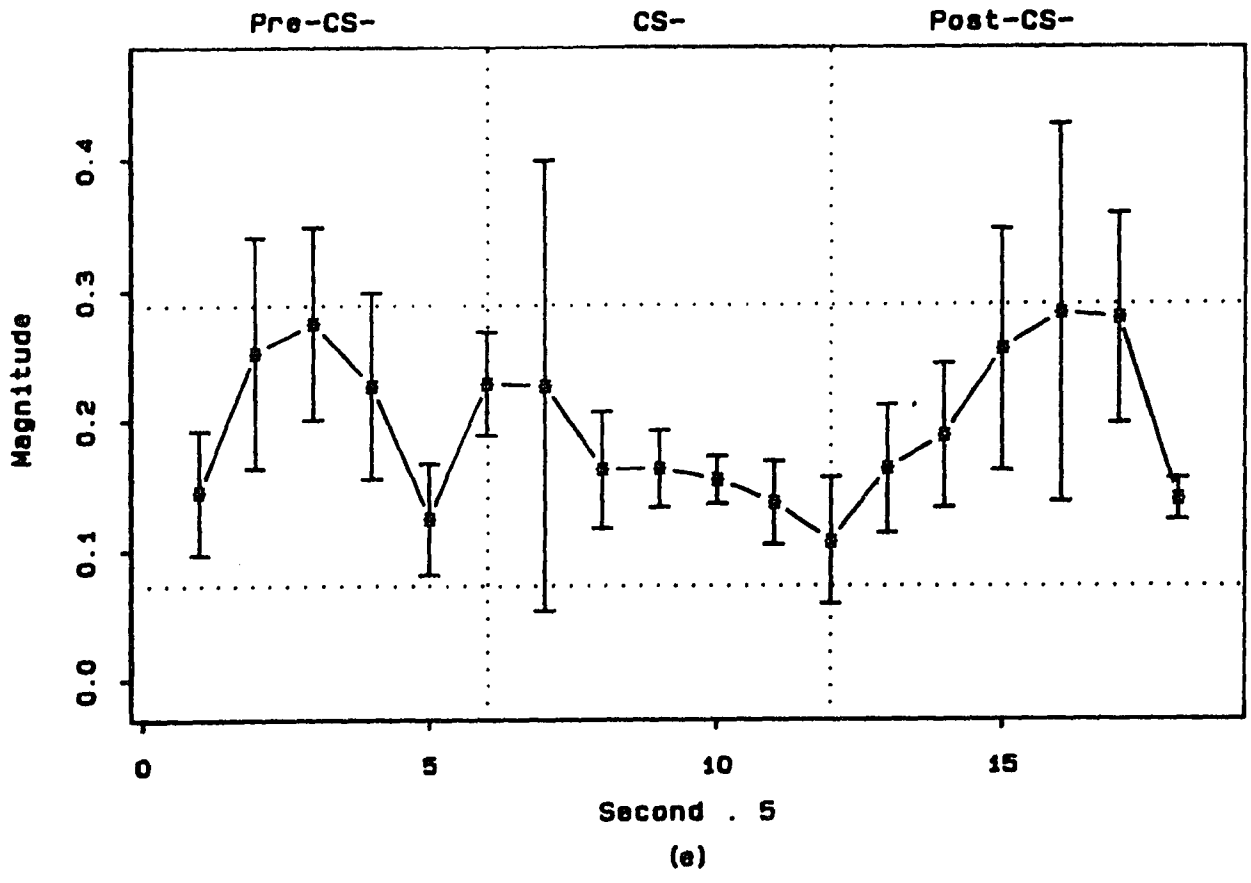

FIGURE 4.9 (e) THE 5-SECOND AVERAGE OF (d) WITH STANDARD ERROR AND 95% CONFIDENCE INTERVAL.

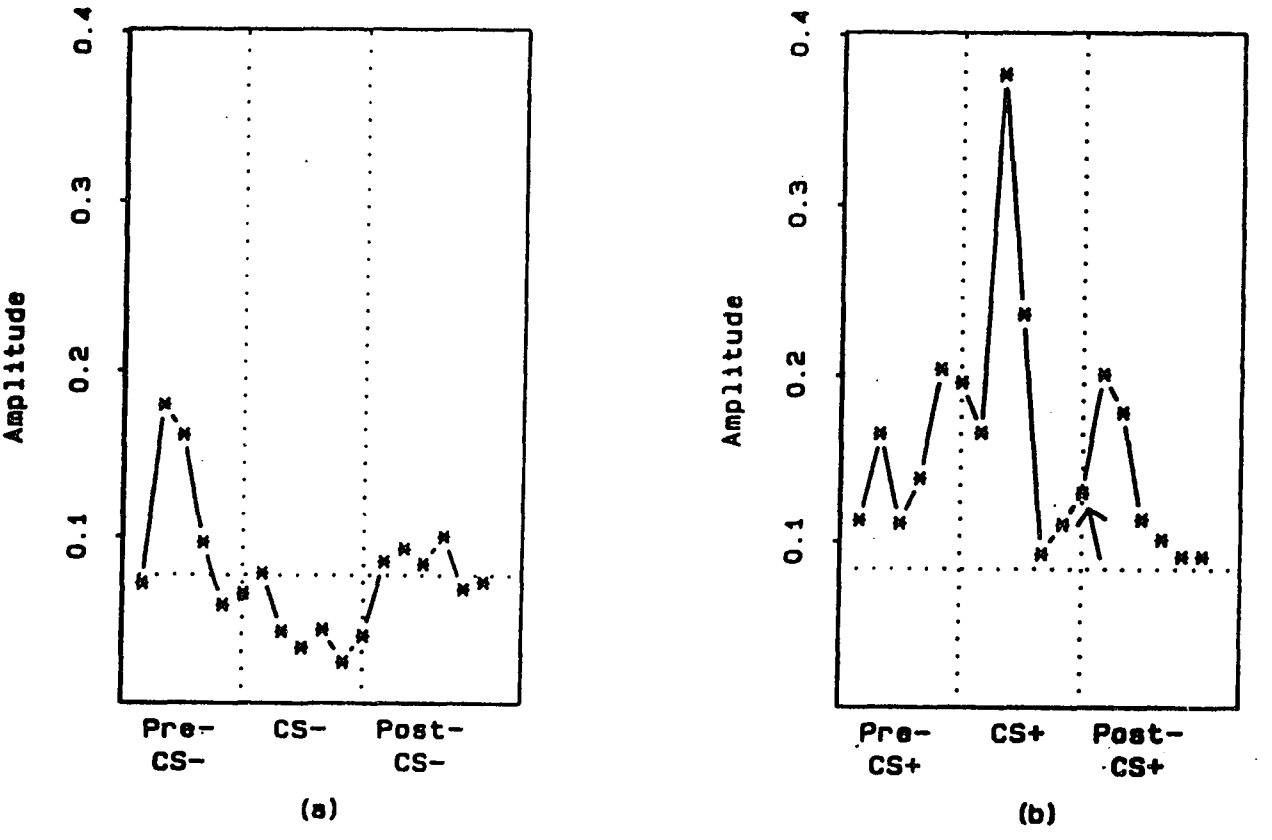

FIGURE 4.10 (a) THE 5-SECOND AVERAGE OF THE LOW FREQUENCY RESPONSE MAGNITUDE RESULT UNDER CS- TRIAL WITH A REFERENCE DOTTED LINE TAKEN FROM THE AVERAGE OF THE 30-SECOND DATA BEFORE PRE-CS-.

(b) THE 5-SECOND AVERAGE OF THE LOW FREQUENCY RESPONSE MAGNITUDE RESULT UNDER CS+ TRIAL WITH A REFERENCE DOTTED LINE TAKEN FROM THE AVERAGE OF THE 30-SECOND DATA BEFORE PRE-CS+.

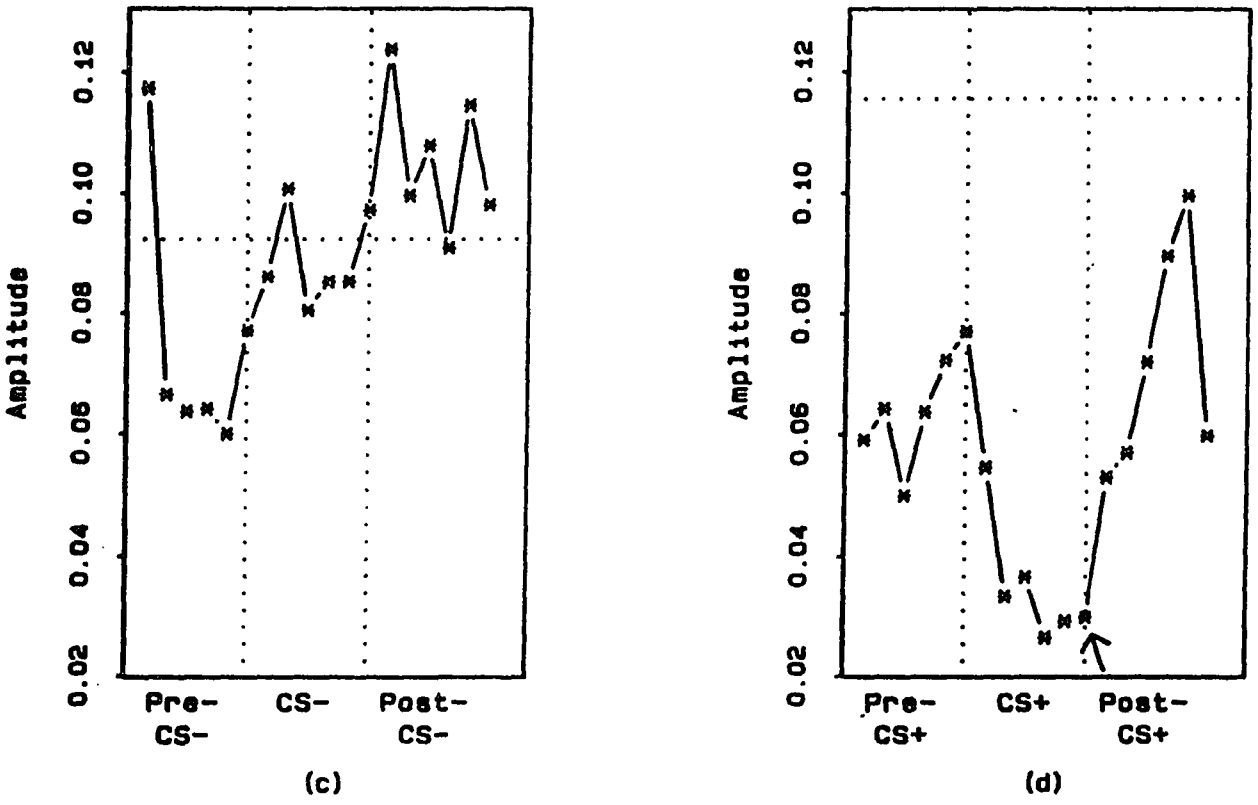

FIGURE 4.10 (c) THE 5-SECOND AVERAGE OF THE RESPIRATION FREQUENCY RESPONSE MAGNITUDE RESULT UNDER CS- TRIAL WITH A REFERENCE DOTTED LINE TAKEN FROM THE AVERAGE OF THE 30-SECOND DATA BEFORE PRE-CS-.

(d) THE 5-SECOND AVERAGE OF THE RESPIRATION FREQUENCY RESPONSE MAGNITUDE RESULT UNDER CS+ TRIAL WITH A REFERENCE DOTTED LINE TAKEN FROM THE AVERAGE OF THE 30-SECOND DATA BEFORE PRE-CS+.

increase of sympathetic activity and a decrease of parasympathetic activity.

(ii) For CS+, the low frequency response increased in the pre-CS+ period and CS+ period, while the respiration frequency response decreased in these two periods.

This suggests an increase of sympathetic activity and a decrease of parasympathetic activity in both the pre-CS+ and CS+ periods.

Comparing the graphs in Fig. 4.11, we can see that the respiration frequency response is higher than the reference dotted line but the pattern maintains a very stable state. This means the parasympathetic activity increased slightly with respect to the reference data but remains stable during the pre-REF, REF, and post-REF peiods. The low frequency response has almost the same pattern as the respiration frequency response except that it decreased at the end of the post-REF period. We conclude that the sympathetic activity also remains stable during the whole pre-REF, REF, and post-REF periods.

Fig. 4.12 shows the average heart rates corresponding to CS+, CS-, and REF trials. If we compare these average heart rates with the interpretation of the respiration frequency responses and the low frequency responses discussed above, we conclude that an increase in heart rate corresponds to a decrease of the parasympathetic activity, with a concomitant increase of sympathetic activity.

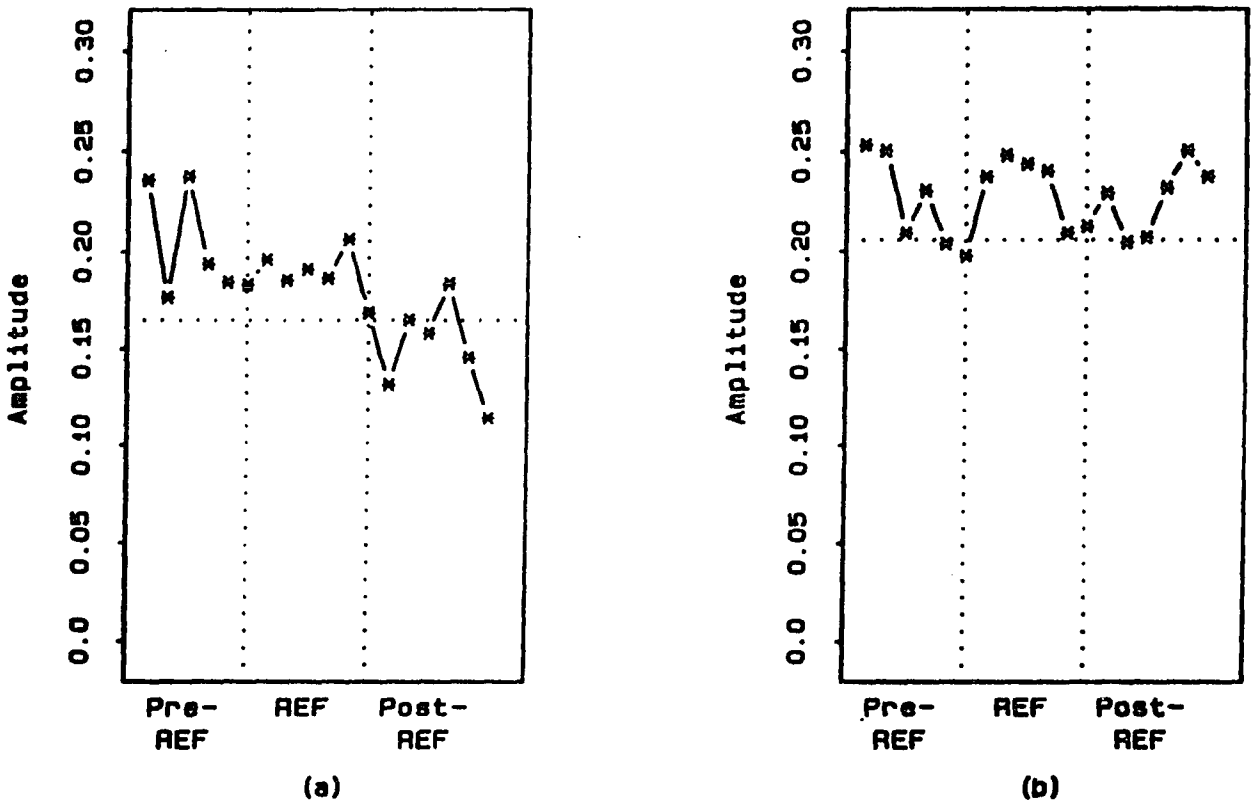

FIGURE 4.11 (a) THE 5-SECOND AVERAGE OF THE LOW FREQUENCY RESPONSE MAGNITUDE RESULT UNDER REF TRIAL WITH A REFERENCE DOTTED LINE TAKEN FROM THE AVERAGE OF THE 30-SECOND DATA BEFORE PRE-REF.

(b) THE 5-SECOND AVERAGE OF THE RESPIRATION FREQUENCY RESPONSE MAGNITUDE RESULT UNDER REF TRIAL WITH A REFERENCE DOTTED LINE TAKEN FROM THE AVERAGE OF THE 30-SECOND DATA BEFORE PRE-REF.

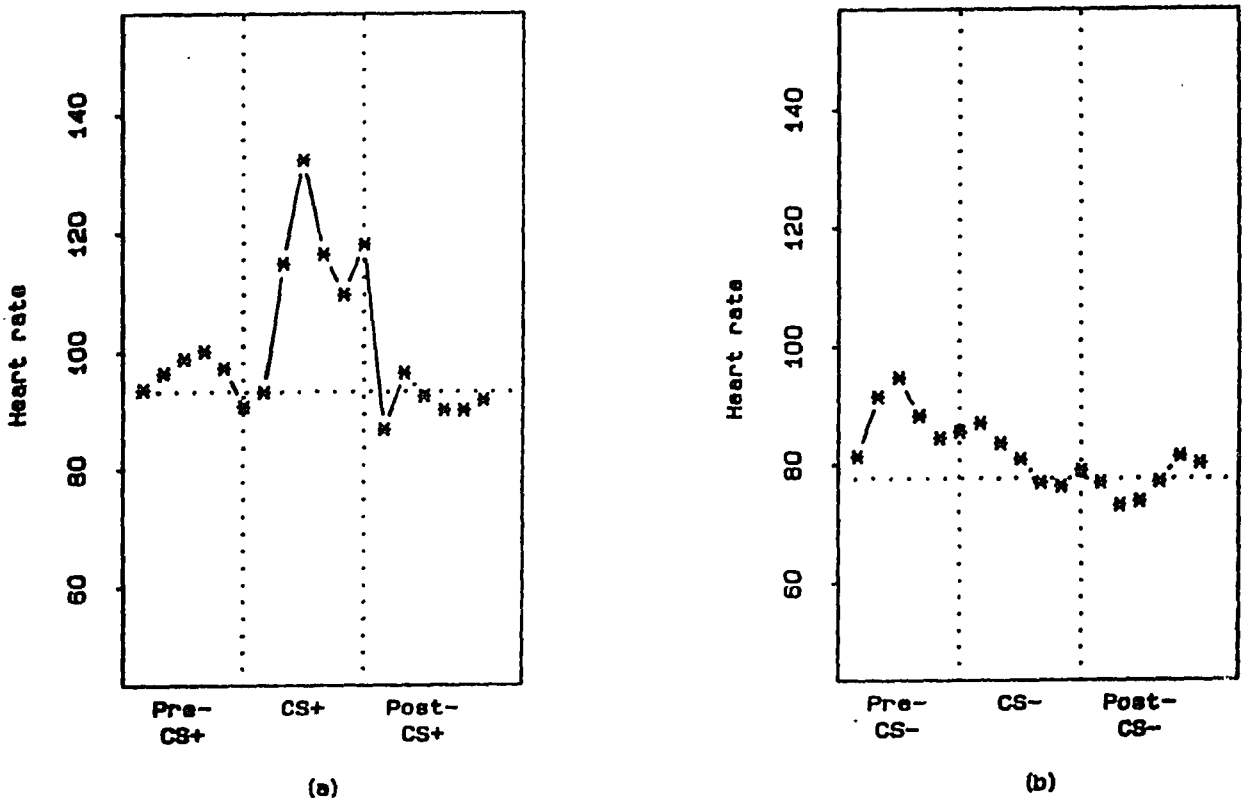

FIGURE 4.12 (a) THE AVERAGE HEART RATE UNDER CS+ TRIAL.
(b) THE AVERAGE HEART RATE UNDER CS- TRIAL.

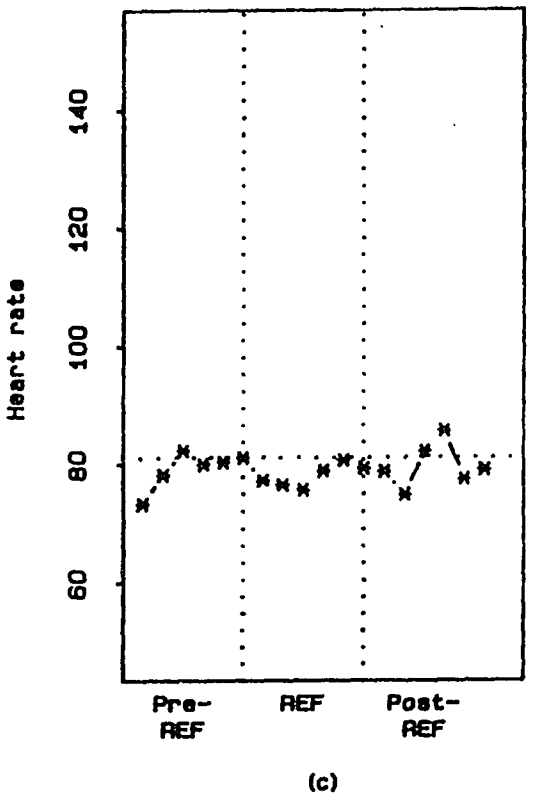

FIGURE 4.12 (c) THE AVERAGE HEART RATE UNDER REF TRIAL.

4-3 DISCUSSION OF RESULTS

For COND dogs, CS+ elicits a reliable sequence of autonomic responses with a consistent time course. The CS+ elicits a tachycardia which is due to an increase of sympathetic activity and a decrease of parasympathetic activity. When shock is delivered at the end of the CS+ period, a tachycardia is again elicited. In the post CS+ period, the sympathetic and the parasympathetic activity return to their normal states. Therefore, we expect the results from complex demodulation to show a decrease in the amplitude of the respiration frequency response (which is mediated by the parasympathetic nervous system) during the CS+ period and at the time when the shock is delivered. The amplitude of the respiration frequency response should then return to its normal level. In Fig. 4.2, and Fig. 4.10 (d), we can see that the amplitude of the respiration frequency response indeed decreased during the CS+ period and remains at its low state when the shock was delivered. It then returned to its normal state (the dotted line in each figure) in the post CS+ period as expected.

Since the low frequency response is mediated by both the sympathetic and parasympathetic nervous systems, the interpretation of the low frequency responses becomes complicated. An increase of low frequency response could be caused by an increase of parasympathetic activity or an

increase of sympathetic activity. However, during the CS+ period of the conditioning trials (see Fig. 4.2, Fig. 4.3 and Fig. 4.10 (b) and (d)), we found times when the amplitude of the low frequency response increased while the respiration frequency response decreased. We believe that these cases where the parasympathetic tone is clearly decreasing in the respiration frequency response while the low frequency response increases, reflect an increase of the sympathetic activity. This interpretation strongly indicates an increase of sympathetic activity that then returned toward normal activity until the shock was delivered. At the time of shock delivery, the amplitude of the low frequency response rises again and returns toward its normal activity in the post CS+ period as expected. Also, from Fig. 4.12 (a), the average heart rate increases in the CS+ period, and after it reached the maximum rate, it decreased until the shock was delivered.

This observation is important because it suggests that sympathetic and parasympathetic contributions to the low frequency peak can be separated procedurally. This means that other procedures (i.e. postural change, cold pressor test, etc.) that produce reciprocal vagal withdrawal and sympathetic activation should also allow us to separate these two components in the low frequency peak. Clearly, such a method would require a time domain view of results as provided by complex demodulation and with further

development such procedures might be extended to clinical applications.

CS- should not elicit any specific autonomic response. Therefore, the results from complex demodulation should show the amplitude of the low and respiration frequency responses randomly fluctuating around the reference line in the CS- and post CS- regions. From Fig. 4.4, Fig 4.5, and Fig. 4.10 (a) and (c), we see the respiration and low frequency responses fluctuating within or near the 95% confidence interval [or around the mean value (dotted line) in Fig. 4.10 (a) and (c)] as expected.

Suprisingly, Fig. 4.10 shows the amplitude of the respiration frequency response decreasing and the amplitude of the low frequency response increasing at the beginning of both pre CS+ and pre CS- regions, indicating a decrease in the activity of the parasympathetic nervous system and an increase in the activity of the sympathetic nervous system. Comparing with Fig. 4.12 (a) and (b), the average heart rates do increase at the beginning of the pre-CS+ and pre-CS- periods. Although these dogs were housed in a double sound-attenuated chamber during the trials, they still exhibited a specific behavior (as observed by a video camera) and increased heart rate when the pre-CSs began. This phenomenon could have been caused by the dogs knowing when the trial began by hearing the noises made by the recording pens of the chart recorder which started to move

at that time. Since the dogs didn't know whether the trial would be a CS+ or a CS- trial, they demonstrated increased arousal at the beginning of the trial.

For NCOND dogs, neither the CS+ or CS- tones predicted any event that would be expected to systematically alter the autonomic nervous system. Therefore, the dogs should ignore the tones and should not respond. From Fig. 4.6, Fig. 4.7, Fig. 4.8, Fig. 4.9, and Fig. 4.11 (a) and (b), we can see that amplitude variation of both respiration and low frequency responses fluctuated randomly within or near the 95% confidence interval (or around the reference lines in Fig 4.11).

4-4 GENERAL DISCUSSION

The respiration frequency magnitude variation of the complex demodulation reflects the activity of the parasympathetic nervous system, and the low frequency magnitude variation of the complex demodulation reflects the activities of both the parasympathetic and sympathetic nervous systems. By monitoring changes in respiration and low frequency responses, we can separately monitor the activities of the sympathetic and parasympathetic nervous systems in certain cases. For example, When the amplitude of the respiration frequency response decreases and low frequency response increases, we can say that the parasympathetic activity has decreased and the sympathetic

activity has increased. However, if the respiration frequency response increases and the low frequency response also increases, we can say that the parasympathetic activity has increased but the sympathetic activity is unknown.

The most important characteristics of the complex demodulation method are first, the ability to examine the dynamics of a system and second, the ability to separate different frequency bands in the time series. The spectral technique, on the other hand, allows us to examine the more steady state phenomena. A limitation of the complex demodulation technique is its inability to separate the effects of two peaks which are very close together in frequency due to practical limitations on the minimum width of the lowpass filter. This limitation is not seen to be a major one in our application since the frequency peaks of interest are far enough apart to be separated. It should be noted that some narrow bandwidth lowpass filters will produce large ripples in the passband and cause a smearing of the result. The choice of a Butterworth filter for this application produces a maximally flat amplitude approximation in the passband.

To increase the speed of processing, the data series can be decimated before complex demodulation which would cause very little information loss, since these data will be lowpass filtered during the process.

CHAPTER V

CONCLUSION

The complex demodulation method allows us to examine both divisions of the autonomic nervous system acting in concert without the use of drugs. It enables us to track changes of amplitude in the respiration frequency and low frequency responses as a function of time. The respiration frequency response reflects the activity of the parasympathetic nervous system, and the low frequency response reflects the activities of both the parasympathetic and sympathetic nervous systems. By monitoring changes in the respiration and low frequency responses, we can separately monitor the activities of the sympathetic and parasympathetic nervous systems under some circumstances.

The " biphasic " response of heart rate (heart rate accelerated and then decelerated) due to a conditioned stimulus (CS) paired with an unconditioned stimulus interval (CS+ paired with a shock in our experiment) has been reported by Turkkan and Kadden (39) for monkeys, and appears to be mediated mostly by vagal release followed by vagal restraint with some sympathetic contribution. Also, Dykman and Gantt (13) concluded that the heart rate acceleration in dogs in response to mild and moderate stimuli is dependent in large part upon a decrease in parasympathetic (vagal)

inhibition. Schoenfeld et al. (35) found that the initial increases in heart rate of monkeys during classical delay conditioning appeared to be the result of increased sympathetic activity and a concomitant decrease in the parasympathetic activity, and toward the end of the CS, an increase in the parasympathetic activity was indicated. They all used the pharmacological neural blockade method to draw their conclusions.

The biphasic heart rate response was also observed in our experiment during the CS+ trial of COND dogs. From the results of complex demodulation, the respiration frequency response at the beginning of the CS+ decreased, indicating the withdrawal of the parasympathetic activity; the low frequency response increased at the same time indicating the activation of the sympathetic activity because the parasympathetic activity is withdrawing. This information suggests that the increase of heart rate involves the withdrawal of the parasympathetic activity and the activation of the sympathetic activity.

Even though the autonomic nervous system is the primary control of the heart rate, the blood pressure and the respiration would also affect the heart rate through the autonomic nervous system as discussed in section 1-3, and Fig. 1.3 shows the simplified block diagram for the regulation of the heart rate. We repeat Fig. 1.3 here as Fig. 5.1.

Therefore, to examine the contribution of the blood pressure and respiration on affecting the two different divisions of the autonomic nervous system is very helpful in investigating the heart regulation, and can be considered as our future work.

To take blood pressure into account, a pneumatic cuff can be placed around the inferior vena cava of a dog, just above the diaphragm, that will cause a decrease in the blood pressure when the pneumatic cuff is inflated. A pneumatic cuff can also be placed at the descending aorta of a dog, that will cause an increase in the blood pressure when the cuff is inflated.

To consider the effect of respiration rate, humans should be used since it is hard to control a dog's respiration rate. We have already performed this kind of experiment at the East Orange VA medical center on five normal subjects (3 male, 2 female) with ages ranging from 22 to 33 years. The ECG and respiration signals were recorded every day at the same time of day with a constant respiration rate set by a metronome. The power spectra of the heart rate variability signal were calculated and compared by using a correlation method. It was found that the power spectrum of HRV from one person is not usually highly correlated with the pattern of the others.

It is also worthwhile to design the hardware and software so that an IBM PC can be used to acquire signals

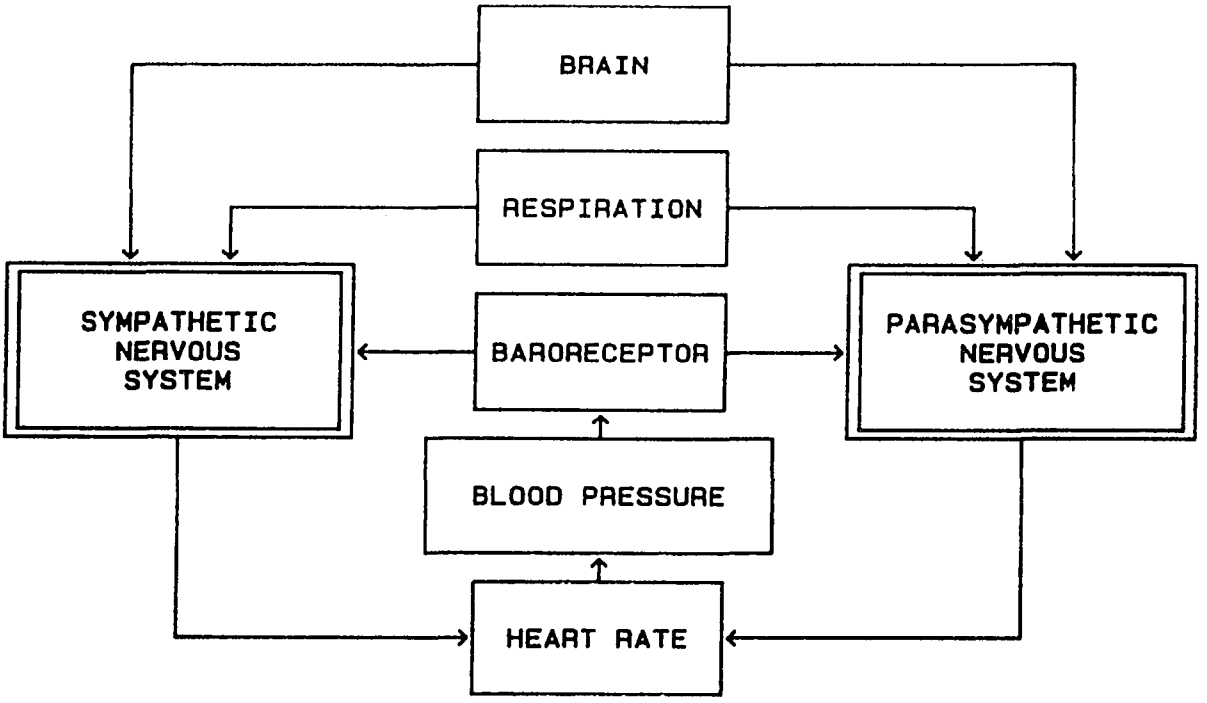

FIGURE 5.1 A SIMPLIFIED BLOCK DIAGRAM WHICH DESCRIBES THE REGULATION OF THE HEART RATE.

and to analyze them in real time by using complex demodulation, which would have important advantages such as the reduction of human error and the tedium involved in the long processing procedure.

When the complex demodulation process is used as a non-invasive method to investigate the activities of the sympathetic and parasympathetic nervous systems, there are some conditions which exist that cause decisions to be difficult to make. For example, when the amplitudes of both the respiration frequency and the low frequency responses rise or fall at the same time, the information about the sympathetic activity is buried in the parasympathetic activity and becomes very hard to assess. Usually, we assume that the heart rate is regulated under the reciprocal effect of the two divisions of the autonomic nervous system. To verify how true the assumption is, more complex demodulation on normal HRV signals is needed.

REFERENCES

1. Akselrod, S., D. Gordon, F. A. Ubel, D. C. Shannon, A. C. Barger, and R. J. Cohen, "Power Spectrum Analysis of Heart Fluctuation: A Quantitative Probe of Beat-to-Beat Cardiovascular Control", Science 213:220-222, 1981
2. Baker, L. E., T. W. Conlter, and J. D. Bourland, "Simple Versatile Instrument for Measuring Impedance Changes Accompanying Physiological Events", Medical and Biological Engineering, March, 1973. pp. 221-229
3. Berne, R. M. and M. V. Levy, Cardiovascular Physiology, Fifth Edition, The C. V. Mosby Company
4. Bloomfield, P., Fourier Analysis of Time Series: An Introduction, John Wiley & Sons
5. Burden, R. L., J. D. Faires, A. C. Reynolds, Numerical Analysis, Prindle, Weber & Schmidt
6. Chess, G. F., R. M. K. Tam, and F. R. Calresu, "Influence of Cardiac Neural Inputs on Rhythmic Variations of Heart Period in the Cat", Am. J. Physiol. 228:775-780, 1975
7. Cleveland, W. S., "Robust, Locally-weighted Regression and Smoothing Scatterplots", J. Am. Stat. Assoc. 74:829-836, 1979
8. Cohen, D. H. and D. C. Randall, "Classical Conditioning of Cardiovascular response", Am. Rev. Physiol. 46:187-197, 1984
9. Cooper, J. R., F. E. Bloom, R. H. Roth, The Biochemical

Basis of Neuropharmacology. Second Edition, Oxford University Press, Inc.

10. Cruz, Frank da, "KERMIT USER GUIDE, Sixth Edition, Revision 1", Columbia University Center for Computing Activities, New York, New York 10027, June, 1985
11. de Boer, R. W., J. M. Karemaker, J. Strackee, "Comparing Spectra of a Series of Point Events Particularly for Heart Rate Variability Data", IEEE Trans. Biomed. Eng.,Vol. BME-31, pp. 384-387, April 1984
12. de Boer, R. W., J. M. Karemaker, J. Strackee, "Description of Heart-Rate Variability Data in Accordance With a Physiological Model for the Genesis of Heartbeats", Psychophysiology, Vol. 22, No. 2, 147-155, March, 1985
13. Dykman, R. A., W. H. Gantt, "The Parasympathetic Component of Unlearned and Acquired Cardiac Responses", Journal of Comparative and Physiological Psychology. Vol. 52, No. 2, April 1959. 163-167
14. Federici, A., A. Rizzo, and A. Cevese, "Role of the autonomic nervous system in the control of heart rate and blood pressure in the defence reaction in conscious dogs", Journal of the Autonomic Nervous System, 12 (1985), 333-345
15. Fredericks, A., J. W. Moore, F. U. Metcalf, J. S. Schwaber, and N. Schneiderman, (1974) "Selective Autonomic Blockade of Conditioned and Unconditioned Heart Rate Changes in Rabbits", Pharmacology Biochemistry and

Behavior, Vol. 2, PP 493-501

16. Fitzgerald, R. D., G. K. Martin, and J. H. O'brien, "Influence of Vagal Activity on Classically Conditioned Heart Rate in Rats", Journal of Comparative and Physiological Psychology, 1973, Vol.83, No.3 485-491

17. Furukawa, Y., and M. N. Levy, "Temporal Changes in the Sympathetic-Parasympathetic Interactions that Occur in the Perfused Canine Atrium", Circulation Research, Vol. 55, No. 6, December 1984. 835-841

18. Ganong, W. F., Review of Medical Physiology, Lange Medical Publications

19. Hatch, J. P., K. Klatt, S. W. Porges, L. Schroeder-Jasheway and J. D. Supik."The Relation Between the Rhythmic Cardiovascular Variability and Reactivity to Orthostatic, Cognitive, and Cold Pressor Stress". Psychophysiology, 23:48-56, 1986

20. Hatton, D. C., Buchholz, R. A., and Fitzgerald, R. D., (1981) "Autonomic Control of Heart Rate and Blood Pressure in Spontaneously Hypertensive Rats During Aversive Classical Conditioning", Journal of Comparative and Physiological Psychology, Vol.95, 978-990

21. Hays, W. L., and R. L. Winkler, Statistics, Volume1, Probability, Inference, and Decision, Holt, Rinehart and Winston, Inc.

22. Hoffman, J. W., and Fitzgerald, R. D., (1978) "Classically Conditioned Heart Rate and Blood Pressure

in Rats Based on Either Electric Shock or Ammonia Fumes Reinforcement", Physilogy and Behavior, 21, 735-741

23. Johnson, A. T., "Filter Design Program (4.2)", The University of Maryland Remote site at Darlington, Maryland.

24. Katcher, A. H., R. L. Solomon, L. H. Turner, V. LoLordo, J. B. Overmier, and R. A. Rescorla, "Heart Rate and Blood Pressure Responses to Signaled and Unsignaled Shocks: Effects of Cardiac Sympathectomy", Journal of Comparative and Physiology Psychology, 1968, Vol. 68, No. 2, 163-174

25. Kazis, E., W. L. Milligan, and D. A. Powell,"Autonomic-Somatic Relationships: Blockade of Heart Rate and Corneo-Retinal Potential Responses", Journal of Comparative and Physiological Psychology, 1973 Vol. 84 No. 1, 98-110

26. Kitney, R. I., O. Rompelman. "Signal Analysis of Heart Rate Variability. in The Study of Heart Rate Variability", Eds. Oxford, England: Clarendon, 1980, pp. 27-58

27. Klose, K. J., J. S. Augenstein, N. Schneiderman, K. Manas, B. Abrams and L. J. Bloom, "Selective Autonomic Blockade of Conditioned and Unconditioned Cardiovascular Changes in Rhesus Monkeys (Macaca Mulatta)", Journal of Comparative and Physiological Psychology,

1975, Vol. 89, No. 7, 810-818

28. Luczak, H. and W. Lanrig, "An Analysis of Heart Rate Variability", Ergonomics, 1973, Vol. 16, No. 1, 85-97

29. McCabe, P. M., Yongue, B. G., Porges, S. W., & Ackles, P. K. (1984), "Changes in Heart Period, Heart Period Variability and a Spectral Analysis Estimate of Respiratory Sinus Arrhythmia During Aortic Nerve Stimulation in Rabbits", Psychophysiology, 21, 149-158

30. Pomeranz, B., R. J. B. Macaulay, M. A. Caudill, I. Kutz, D. Adam, D. Gordon, K. M. Kilborn, A. C. Barger, D. C. Shannon, R. J. Cohen, H. Benson, "Assessment of Autonomic function in Humans by Heart Rate Spectral Analysis", The Ame. Physiol. Society, 0363-6135/85 H151-H153

31. Porges, S. W., McCabe, P. M., & Yongue, B. G. (1982), "Respiratory-Heart Rate Interaction: Psychophysiological Implications for Pathophysiology and Behavior", In J. J. Cacioppo & R. E. Petty (Eds.), Perspectives in Cardiovascular Psychophysiology, pp. 223-264, New York: Guilford.

32. Randall, D., C. M. Cottrill, E. P. Todd, M. A. Price, and C. C. Wachtel, "Cariac Output and Blood Flow Distribution During Rest and Classical Aversive Conditioning in Monkey", Am. J. Physil. 1982, Vol. 19 No. 5, 490-497

33. Reisman, S. S. and W. N. Tapp. "A Variable Threshold

Adaptive R-wave Detector", Physiol. Behav. 35:111-115, 1985

34. Sayers, B. McA., "Analysis of Heart Rate Variability", Ergonomics

35. Schoenfeld, W. N., R. M. Kadden, P. J. Tremont, M. R. McCullough and W. A. Steele, "Effects of Pharmacological Autonomic Blockade upon Cardiac Rate and Blood Pressure Conditioned and Unconditioned Responses in Macaca Mulatta", Journal of the Autonomic Nervous System, 2(1980) 365-375

36. Snapper, A. G., Western Michigan University, G. Inglis, University of Rochester, "SKED SOFTWARE SYSTEM, SKED USERS GROUP", Psychology Department, Western Michigan University, Kalamazoo, Michigan 49008

37. Tompkins, W. J., J. G. Webster, Design of Microcomputer Based Medical Instrumentation, Prentice-Hall, Inc. Englewood Cliffs, New Jersey

38. Tukey, J. W. and R. B. Blackman, The Measurement of Power Spectra. From the Point of View of Communications Engineering, Dover Publications, Inc. New York

39. Turkkan, J. S., and R. M. Kadden, "Classically Conditioned Heart Rate Response in Macaca Mulatta after Beta-Adrenergic, Vagal and Ganglionic Blockade", Journal of the Autonomic Nervous System, 1, 1979, 211-227

40. Warner, H. R. and A. Cox, J. Appl. Physiol. 17a 349

1962

41. Yehle, A., Dauth, G., and Schneiderman, N., "Correlates of Heart-Rate Classical Conditioning in Curarized Rabbits", Journal of Comparative and Physiological Psychology, 1967, 64, 98-104

42. Yongue, B. G., McCabe, P. M., Porges, S. W., Rivera, M. E., Kelly, S. L., & Ackles, P. K. (1982), "The Effects of Pharmacological Manipulations that Influence Vagal Control of the Heart on Heart Period, Heart Period Variability and Respiration in Rats", Psychophysiology, 19, 426-432

APPENDIX A

The signal acquisition circuit consists of two parts: the excitation circuit and the pick-up circuit. The excitation circuit provides a 3 ma. peak, 50K Hz sinusoidal current to the subject. The pick-up circuit simultaneously picks up the ECG signal and the modulated respiration signal from the subject, separates them, and produces separate outputs consisting of the filtered ECG signal and the demodulated respiration signal. Figure A.1 is the schematic of this signal acquisition circuit. The component values are listed in TABLE A.1.

A-1 DESCRIPTION OF THE SIGNAL ACQUISITION CIRCUIT

In the excitation circuit, IC1 generates a 50 K Hz sine wave with peak values $\pm$1.32 V, and then feeds this sine wave into the base of TR1. TR1 is a common-emitter amplifier with an emitter resistor R8. This amplifier has a very large AC load impedance Z_1 at 50K Hz, which is the resonant frequency.

The voltage gain of this amplifier at 50K Hz is

$$A_v = - Z_1' / R8$$

where $Z_1' = Z_1 \,||\, Z_{in}$

and Z_{in} is the impedance across the excite electrodes. Typically Z_{in} = 250 ohms.

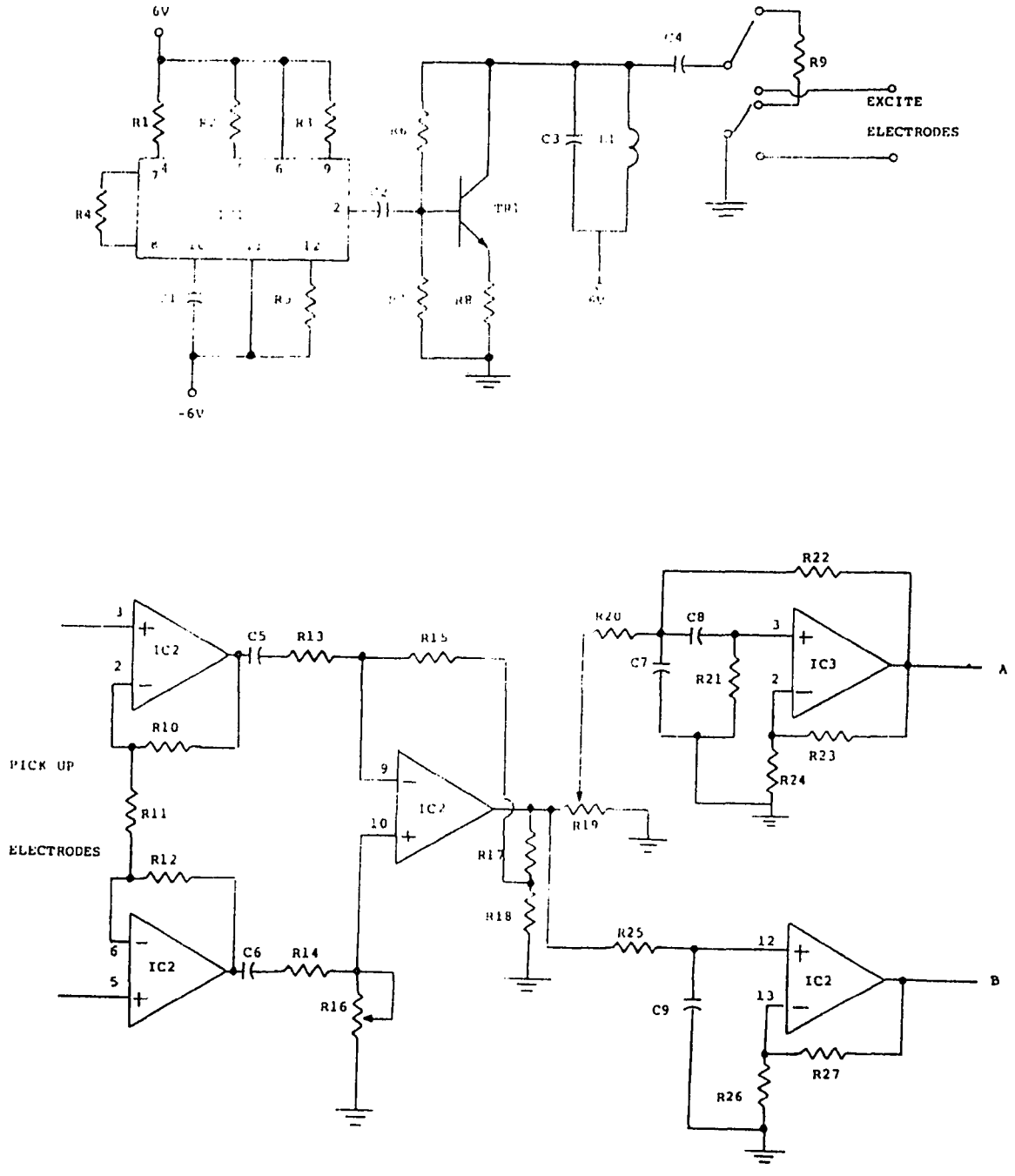

FIGURE A .1 THE CIRCUITRY OF THE SIGNAL ACQUISITION SYSTEM

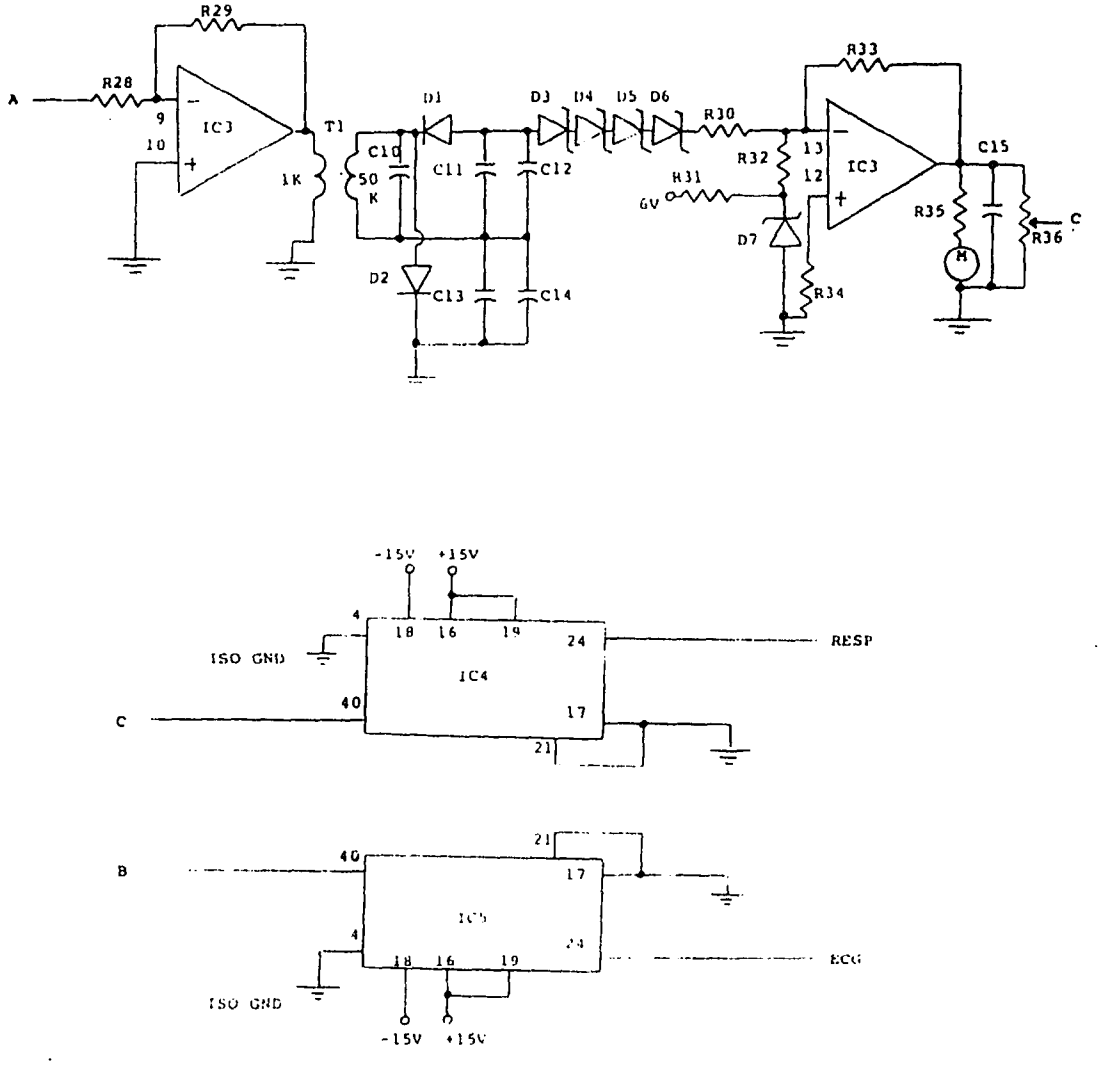

FIGURE A .1 THE CIRCUITRY OF THE SIGNAL ACQUISITION SYSTEM

Therefore, Z_1' is approximately equal to 250 ohms, and A_V is approximately equal to -0.54, and the typical current passing through the excite electrodes is about 3 ma.. If the impedance across the excite electrodes changes because of the movement of inspiration and expiration, A_V changes, so output voltage waveform amplitude changes. From the current point of view, this circuit supplies a constant 50K Hz, AC current to the excite electrodes, and the voltage across the excite electrodes changes when the impedance across the excite electrodes changes due to the inspiration and expiration. Therefore, a modulated respiration signal can be acquired. R9 is used to pass the DC charging current at the moment when the power is turned on. Without R9, a current of about 24 ma. passes through the subject at the time when the power is turned on and C4 is charged up. This current would be felt like a shock to the subject.

In the pick-up circuit, the 3/4 IC2, R10 to R18, and C5, C6 form a difference amplifier with a very high imput impedance and the gain of approximately 25. Then the circuit splits into two parts: 1/4 IC3, R19 to R24, and C7, C8 form a bandpass filter centered at 50K Hz to pass the modulated respiration signal; 1/4 IC2, R21 to R27, and C9 form a lowpass filter to pass the ECG signal. C10 to C14, D1, and D2 form a conventional voltage doubling circuit which rectifys the input modulated signal and demodulates the signal down to low frequency range. D3 to D6 are four 15-

volt zener diodes which drop 60 Volts DC from the demodulated signal. 1/4 IC3, R30 to R36, C15 and D7 form a subtraction ciruit which subtracts the input signal from a fixed reference value determined by the drop across the zener diode D7. R19 is a pot which is used to adjust the input modulated respiration signal so that the output demodulated respiration across R36 contains no DC component, which can be observed from the ammeter below R35. R36 is a pot used to adjust the range of the output demodulated respiration signal within -5 to +5 Volts which is the range of the A/D converter. Finally, the ECG signal and the demodulated respiration signal pass through the isolation circuits IC4 and IC5, and then appear at the output. The isolation circuit is used here because the output signals will be recorded on tape which is powered with an AC source. Without this isolation circuit, the AC source from the tape recorder may feed into the pick-up circuit and hurt the subject.

A-2 DESCRIPTION OF THE A / D CONVERTER CIRCUIT

Figure A.2 is the circuitry of the A/D converter. The values of components are listed in TABLE A.2.

The A/D converter converts an analog signal in the range from -5 Volts to +5 Volts into 12-bit digital value. Also, the A/D converter is so designed that it starts to convert when the PDP-8 computer gets the first R-wave pulse.

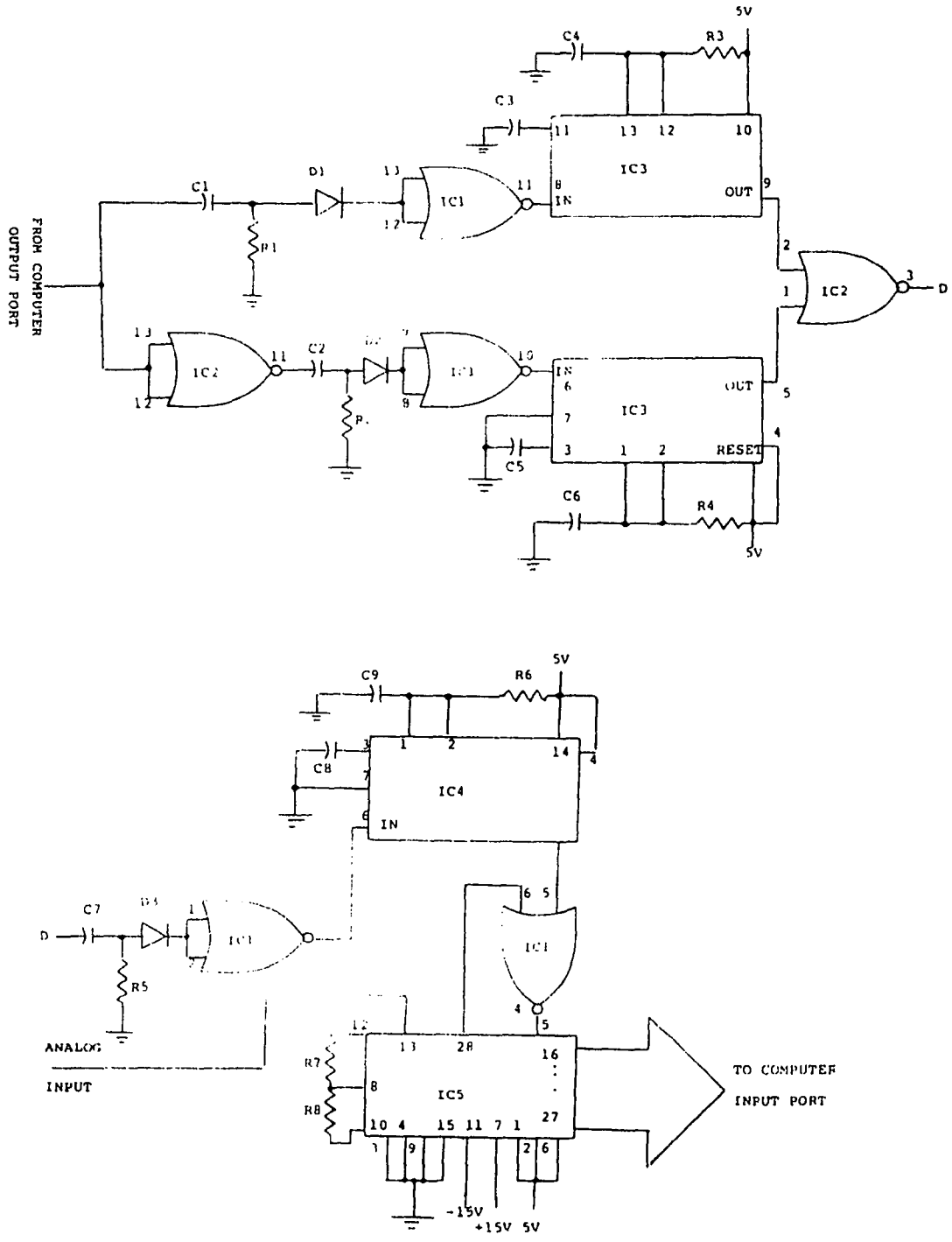

FIGURE A.2 THE CIRCUITRY OF THE 12-BIT A/D CONVERTER.

The signal sent from PDP-8 computer to this A/D converter for conversion triggering is a 5 Hz, 50 % duty cycle square wave, but a sampling rate of 10 Hz is desired. Therefore, IC1 to IC4, C1 to C9, R1 to R6 form a circuit to convert the 5 Hz input square wave into a 10 Hz square wave. IC5, R7 and R8 form a circuit to sample the analog input signal with a 10 Hz sampling rate.

TABLE A.1

COMPONENT VALUES

Resistors

R1	5K	Ohms	R19	20K	Ohms
R2	5K	Ohms	R20	33K	Ohms
R3	10K	Ohms	R21	10K	Ohms
R4	5K	Ohms	R22	11K	Ohms
R5	82K	Ohms	R23	56K	Ohms
R6	10K	Ohms	R24	56K	Ohms
R7	10K	Ohms	R25	16K	Ohms
R8	460	Ohms	R26	20K	Ohms
R9	2.2K	Ohms	R27	82K	Ohms
R10	120K	Ohms	R28	7.5K	Ohms
R11	10K	Ohms	R29	75K	Ohms
R12	120K	Ohms	R30	200K	Ohms
R13	680K	Ohms	R31	8.2K	Ohms
R14	680K	Ohms	R32	200K	Ohms
R15	680K	Ohms	R33	470K	Ohms
R16	1M	Ohms	R34	100K	Ohms
R17	82K	Ohms	R35	62K	Ohms
R18	4.3K	Ohms	R36	10K	Ohms

Capacitors

C1	0.001	Microfarad	C9	0.01	Microfarad
C2	0.063	Microfarad	C10	82	Picofarad
C3	0.004	Microfarad	C11	0.1	Microfarad
C4	100	Microfarad	C12	0.1	Microfarad
C5	470	Nanofarad	C13	0.1	Microfarad
C6	470	Nanofarad	C14	0.1	Microfarad
C7	220	Picofarad	C15	0.22	Microfarad
C8	220	Picofarad			

Inductor

L1	2.5	Milihenry

Diodes

D1	IN914	D5	15 v Zener
D2	IN914	D6	15 v Zener
D3	15 v Zener	D7	5 v Zener
D4	15 v Zener		

Transformer

T1	SP-5 1K-50K

Transistor

TR1	2N2222

Integrated Circuits

IC1	ICL8038	IC4	AD293
IC2	LM7641	IC5	AD293
IC3	LM7641		

Meter

M	Milliammeter

TABLE A.2

COMPONENT VALUES

Resistors

R1	1.5K	Ohms	R5	1.5K	Ohms
R2	1.5K	Ohms	R6	10K	Ohms
R3	10K	Ohms	R7	47	Ohms
R4	10K	Ohms	R8	47	Ohms

Capacitors

C1	0.01	Microfarad	C6	0.001	Microfarad
C2	0.01	Microfarad	C7	0.001	Microfarad
C3	0.01	Microfarad	C8	0.01	Microfarad
C4	0.001	Microfarad	C9	0.001	Microfarad
C5	0.01	Microfarad			

Diodes

D1	IN914	D3	IN914
D2	IN914		

Integrated Circuits

IC1	CD4001	IC4	LM556
IC2	CD4001	IC5	AD574
IC3	LM556		

APPENDIX B

In order to transfer data from the PDP-8 computer to the PDP-11 computer, and then from the PDP-11 computer to the VAX 11/750 computer, we first used keyboard and screen from the PDP-8 computer to run Kermit on the PDP-8 computer. Then we connected to the PDP-11 computer through the serial ports from the same keyboard and screen of the PDP-8 computer, and ran Kermit on the PDP-11 computer. We then returned to the PDP-8 computer, and sent data files to the PDP-11 computer. Once the data files had been sent, we exited from Kermit on the PDP-11 computer, and escaped back to the PDP-8 computer. Using the same procedure, we transfered data files from the PDP-11 computer to the VAX 11/750 computer. The following commands were used while transfering data files:

From the PDP-8 computer terminal,

```
R KERMIT                        # GET INTO KERMIT ON PDP-8
KERMIT-8 >                      # INDICATE THE PDP-8 KERMIT
                                # IS READY
KERMIT-8 > CONNECT              # CONNECT TO PDP-11
> LOG KERMIT/KERMIT             # LOG IN PDP-11 KERMIT DIR.
Kermit -11 >                    # INDICATE THE PDP-11 KERMIT
Kermit -11 > server             # " RECEIVE " COMMAND
Control \ c                     # ESCAPE BACK TO PDP-8
KERMIT-8 > SEND FILENAME        # SEND DATA FILE FROM PDP-8
```

```
                                    # TO PDP-11
KERMIT-8 > BYE                      # SHUT OFF  " RECEIVE " MODE
                                    # IN PDP-11
KERMIT-8 > CONNECT                  # CONNECT TO PDP-11 AGAIN
Kermit -11 > SET LINE TT3:          # SET THE TRANSMISSION LINE
Kermit 11 > connect                 # CONNECT TO VAX 11/750
Login: password                     # LOGIN VAX 11/750
% kermit                            # RUN KERMIT IN VAX 11/750
c -kermit >                         # INDICATE VAX 11/750 KERMIT
                                    # IS READY
c -kermit > server                  # " RECEIVE " COMMAND
Control \ c                         # ESCAPE BACK TO PDP-11
Kermit -11 > send filename          # SEND DATA FILE FROM PDP-11
                                    # TO VAX 11/750
Kermit -11 > finish                 # SHUT OFF " RECEIVE " MODE
                                    # IN VAX 11/750
Kermit -11 > connect                # CONNECT TO VAX 11/750 AGAIN
c -kermit > ex                      # EXIT FROM KERMIT IN
                                    # VAX 11/750
% logoff                            # LOGOFF FROM VAX 11/750
Control \ c                         # ESCAPE BACK TO PDP-11
Kermit -11 > ex                     # EXIT FROM KERMIT IN PDP-11
> logoff                            # LOGOFF FROM PDP-11
Control \ c                         # ESCAPE BACK TO PDP-8
KERMIT-8 > EX                       # EXIT FROM KERMIT IN PDP-8
```

APPENDIX C

```
c-------------------------------------------------------------c
c                                                             c
c     demobu:   demodulation monitor - main program for       c
c               complex demodulation                          c
c                                                             c
c      note:  data should be detrended prior to               c
c               demodulation (e.g. with LOWESS in S of        c
c               VAX 11/750) to remove the power very near     c
c               frequency 0                                   c
c                                                             c
c-------------------------------------------------------------c
c
      real x(32768), d1(32768), d2(32768), y(60)
      real omega
      real sum, mean
      real twopi
      real num
      integer n, nd, n1
      integer ierr, iquery
      integer start, step
      character *40 name, magname, phasename, filname
      character *1 ans
c
c input data series
c
      write(6,'(t20,"input ",$)')
      read(5,*) name
c
c store result magnitude to which file
c
      write(6,'(t20,"output magnitude to ",$)')
      read(5,*) magname
c
c store result phase to which file
c
      write(6,'(t20,"output phase to ",$)')
      read(5,*) phasename
c
c complex demodulation at period T = np/nf which
c np = # of points for FFT, such as 512, 1024 ...
c nf = which point from FFT where you want to
c      complex demodulate at
c example : nom = T = 4096/30
c
      write(6,'(t20,"demodulate at period ",$)')
      read(5,*) nom
c
c # of points to be flipped over for both ends of data
c series before lowpass filtering
```

```
c
      write(6,'(t20,"How many points to be flipped over for
     * each side ",$)')
      read(5,*) n1
c
c input coefficient filename for lowpass filter
c
      write(6,'(t20,"filter coefficients filename ",$)')
      read(5,*) filname
c
c decimation the output ?
c
      write(6,'(t20,"decimate? ",$)')
      read(5,*) ans
      if (ans.eq."y") then
           write(6,'(t20,"decimate at what steps ",$)')
           read(5,*) step
      else
           step = 1
      end if
c
c compute omega - the demodulation frequency in radians
c
      twopi = 8.0 * atan(1.0)
      omega = twopi * ( 1.0 / num )
c
c write label
c
      write(6,'(28(/),t10,"COMPLEX DEMODULATION",/,t15,
     * "demodulating ", a40,/,t15,"at freq ',f15.8,///)
     * name, omega
c
c input coefficients for lowpass filter through
c subroutine datin
c
      iquery = 1
      call datin( filname, y, nd, sum, mean, ierr, iquery)
      if ( ierr.gt.0 ) then
      write(6,'(/,t20,"error return from datin filter
     * coefficient ")')
      stop
      else
      continue
      endif
c
c input data series through subroutine datin
c
      iquery = 1
      call datin (name, x, n, sum, mean, ierr, iquery)
      if ( ierr.gt.0 ) then
           write(6,'(/,t20,"error return from datin ")')
           stop
```

```
      else
      continue
      endif
c
c remove DC from data input series
c
      do 10 i = 1,n
      x(i) = x(i) - mean
 10   continue
c
cdemodulate data and return real part in d1 & imaginary
c part in d2 through subroutine demod
c
      call demod (x, n, omega, d1, d2)
c
c flip over data at both ends and lowpass filtering the
c real part and imaginary part forward and backward to
c cancel out phase shift of the lowpass filtering through
c suboutine filo
c
      call filo (d1, x, n, y, nd, n1)
      call filo (d2, x, n, y, nd, n1)
c
c recover magnitude and phase through subroutine polar
c
      call polar(d1, d2, n)
c
c set decimation factor for output
c
      start = step
      iquery = 0
c
c write out magnitude and phase to assigned filenames
c through subroutine datout
c
      call datout(magname,d1,start,n,step,ierr,iquery)
      if (ierr.eq.0) write(6,'(t20,a40,"written")')magname
      call datout(phasename,d2,start,n,step,ierr,iquery)
      if (ierr.eq.0) write(6,'(t20,a40,"written")')phasename
c
c
      end
```

```
c-------------------------------------------------------------c
c                                                             c
c     filop : a subroutine to flip over the data in both      c
c             ends and then pass the flip-overed data         c
c             series through a lowpass filter forward and     c
c             backward to cancel out the phase shift          c
c             caused by filter                                c
c                                                             c
c-------------------------------------------------------------c
c
      subroutine filo (x,y,n,y1,nd,n1)
c
      read x(32768), y(32768), y1(60)
      integer n,n1,i
c
c set the original point for recovering from flip-overed
c data series
c
      n2 = n1+1
c
c flip over n1 points at the beginning of data series
c
      do 20 i = 1,n1
      n4 = n1+2-i
      y(i) = x(n4)
 20   continue
c
c add flip-overed part to original data series
c
      do 10 i = 1,n
      n3 = n1+i
      y(n3) = x(i)
 10   continue
c
c flip over n1 points at the end of data series
c
      do 30 i = n+1,n+n1
      i1 = i-n
      i2 = n-i1
      i3 = n1+i
      y(i3) = x(i2)
 30   continue
c
c calculate the length of the flipped-over data series
c
      n5 = n+n1+n1
c
c pass the flipped-over data series through a lowpass
c Butterworth filter by using subroutine lpbut
c
      call lpbut (y, n5, y1, nd)
```

```
c
c change the order of the filtered data series backward
c in other words x(n) = y(-n)
c
      do 40 i = 1,n5
      i5 = n5+1-i
      x(i) = y(i5)
 40   continue
c
c pass the backward data series through the same filter
c by using the subroutine lpbut
c
      call lpbut (x, n5, y1, nd)
c
c change the backward filtered data into right order
c
      do 50 i = 1,n5
      i5 = n5+1-i
      y(i) = x(i5)
 50   continue
c
c set the ending point for recovering the right data series
c
      n8 = n5-n1
c
c recover the right region of the filtered data series
c
      do 70 i = n2,n8
      j = i-n1
      x(j) = y(i)
 70   continue
c
c
      return
      end
```

```
c-------------------------------------------------------c
c                                                       c
c     butwth :  a subroutine to perform the lowpass     c
c               Butterworth filtering                   c
c                                                       c
c   if                                                  c
c     x(k) : input data series                          c
c     y(k) : filtered data series                       c
c   then there are n stages with the equation           c
c                                                       c
c      y(k)=[x(k)+2x(k-1)+x(k-2)+ay(k-1)+by(k-2)]/c     c
c                                                       c
c      a, b and c are coefficients input from file      c
c                                                       c
c-------------------------------------------------------c
c
      subroutine lpbut (x, n, x1, n1)
c
      real x(n), y(32768), x1(60)
      integer n,n1,is
      real a,b,c
c
c set the first stage
c
      is1 = 1
c
c calculate total stages in the lowpass filtering process
c
      is = n1/3
c
c write out the present stage
c
      write(6,889)is
 889  format(//,3x,'There are  ',i2,' stages')
      write(6,12)is1
 12   format(///,5x,'This is stage ',i2)
c
c get coefficients for the present stage
c
      nm = (is1 - 1) * 3
      m1 = 1 + nm
      m2 = 2 + nm
      m3 = 3 + nm
      a = x1(m1)
      b = x1(m2)
      c = x1(m3)
c
c write out the present coefficients
c
      write(6,40) a,b,c
 40   format(1x,'a= ', f15.6,5x,'b= ',f15.6,5x,'c= ',f15.6)
```

```
c
c lowpass filtering by using the formula above for the
c present stage
c
      y(1) = x(1)/c
      y(2) = (x(2)+2*x(1)+a*y(1))/c
c
      do 10 i = 3,n
      y(i)=(x(i)+2*x(i-1)+x(i-2)+a*y(i-1)+b*y(i-2))/c
 10   continue
c
c put filtered data series from array y to array x
c
      do 20 i = 1,n
      x(i) = y(i)
 20   continue
c
c if the present stage is the last stage, stop
c otherwise continue process
c
      is1 = is1+1
      if(is.ge.is1) go to 100
c
      return
      end
```

```
c-------------------------------------------------------c
c                                                       c
c     stepii : a program to read data from combined data  c
c              file and interpolate the samples with step c
c              function and store interpolated data into  c
c              another file                               c
c                                                       c
c-------------------------------------------------------c
c
      CHARACTER *16 DATFIL, OUTFIL
      CHARACTER *80 LINE
      INTEGER CODE, VALUE
      INTEGER U(17), UN
      LOGICAL EXIST
C
      DIMENSION X(4096), Y(4096), XR(25240)
C
      DATA U/1,2,3,4,7,8,9,10,11,12,13,14,15,16,17,18,19/
C
C READ INPUT DATA FILENAME
C
 1    WRITE(6,10)
 10   FORMAT(' DATA INPUT FILE -----> ',$)
      READ(5,20) DATFIL
C
C READ OUTPUT FILENAME
C
      WRITE(6,11)
 11   FORMAT(' IBI INTERPOLATED DATA OUTPUT FILE -----> ',$)
      READ(5,20) OUTFIL
 20   FORMAT(A16)
C
C CHECK IF INPUT-OUTPUT UNIT IS AVAILABLE
C
      DO 5 I = 1,17
      INQUIRE(UNIT=U(I),EXIST=L)
      IF(.NOT.EXIST) GO TO 8
 5    CONTINUE
      WRITE(6,'(T20,"NO UNIT AVAILABLE ")')
      GO TO 113
C
C SET INITIAL VALUE OF TIME INDEX
C
 8    X(1) = 0.
      VA = 0.
      K = 0
C
C OPEN INPUT FILE
C
      UN = U(I)
      OPEN(UN,FILE=DATFIL,STATUS='OLD')
```

```
C
C READ FIRST FOUR LINES OF HEADER & KERMIT GREP
C
      READ(UN,9999) LINE
      READ(UN,9999) LINE
      READ(UN,9999) LINE
      READ(UN,9999) LINE
 9999 FORMAT(80A)
C
C READ 'CODE' AND 'VALUE' FROM INPUT FILE
C
 25   READ(UN,*,END=200) CODE, VALUE
 23   FORMAT(I1,/,I5)
C
C CODE=1 RESPIRATION VALUE
C CODE=2 IBI VALUE
C IF CODE = 2, THEN TAKE OUT IBI VALUE
C
      IF(CODE .NE.1 .AND. CODE .NE.2) GO TO 200
      IF(CODE .EQ.2) THEN
      K = K+1
      Y(K) = VALUE/100
      VA = VA+Y(K)
      X(K+1) = VA
C
C IF IBI VALUE <0.1, DON'T COUNT IT AS A REFERENCE
C TO PREVENT ARTIFACT
C
      IF(Y(K) .LT. 0.1) K=K-1
      ENDIF
      GO TO 25
C
C CLOSE INPUT-OUTPUT UNIT
C
 200  CLOSE(UN)
C
C SET TOTAL POINTS FOR INTERPOLATION
C
      IVAL = 10*VA + 1
      NI = 2
C
C DO THE INTERPOLATION BY USING THE STEP FUNCTION
C VALUES BETWEEN T(M) AND T(M+1) ARE THE VALUE AT
C TIME T(M+1)
C
      DO 56 J = 1, IVAL
      XK = 0.1* J
      IF(XK .GE. X(NI)) NI= NI+1
      XR(J) = Y(NI-1)
 56   CONTINUE
C
C IF THE INPUT-OUTPUT UNIT IS AVAILABLE
```

```
C
      DO 55 K = 1,17
      INQUIRE(UNIT=U(K), EXIST=L)
      IF(.NOT.EXIST) GO TO 38
 55   CONTINUE
      WRITE(6,'(T20,"NO UNIT AVAILABLE ")')
      GO TO 113
C
C OPEN OUTPUT FILE
C
 38   UN = U(K)
      OPEN(UN,FILE=OUTFIL,STATUS='NEW')
C
C WRITE OUT THE RESULT TO OUTPUT FILE
C
      WRITE(UN,*)(XR(J),J=1,IVAL)
C
C CLOSE INPUT OUTPUT UNIT
C
      CLOSE(UN)
 113  STOP
      END
```

```
c-------------------------------------------------------c
c                                                       c
c     datin : a subroutine to open and read files       c
c             containing a single variable per line     c
c             uses logical unit other than 0, 5 or 6    c
c                                                       c
c     inputs:                      on return:           c
c                                                       c
c     name  name of input file     name of input file   c
c      x    a real array           array with data      c
c      n                           length of data in x  c
c     sum                          sum of x             c
c     mean                         mean of x            c
c     ierr  error code = 0         0 if no problems     c
c                                  1 if unsolved error  c
c                                  2 if no unit is availablec
c   iquery  1 prompts for new filename                  c
c           when file not found          unchanged      c
c           0 no prompt for new filename                c
c           returns with ierr =1                        c
c                                                       c
c-------------------------------------------------------c
c
      subroutine datin (name,x,n,sum,mean,ierr,iquery)
c
      character * 40 name
      real x(32768), v, sum, mean
      integer n, ierr, iost
      integer iquery
      integer u(17), un
      logical exist
      data u/1,2,3,4,7,8,9,10,11,12,13,14,15,16,17,18,19/
c
      ierr = 0
c
c find an available unit
c
      do 5 i = 1, 17
      inquire(unit = u(i), exist =1)
      if (.not.exist) go to 20
 5    continue
c
c if no unit available
c
      write( 6, '(t20, "no unit available ")')
      ierr = 2
      return
c
c open file on unit u(i) and read the data
c
 20   uerr = 0
```

```
      un = u(i)
      open(un,file=name,status='old',err=50,iostat=iost)
      n = 0
      sum = 0.
 30   read(un,*,end=40) v
c
c calculate the sum of the series
c
      n = n+1
      x(n) = v
      sum = sum + x(n)
      go to 30
c
c close input-output unit
c
 40   close(un)
c
c calculate the mean
c
      mean = sum /real (n)
      return
c
c if error opening file - fix if appropriate
c
 50   ierr = 1
      if (iost.eq.118) then
      write(6,'(t20,"file not found")')
      if (iquery.gt.0) then
      write(6,'(t20,"input file ",$)')
      read(5,*) name
      go to 20
      else
      return
      end if
      else
      return
      end if
      end
```

```
c-------------------------------------------------------------c
c                                                             c
c     demod : a subroutine to demodulate series x at          c
c             frequency omega, real and imaginary parts       c
c             of the demodulated series are returned in       c
c             d1 and d2 respectively                          c
c                                                             c
c-------------------------------------------------------------c
c
      subroutine demod(x,n,omega,d1,d2)
c
      real x(n), d1(n), d2(n)
      real arg
      real omega
      integer n
c
c calculate demodulated real part and imaginary part of
c a data series x(n)
c
      do 10 i = 1,n
      arg = real (i-1) * omega
      d1(i) = x(i) * cos(arg) * 2.0
      d2(i) = -x(i) * sin(arg) * 2.0
 10   continue
      return
      end
```

```
c-------------------------------------------------------c
c                                                       c
c     datout : a subroutine to write real data into an  c
c              ascii file -- 1 obs / line, using logical c
c              unit other than 0, 5 or 6                c
c                                                       c
c     inputs:                              on return:   c
c                                                       c
c    name  name of file to be written     unchanged     c
c     x    a real array to be written     unchanged     c
c    wbeg  1st point to be written        unchanged     c
c    wlast last point be be written       unchanged     c
c                                                       c
c    ierr  0                0 if file written successfully c
c                           1 if unsolved problems      c
c                           2 if no unit available      c
c                                                       c
c   iquery 0 if existing files with name                c
c          are overwritten without warning              c
c          1 to query before overwritten                c
c                                                       c
c-------------------------------------------------------c
c
      subroutine datout(name,x,wbeg,wlast,wstep,ierr,iquery)
c
      character * 40 name
      character * 1 ans
      real x(n)
      integer n,ierr,iost,iquery
      integer u(17),un
      integer wbeg,wlast,wstep
      logical exist
      data u/1,2,3,4,7,8,9,10,11,12,13,14,15,16,17,18,19)
c
      ierr = 0
      iost = 0
c
c find an available unit
c
      do 5 i = 1,17
      inquire (unit=u(i), exist=1)
      if (.not.exist) go to 20
c
c if no unit available
c
 5    continue
      ierr = 2
      write(6,'(t20," no unit available ")')
      return
 20   continue
c
```

```
c open the file on unit u(i) and write the data into it
c
      un = u(i)
      open( un,file=name,status='new',err=50,iostat=iost)
      do 30 j = wbeg,wlast,wstep
      write(un,*) x(j)
 30   continue
c
c close input-output unit
c
      close(un)
      return
c
c error in file opening - fix if possible
c
 50   if(iost.eq.117 .and. iquery.gt.0) then
      write(6,'(t20,"file exists- overwrite it ? ",$)')
      read(5,*) ans
      if (ans .eq. "y") then
      write(6,'(t20,"output file name ",$)')
      read(5,*)name
      go to 20
      else
      return
      end if
      end if
      else if (iost.eq.117) then
      open(un,file=name,status='unknown',err=90,iostat=iost)
      go to 20
      else
      go to 90
      end if
c
c if all else fails...fall of end of subroutine
c
 90   write(6,'(t20,"error ",i4,"deleting file ")') iost
      ierr = 1
      return
      end
```

```
c-------------------------------------------------------c
c                                                       c
c     polar : a subroutine to convert the pair of series  c
c             x and y from the real and imaginary parts of c
c             complex numbers to their magnitude and phase c
c                                                       c
c     magnitude is computed as sqrt(real*real+imag*imag)  c
c     phase is computed as atan2(imag,real)             c
c                                                       c
c-------------------------------------------------------c
c
      subroutine polar (x,y,n)
c
      real x(n), y(n)
      integer n
c
c calculate the real part and the imaginary part
c
      do 10 i = 1,n
      r = sqrt(( x(i)**2) + (y(i)**2))
      phi = atan2(y(i),x(i))
      x(i) = r
      y(i) = phi
 10   continue
      return
      end
```

```
c-------------------------------------------------------------c
c     resp : a program to read respiration data from        c
c            combined data file and store it to another     c
c            file                                           c
c                                                           c
c-------------------------------------------------------------c
c
      CHARACTER * 16 DATFIL,OUTFIL
      CHARACTER * 80 LINE
      INTEGER CODE,VALUE
      INTEGER U(17),UN
      LOGICAL EXIST
C
      DIMENSION XR(25240)
      DATA U/1,2,3,4,7,8,9,10,11,12,13,14,15,16,17,18,19/
C
C READ INPUT AND OUTPUT FILENAMES
C
 1    WRITE(6,10)
 10   FORMAT(' DATA INPUT FILE -----> ',$)
      READ(5,20) DATFIL
      WRITE(6,11)
 11   FORMAT(' RESPIRATION DATA OUTPUT FILE -----> ',$)
      READ(5,20)OUTFIL
 20   FORMAT(A16)
C
C IF INPUT-OUTPUT UNIT IS AVAILABLE
C
      DO 5 I=1,17
      INQUIRE(UNIT=U(I),EXIST=L)
      IF(.NOT.EXIST)GO TO 8
 5    CONTINUE
      WRITE(6,'(T20," NO UNIT AVAILABLE ")')
      GO TO 113
C
C OPEN INPUT FILE
C
 8    UN = U(I)
      K = 0
      OPEN(UN,FILE=DATFIL,STATUS='OLD')
      READ(UN,9999) LINE
      READ(UN,9999) LINE
      READ(UN,9999) LINE
      READ(UN,9999) LINE
 9999 FORMAT(80A)
C
C READ CODE AND VALUE FROM INPUT FILE
C
 25   READ(UN,*,END=200) CODE, VALUE
 23   FORMAT(I1,/,I5)
C
```

```
C IF CODE NOT EQUAL 1 AND NOT EQUAL 2, CLOSE UNIT.
C
      IF(CODE .NE.1 .AND. CODE .NE.2) GO TO 200
C
C IF CODE EQUAL 1 MEANS VALUE IS A RESPIRATION VALUE
C
      IF(CODE .EQ. 1) THEN
      K = K+1
      XR(K) = VALUE/100.
      ENDIF
      GO TO 25
C
C CLOSE INPUT-OUTPUT UNIT
C
 200  CLOSE(UN)
C
C IF INPUT-OUTPUT UNIT IS AVAILBALE FOR OUTPUT
C
      DO 55 M = 1,17
      INQUIRE(UNIT=U(M),EXIST=L)
      IF(.NOT.EXIST)GO TO 38
 55   CONTINUE
      WRITE(6,'(T20,"NO UNIT AVAILABLE ")')
      GO TO 113
C
C WRITE OUT OUTPUT FILE
C
 38   UN = U(M)
      OPEN(UN,FILE=OUTFIL,STATUS='NEW')
      WRITE(UN,*)(XR(J),J = 1,K)
C
C CLOSE INPUT-OUTPUT UNIT
C
      CLOSE(UN)
 113  STOP
      END
```

```
/FILE RWAVE1.SK
/CREATED 11-JAN-85
/VERSION 1
/
/PROGRAM TO SAMPLE THE DR8E PARALLEL IO BOARD
/THE PROGRAM STARTS WITH OPENING THE OUTPUT FILE AND
/CLEARING THE OUTPUT BUFFER. AFTER .01 SEC. BIT 12 IN THE
/OUTPUT BUFFER IS SET TO ONE SIGNALLING THE A TO D
/CONVERTER TO START CONVERTING THE RESPIRATION WAVE,
/.09 SEC. LATER THE INPUT BUFFER IS SET TO ZERO. .09 SEC.
/LATER THE INPUT BUFFER IS READ AGAIN AND THE WHOLE PROCESS
/STARTS ALL OVER AGAIN.

LIST S=4000        /USED TO SET BIT 12 TO ONE
LIST Z=7777        /USED TO CLEAR THE BUFFER

CTRS=300

S.S.1,
S1,
      Z1:CALL 0[4095,?6515];CALL 0[4095,?6513];SET
      I=0--->S2 /CLEAR THE OUTPUT REGISTER
      Z3---->S1
S2,
      .01":CALL 0[4095,?6516];IF I=300;Z2;THEN;SET
      I=1-->S3   ;ELSE-->S3   /SET OUTPUT REGISTER BIT 12 TO 1
      Z3--->S1
S3,
/GET VALUE IN THE INPUT REGISTER AND THEN CLEAR THE INPUT
/REGISTER
      .09":CALL 0[C(I),?6514];CALL 0[4095,?6513];
      WRITE C(I),1;ADD I-->S4
      Z3--->S1
S4,
      .01":CALL 0[4095,?6515];IF I=300;Z2;THEN;
      SET I=1--->S5 /SET OUTPUT REGISTER TO 0
                 ;ELSE-->S5
      Z3--->S1
S5,
      .09":CALL 0[C(I),?6514];CALL 0[4095,?6513];
      WRITE C(I),1;ADD I-->S2
      Z3--->S1

/STATE SET TO MEASURE IBI
/THE FIRST BEAT WILL START STATE SET 1 AND OPEN THE
/DATA FILE
/DATA WILL BE COLLECTED IN .01 SEC. AND WRITTEN TO
/THE DATA FILE WITH A CODE OF 2

S.S.2,
```

```
S1,
      START:OPEN--->S2
S2,
      R3:SET B=0;Z1-->S3
S3,
      R3:WRITE B,2;SET B=0;Z1--->SX
      .01":ADD B--->SX
      R100:Z3--->S4
S4,
      .01":CLOSE--->S5
S5,
      .01":CLOSE--->S1
S.S.3,
S1,
      Z2:FOR X=1,1,300;SET C(X)=0;NEXT-->SX
      Z3:TYPE
      "!OUTPUT FILE CLOSED;COPY TO FLOPS PLEASE!"-->S2
S2,
      120'---->STOP
      R3-->S1
```

APPENDIX D

In this section, one COND dog's (dog 1) and one NCON dog's (dog 4) results are displayed.

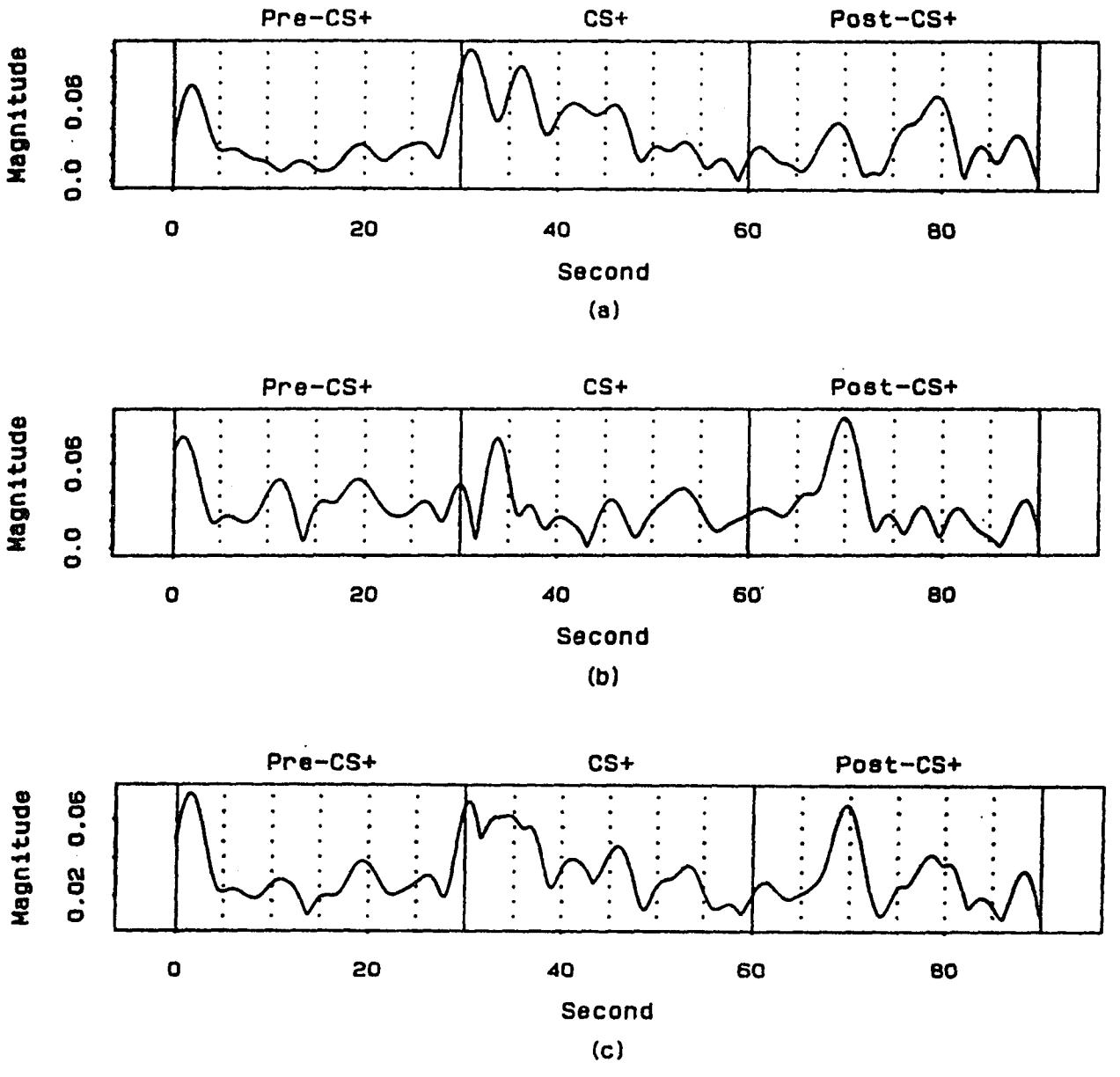

FIGURE D.1 (a) THE RESPIRATION FREQUENCY MAGNITUDE RESULT OF DOG 1 UNDER CS+ TRIAL 1.

(b) THE RESPIRATION FREQUENCY MAGNITUDE RESULT OF DOG 1 UNDER CS+ TRIAL 2.

(c) THE AVERAGE FROM (a) AND (b).

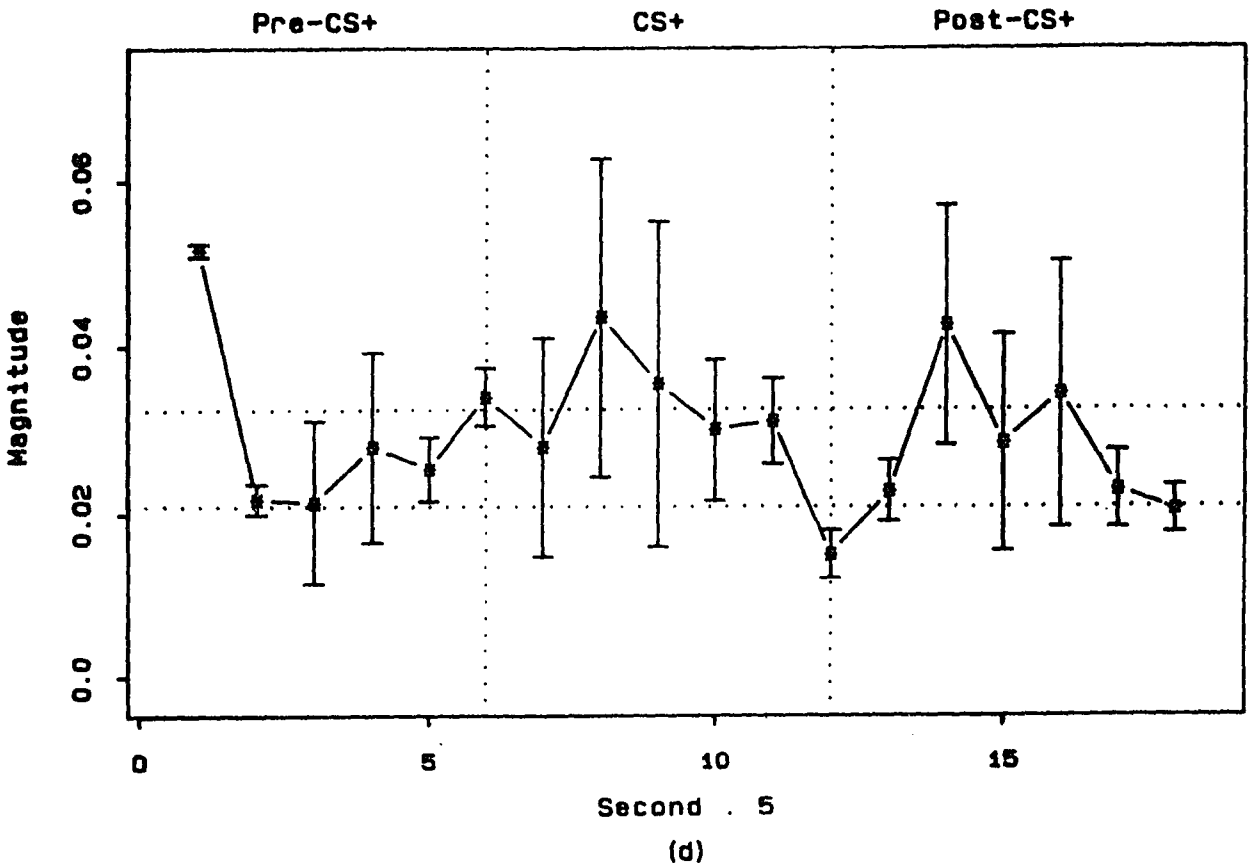

FIGURE D.1 (d) THE 5-SECOND AVERAGE OF (c) WITH STANDARD ERROR AND 95% CONFIDENCE INTERVAL.

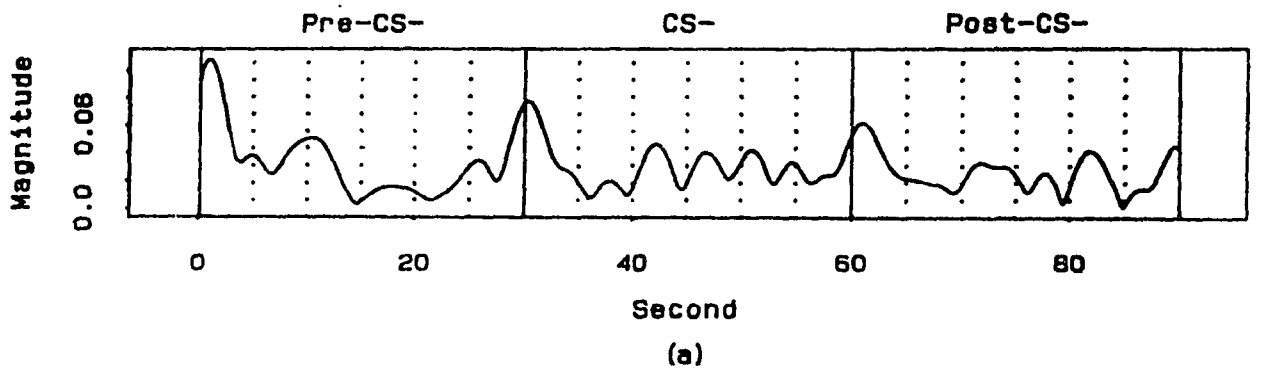

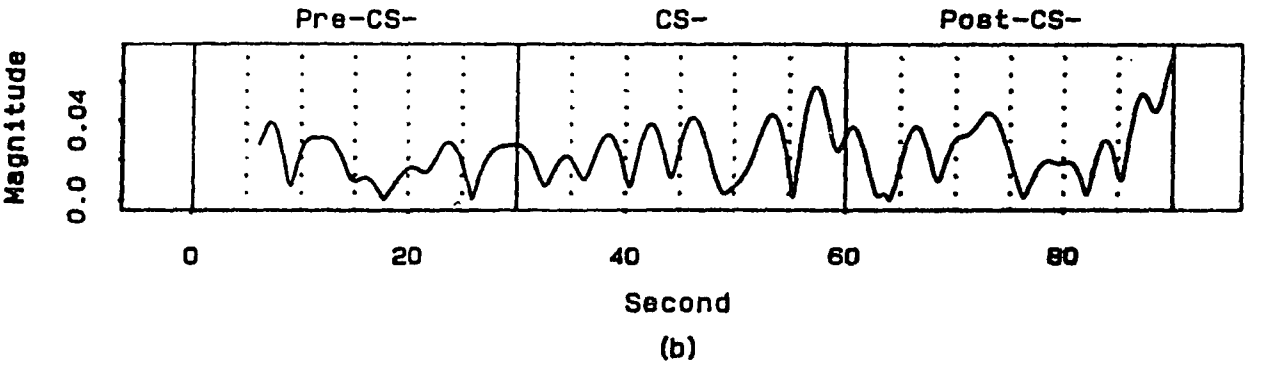

FIGURE D.2 (a) THE RESPIRATION FREQUENCY MAGNITUDE RESULT OF DOG 1 UNDER CS- TRIAL 1.

(b) THE RESPIRATION FREQUENCY MAGNITUDE RESULT OF DOG 1 UNDER CS- TRIAL 2.

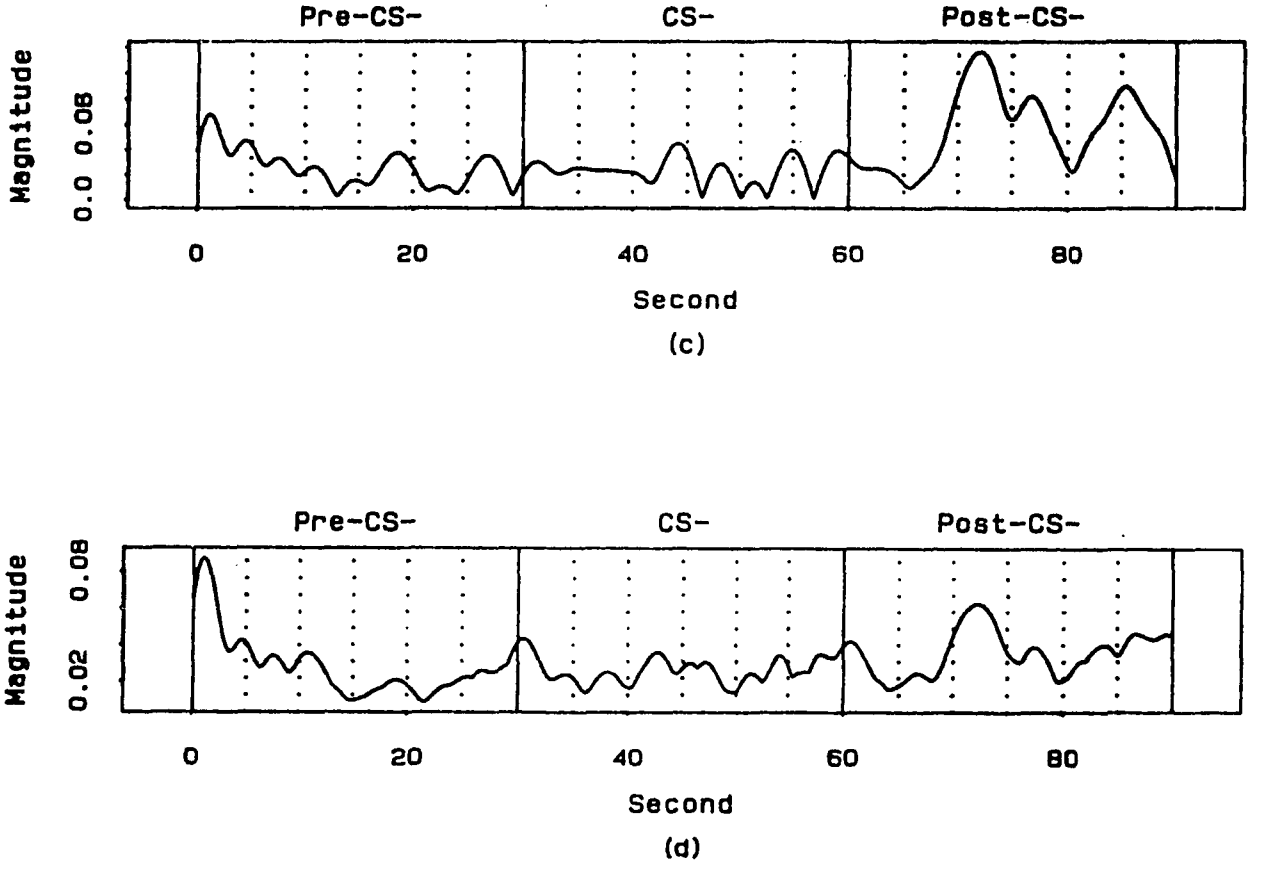

FIGURE D.2 (c) THE RESPIRATION FREQUENCY MAGNITUDE RESULT OF DOG 1 UNDER CS- TRIAL 3.

(d) THE AVERAGE FROM (a) TO (c).

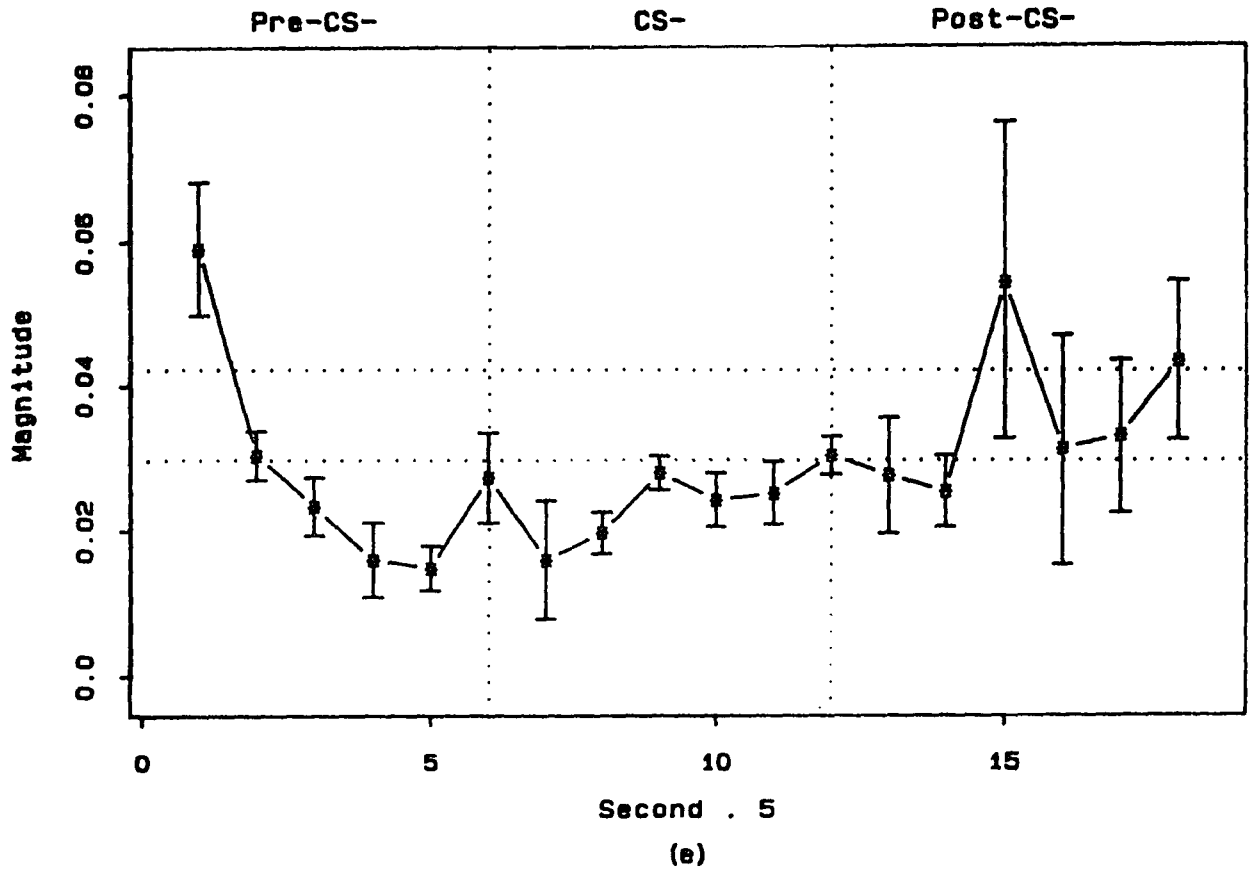

FIGURE D.2 (e) THE 5-SECOND AVERAGE OF (d) WITH STANDARD ERROR AND 95% CONFIDENCE INTERVAL.

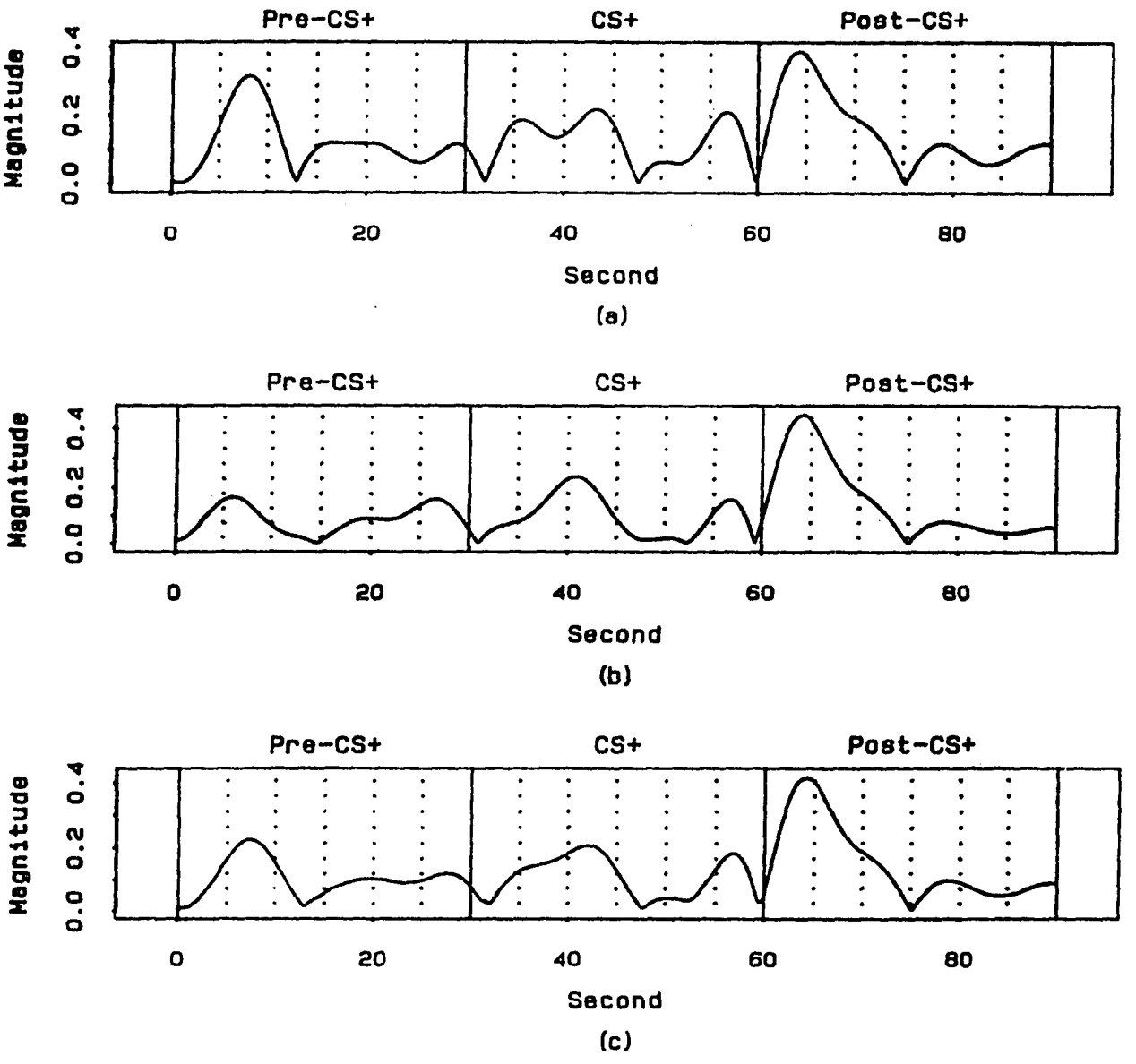

FIGURE D.3 (a) THE LOW FREQUENCY MAGNITUDE RESULT OF DOG 1 UNDER CS+ TRIAL 1.

(b) THE LOW FREQUENCY MAGNITUDE RESULT OF DOG 1 UNDER CS+ TRIAL 2.

(c) THE AVERAGE FROM (a) AND (b).

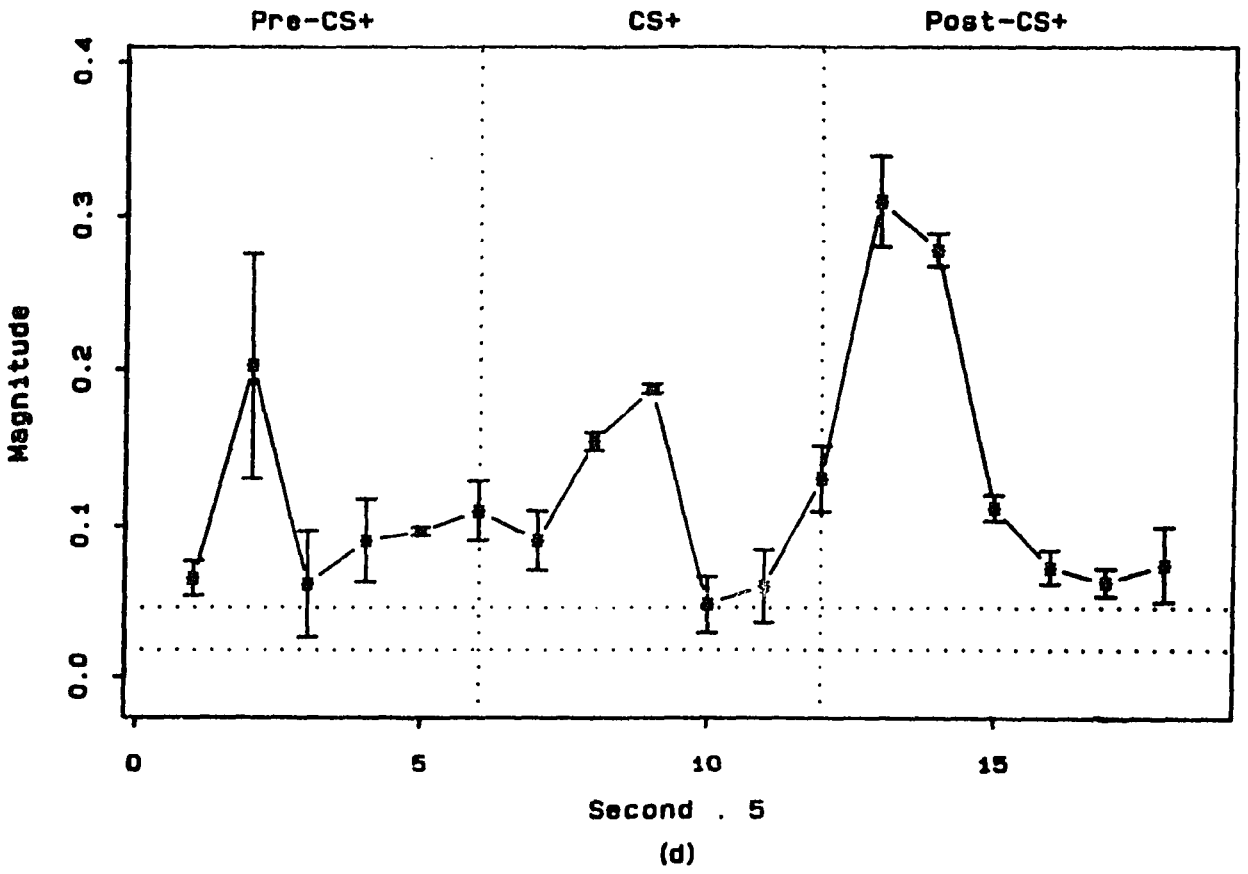

FIGURE D.3 (d) THE 5-SECOND AVERAGE OF (c) WITH STANDARD ERROR AND 95% CONFIDENCE INTERVAL.

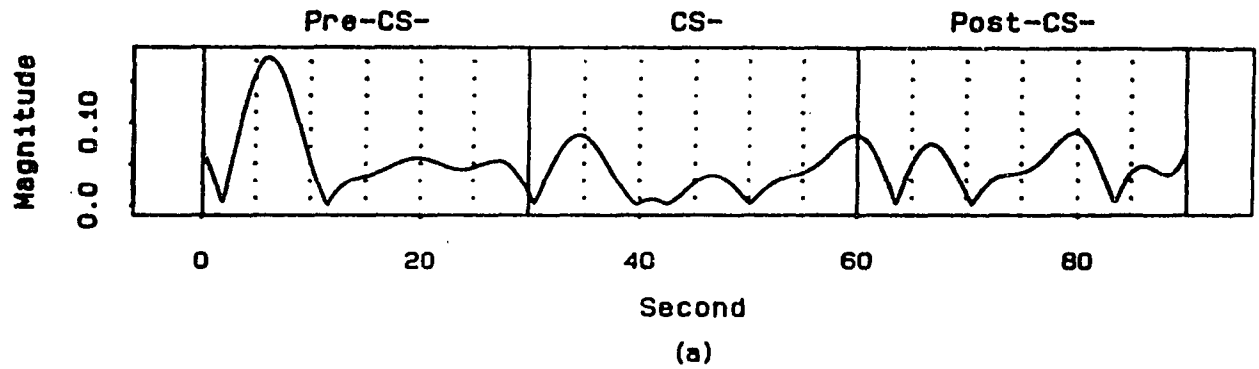

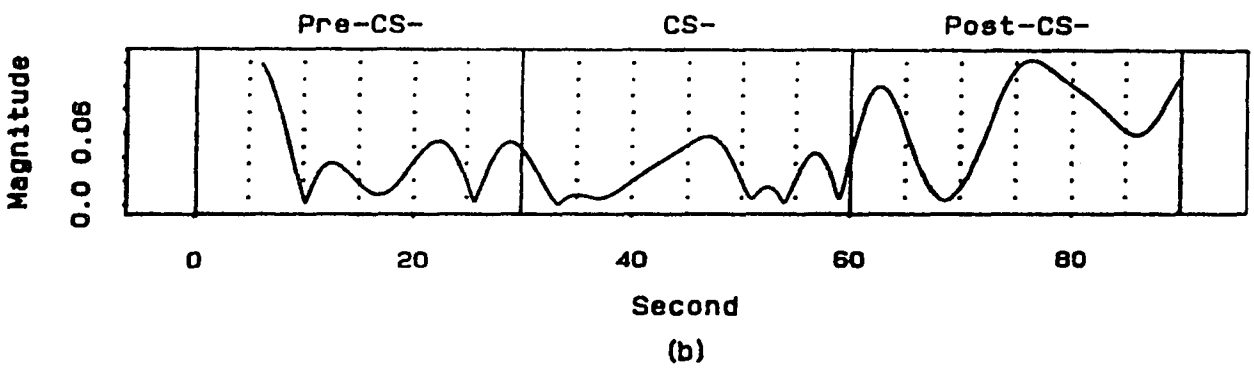

FIGURE D.4 (a) THE LOW FREQUENCY MAGNITUDE RESULT OF DOG 1 UNDER CS- TRIAL 1.

(b) THE LOW FREQUENCY MAGNITUDE RESULT OF DOG 1 UNDER CS- TRIAL 2.

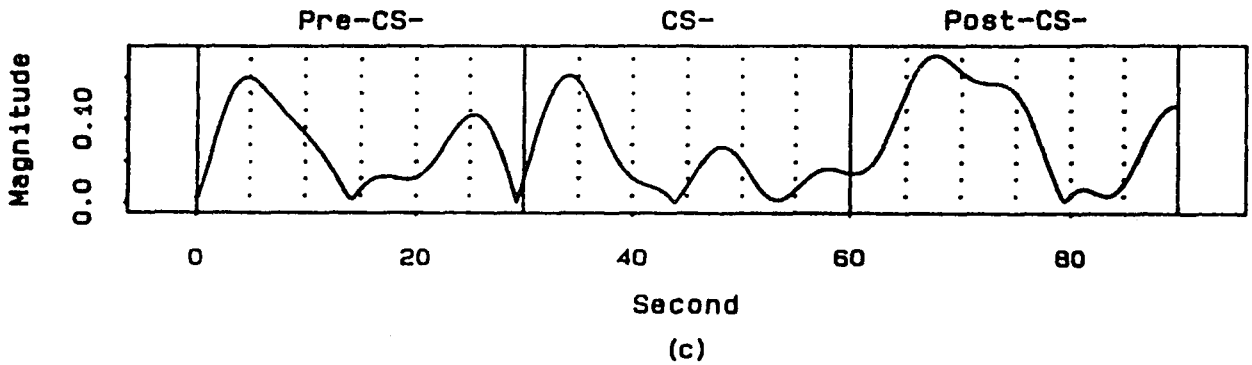

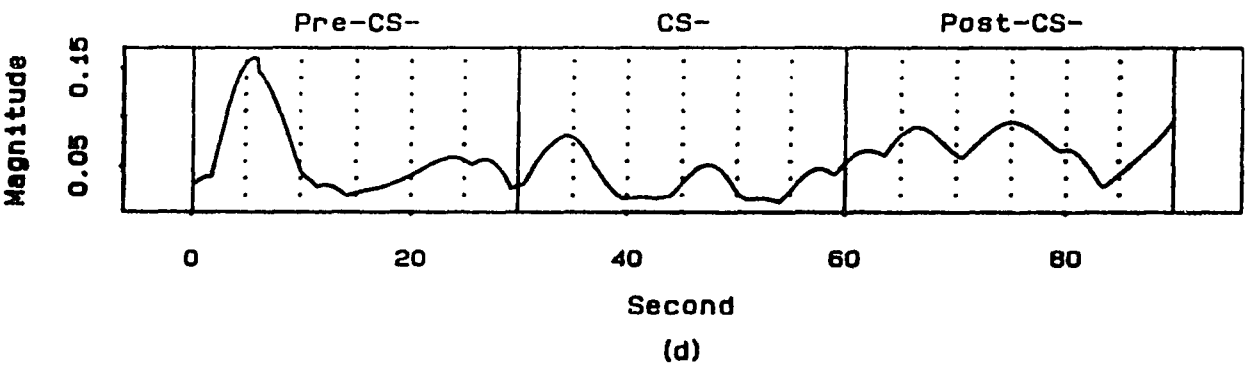

FIGURE D.4 (c) THE LOW FREQUENCY MAGNITUDE RESULT OF DOG 1 UNDER CS- TRIAL 3.

(d) THE AVERAGE FROM (a) TO (c).

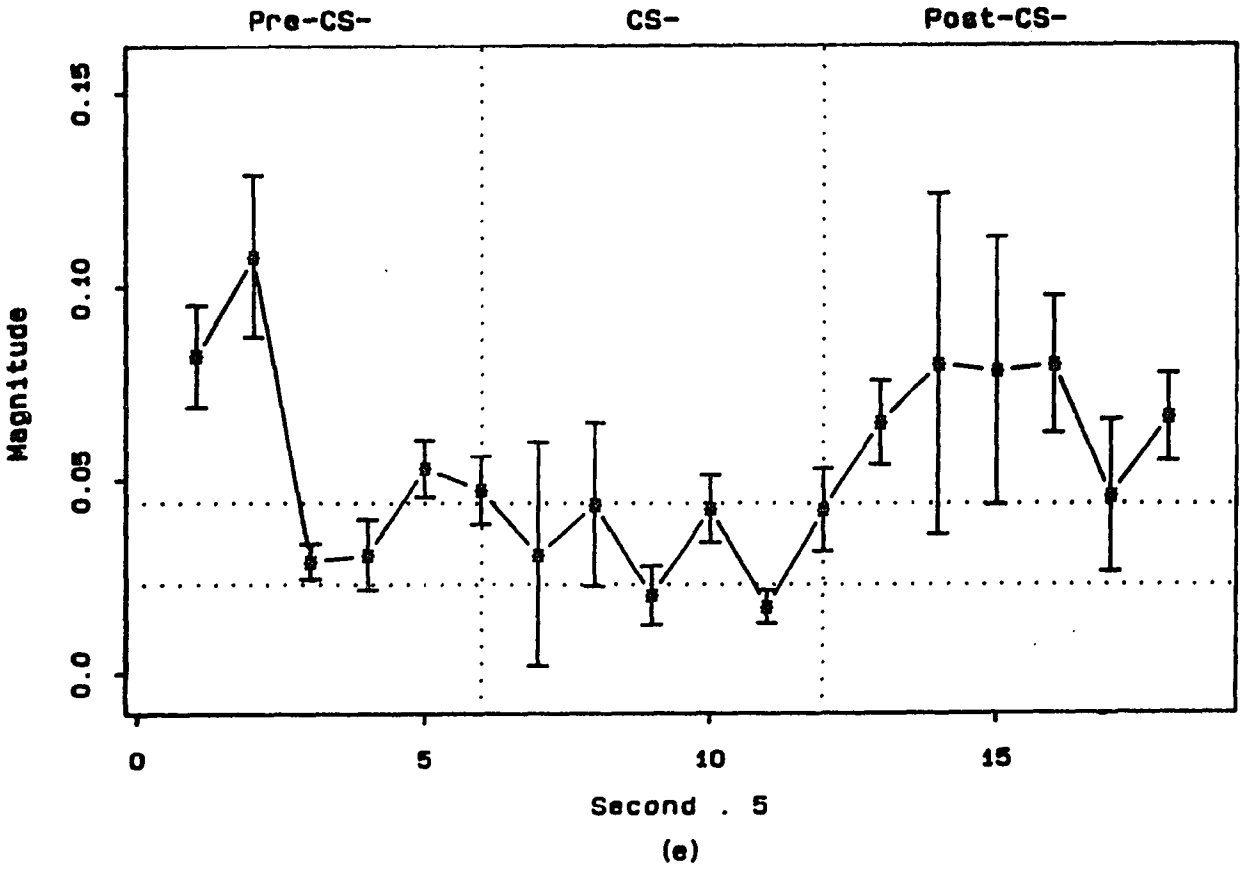

FIGURE D.4 (e) THE 5-SECOND AVERAGE OF (d) WITH STANDARD ERROR AND 95% CONFIDENCE INTERVAL.

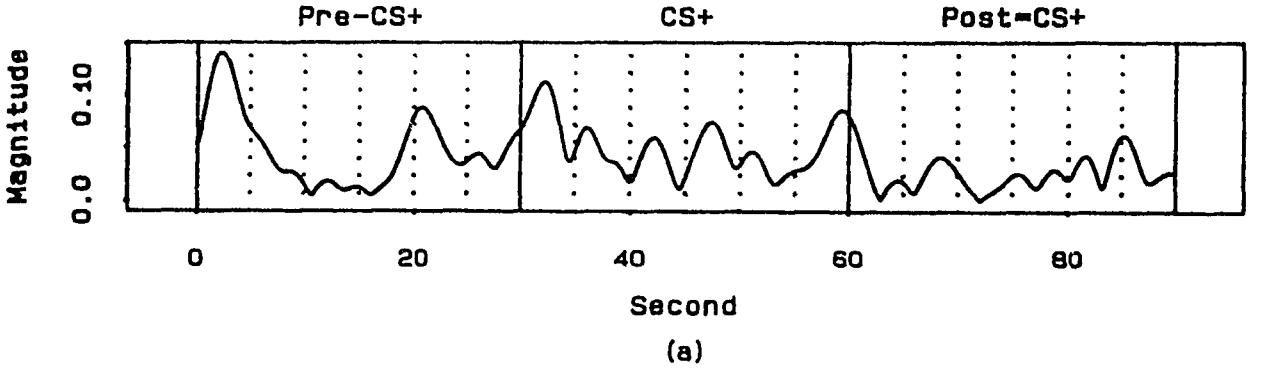

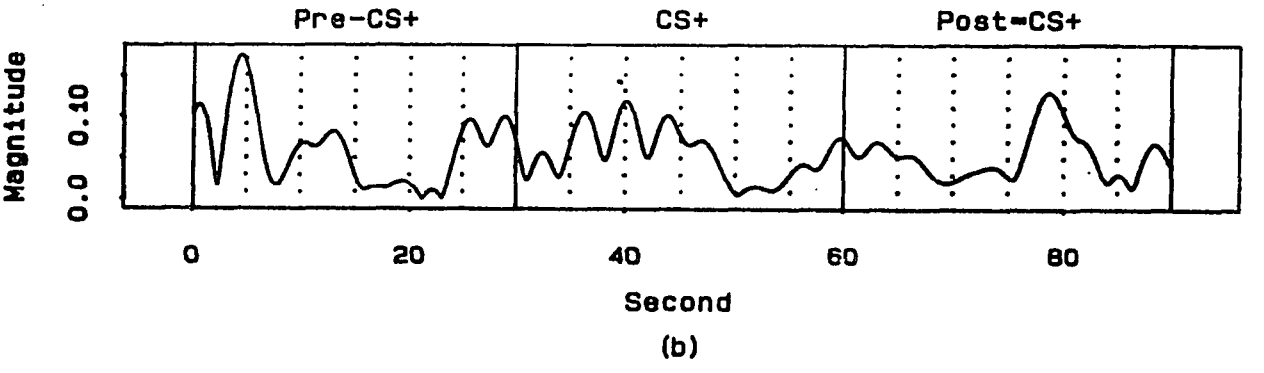

FIGURE D.5 (a) THE RESPIRATION FREQUENCY MAGNITUDE RESULT OF DOG 4 UNDER CS+ TRIAL 1.

(b) THE RESPIRATION FREQUENCY MAGNITUDE RESULT OF DOG 4 UNDER CS+ TRIAL 2.

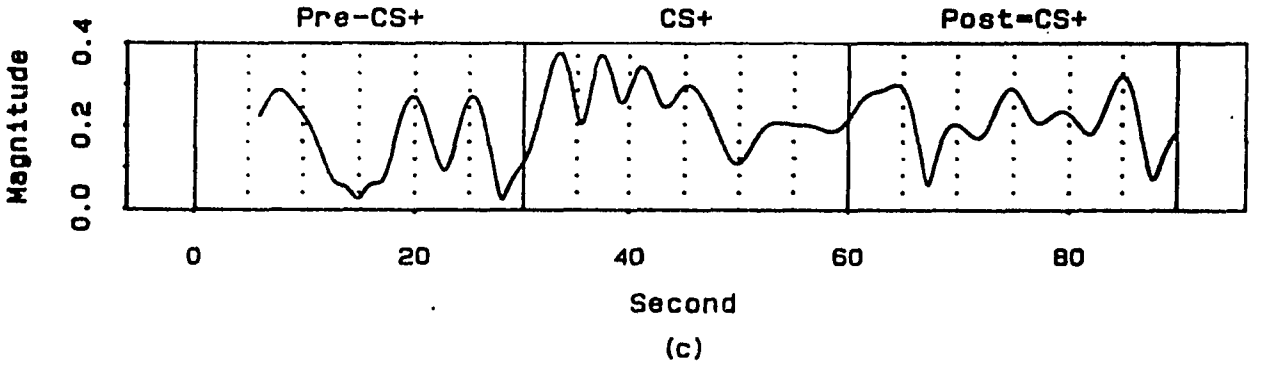

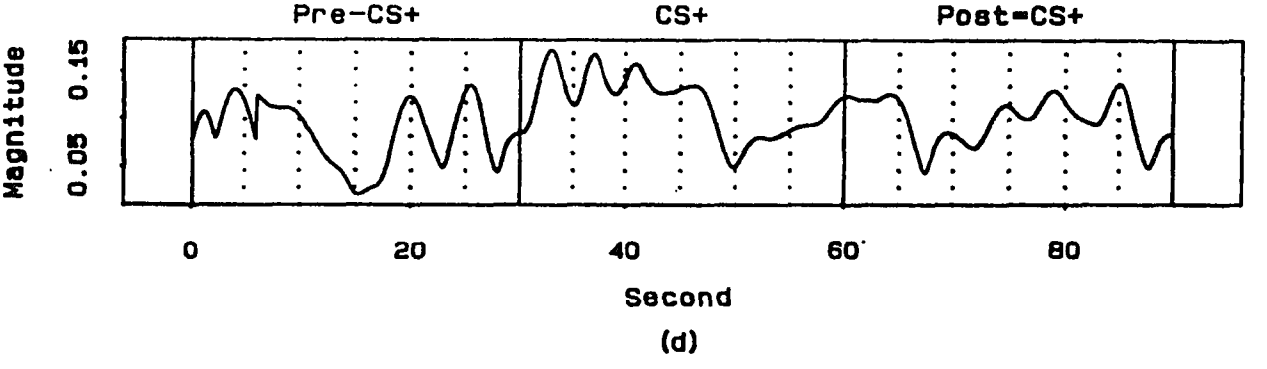

FIGURE D.5 (c) THE RESPIRATION FREQUENCY MAGNITUDE RESULT OF DOG 4 UNDER CS+ TRIAL 3.

(d) THE AVERAGE FROM (a) TO (c).

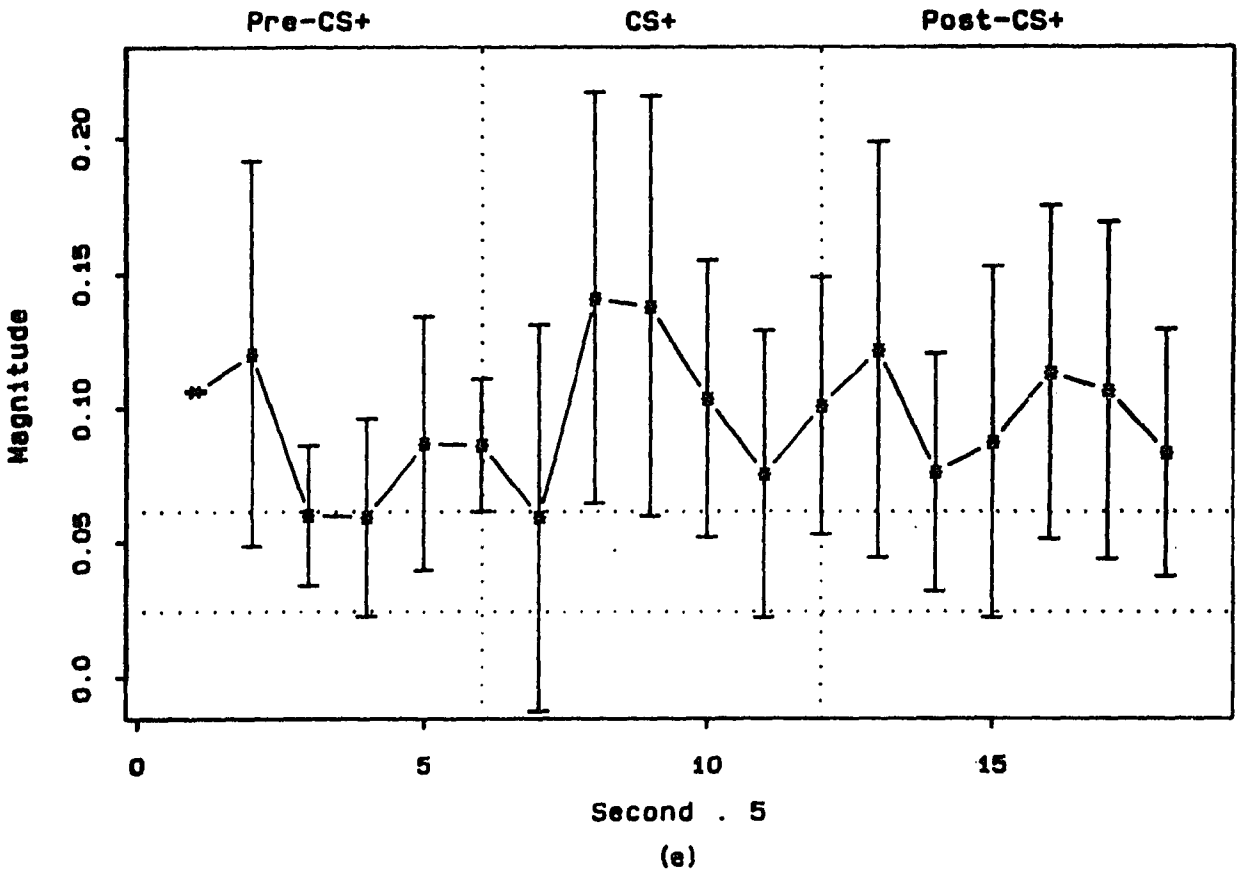

FIGURE D.5 (e) THE 5-SECOND AVERAGE OF (d) WITH STANDARD ERROR AND 95% CONFIDENCE INTERVAL.

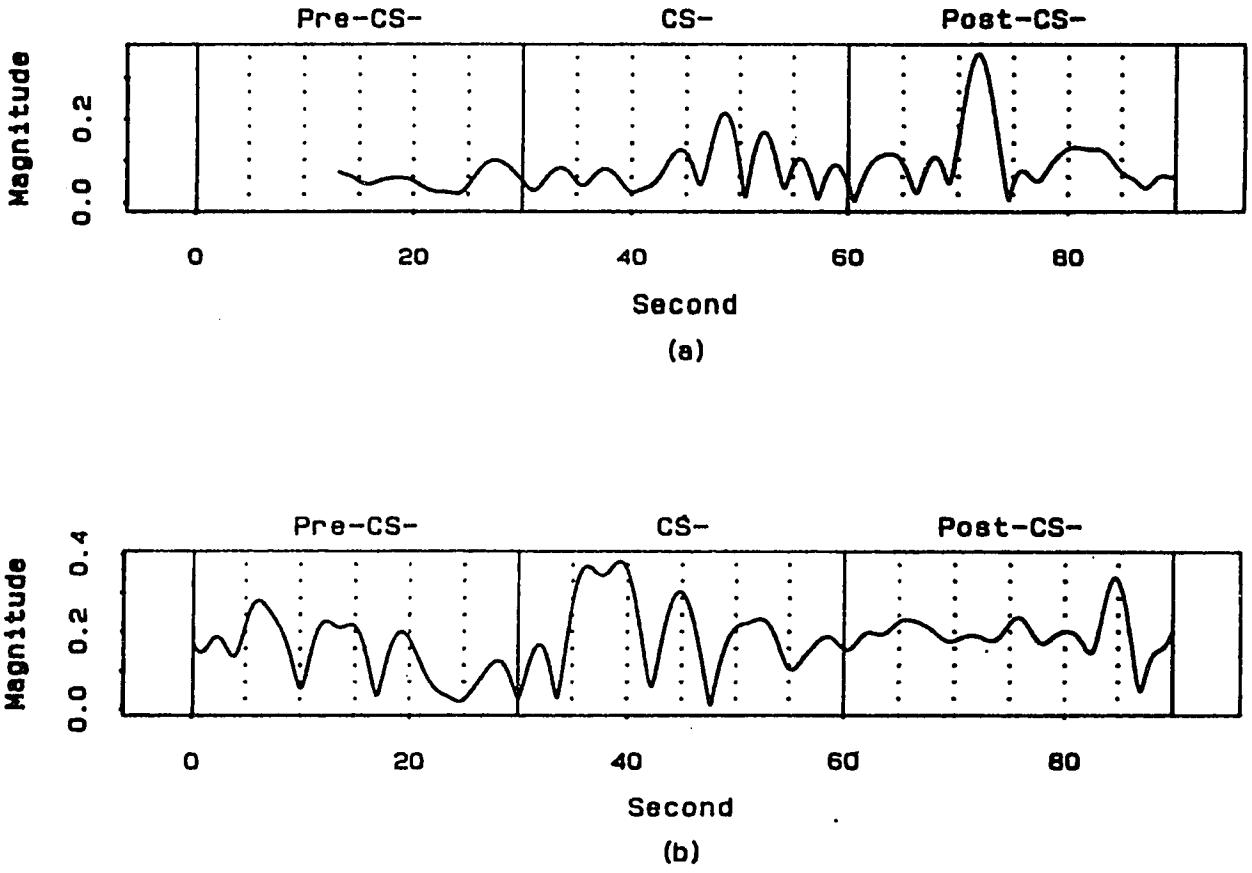

FIGURE D.6 (a) THE RESPIRATION FREQUENCY MAGNITUDE RESULT OF DOG 4 UNDER CS- TRIAL 1.

(b) THE RESPIRATION FREQUENCY MAGNITUDE RESULT OF DOG 4 UNDER CS- TRIAL 2.

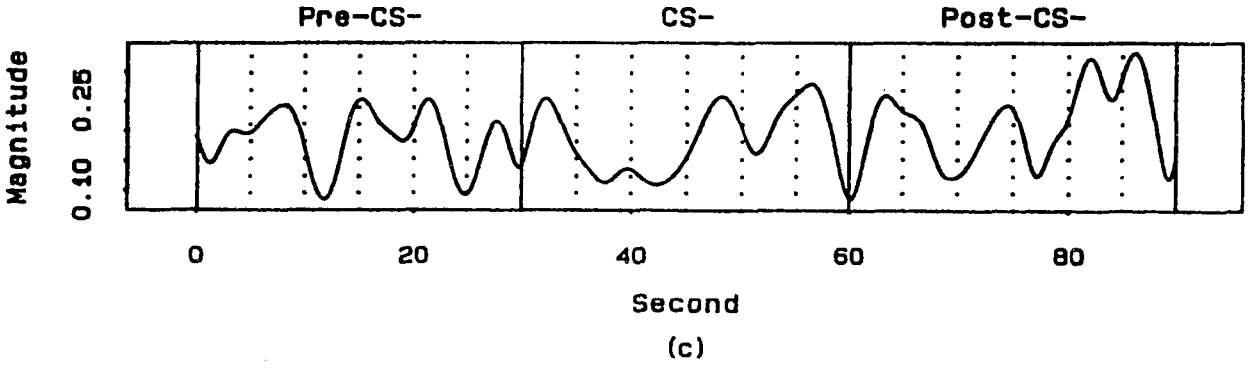

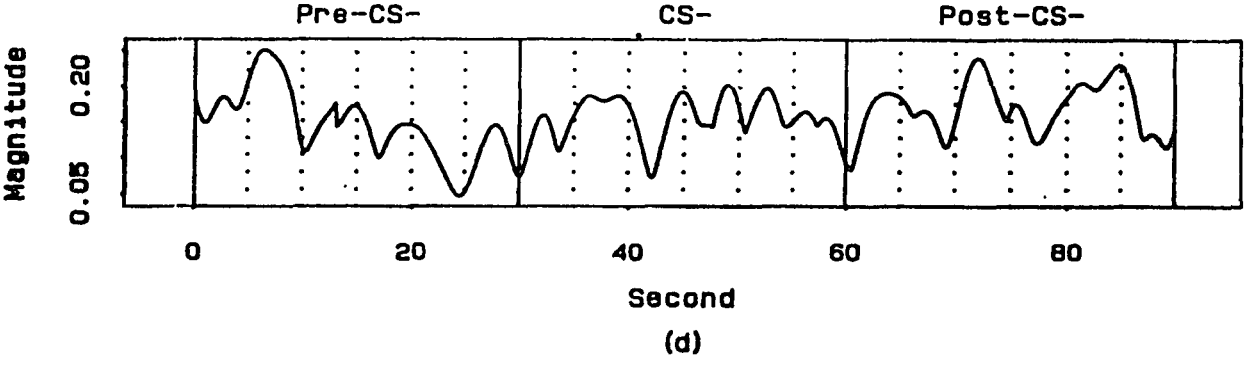

FIGURE D.6 (c) THE RESPIRATION FREQUENCY MAGNITUDE RESULT OF DOG 4 UNDER CS- TRIAL 3.

(d) THE AVERAGE FROM (a) TO (c).

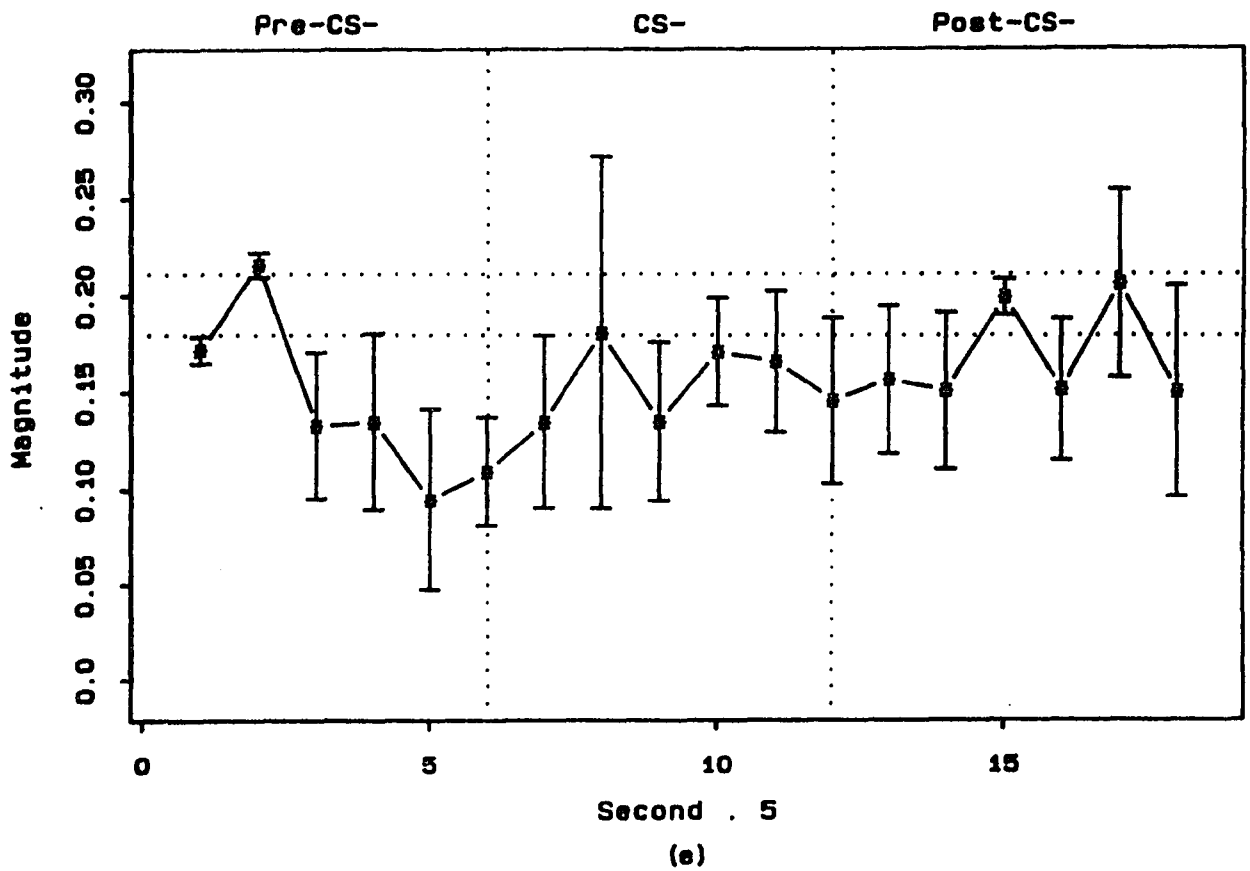

FIGURE D.6 (e) THE 5-SECOND AVERAGE OF (d) WITH STANDARD ERROR AND 95% CONFIDENCE INTERVAL.

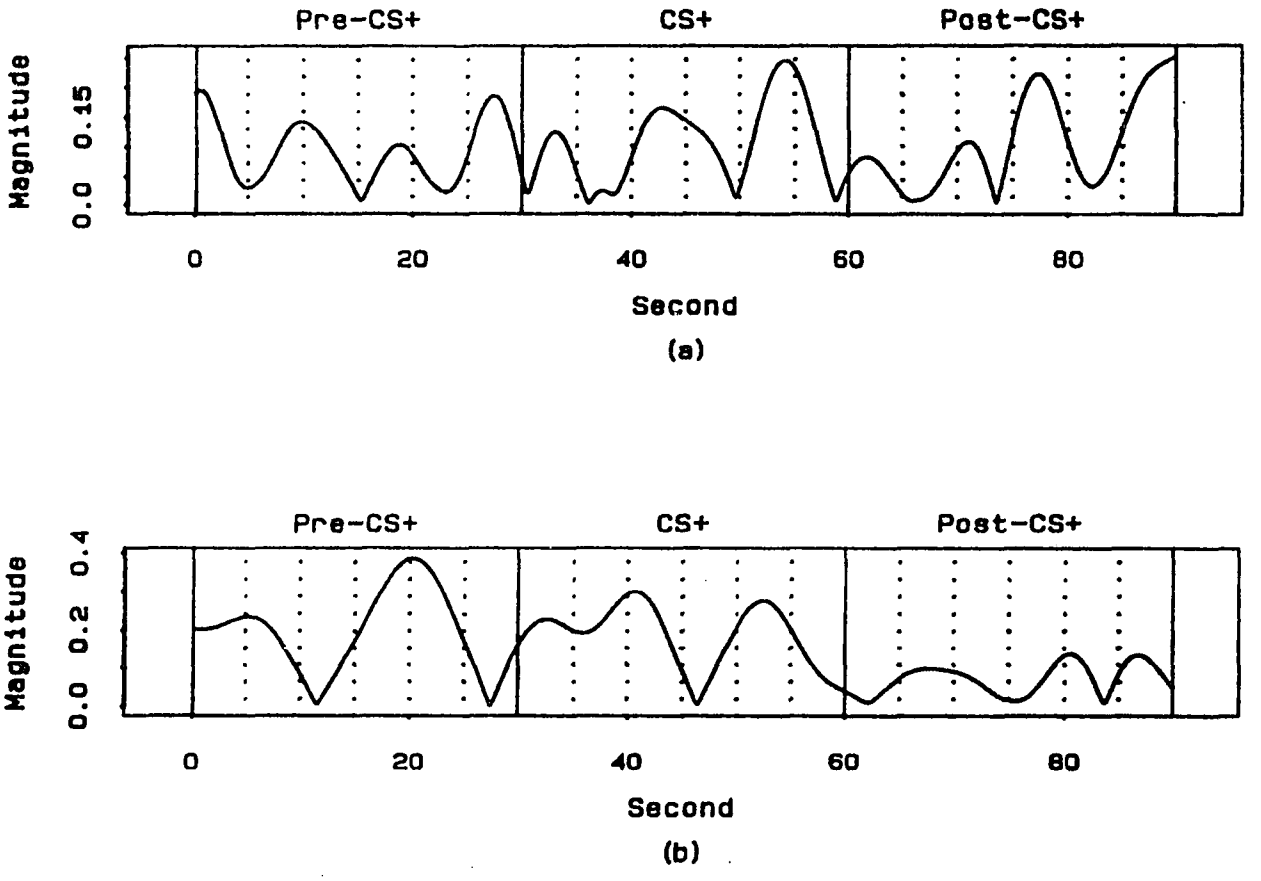

FIGURE D.7 (a) THE LOW FREQUENCY MAGNITUDE RESULT OF DOG 4 UNDER CS+ TRIAL 1.

(b) THE LOW FREQUENCY MAGNITUDE RESULT OF DOG 4 UNDER CS+ TRIAL 2.

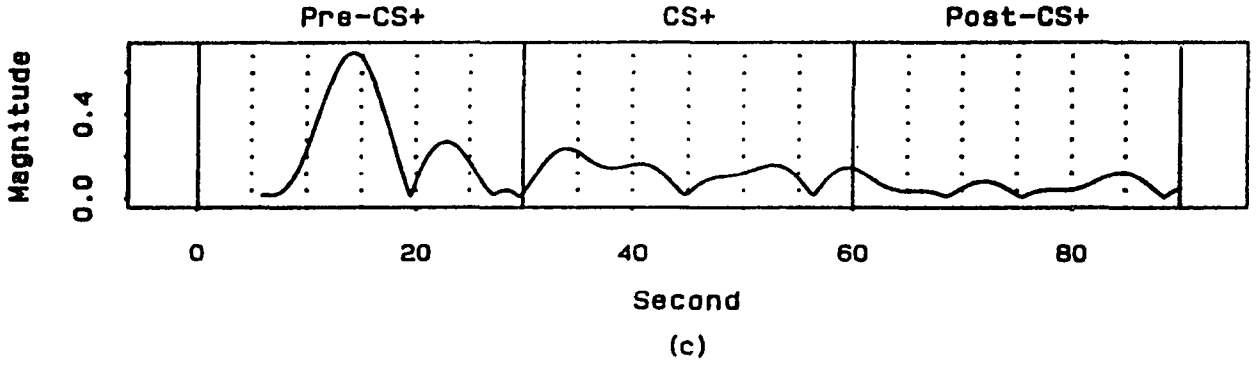

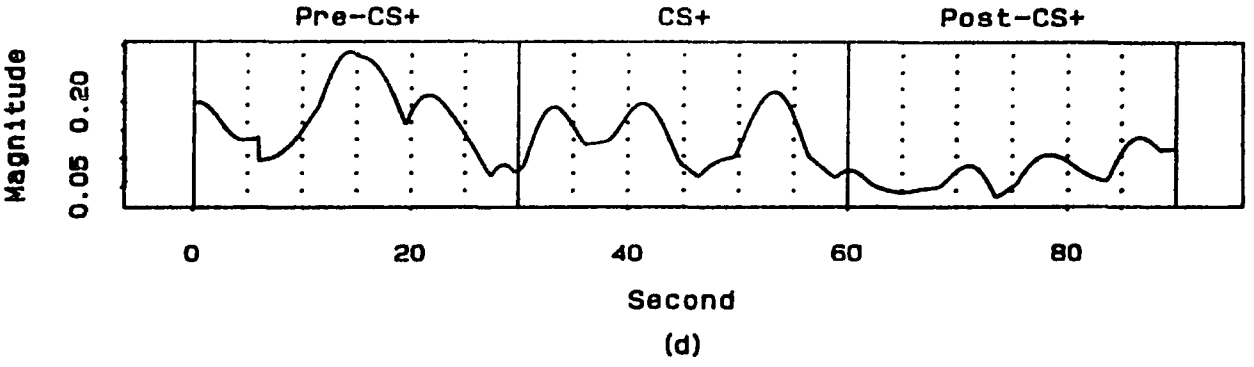

FIGURE D.7 (c) THE LOW FREQUENCY MAGNITUDE RESULT OF DOG 4 UNDER CS+ TRIAL 3.
(d) THE AVERAGE FROM (a) TO (c).

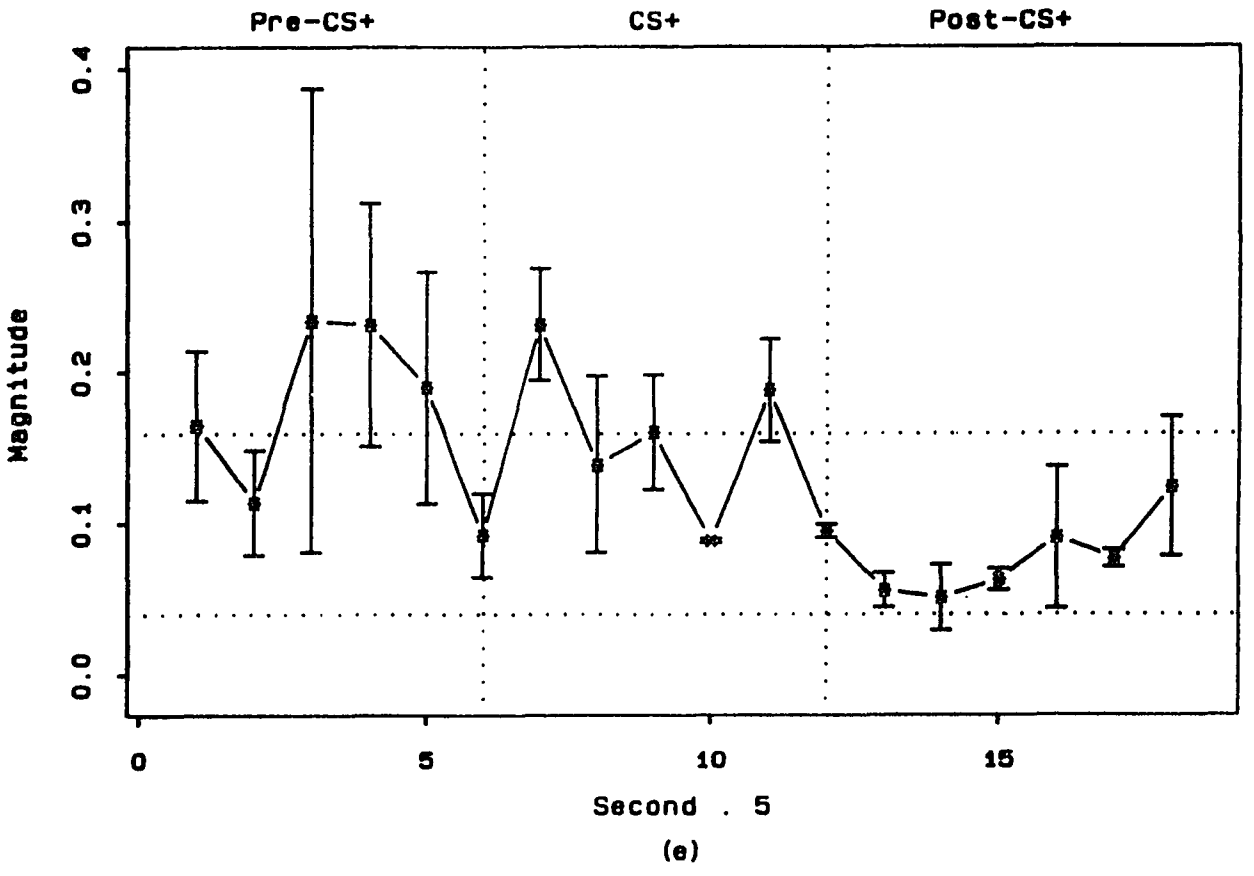

FIGURE D.7 (e) THE 5-SECOND AVERAGE OF (d) WITH STANDARD ERROR AND 95% CONFIDENCE INTERVAL.

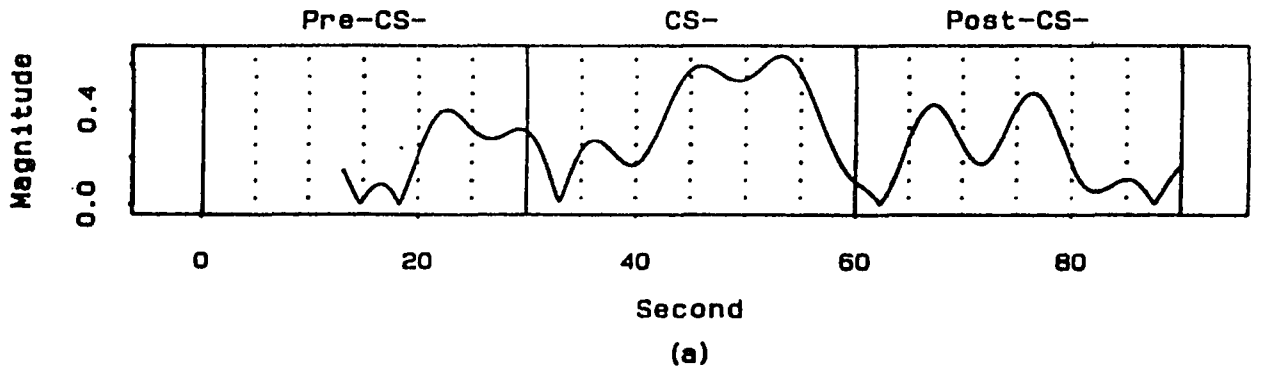

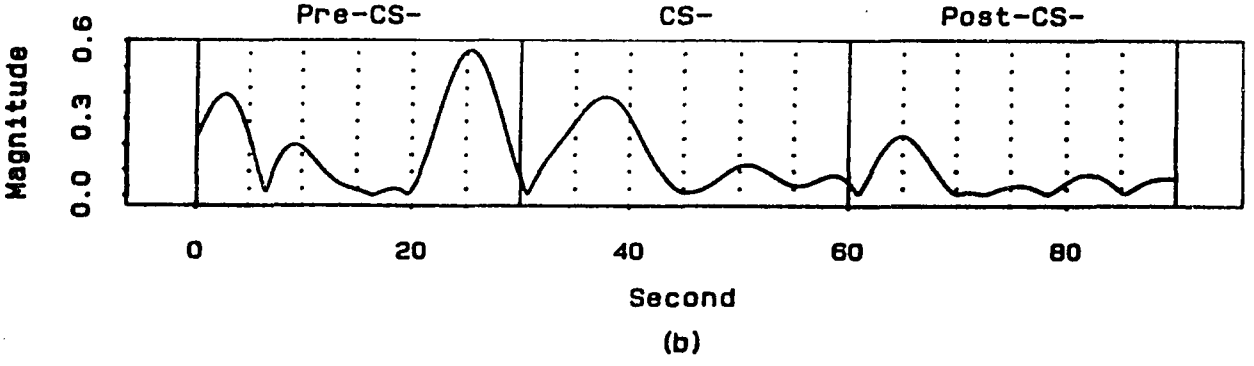

FIGURE D.8 (a) THE LOW FREQUENCY MAGNITUDE RESULT OF DOG 4 UNDER CS- TRIAL 1.

(b) THE LOW FREQUENCY MAGNITUDE RESULT OF DOG 4 UNDER CS- TRIAL 2.

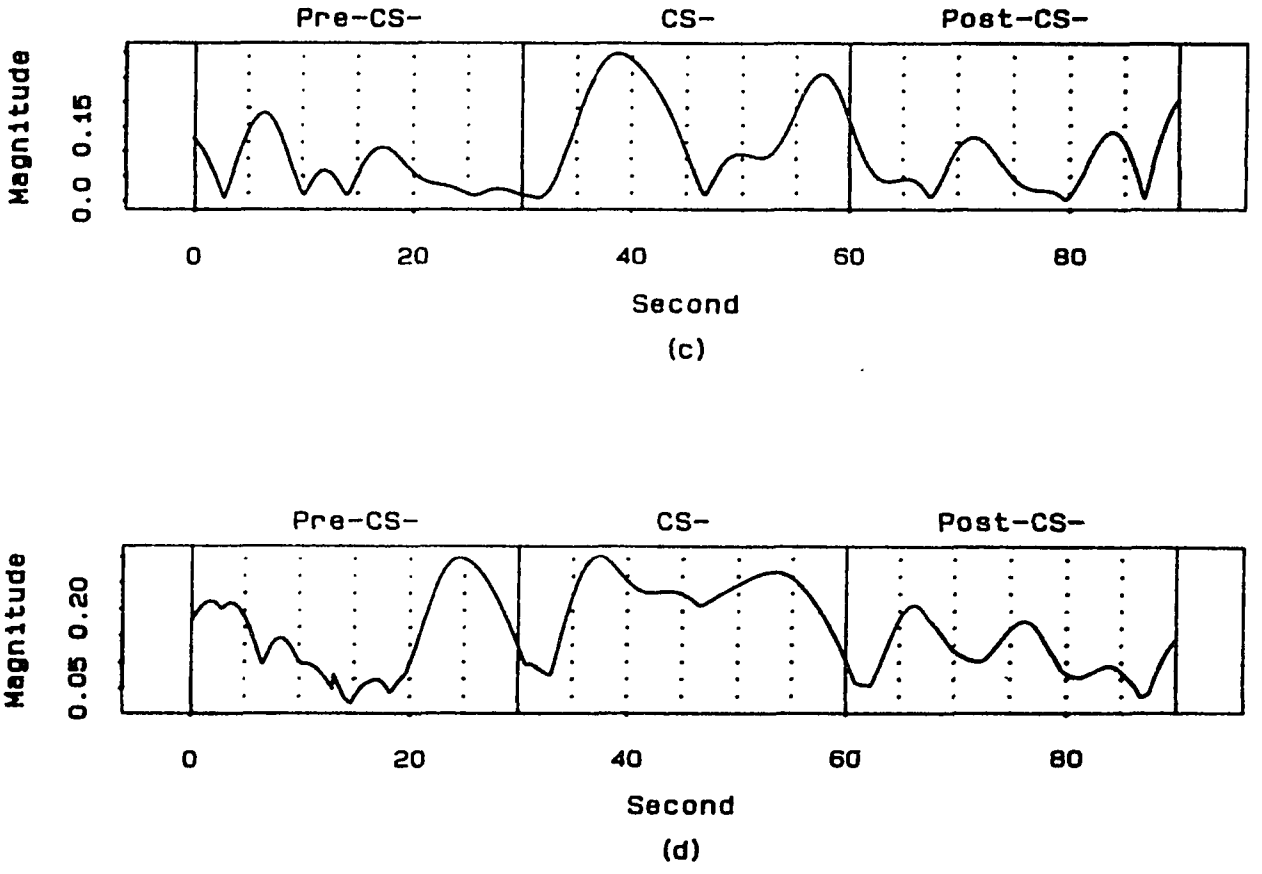

FIGURE D.8 (c) THE LOW FREQUENCY MAGNITUDE RESULT OF DOG 4 UNDER CS- TRIAL 3.

(d) THE AVERAGE FROM (a) TO (c).

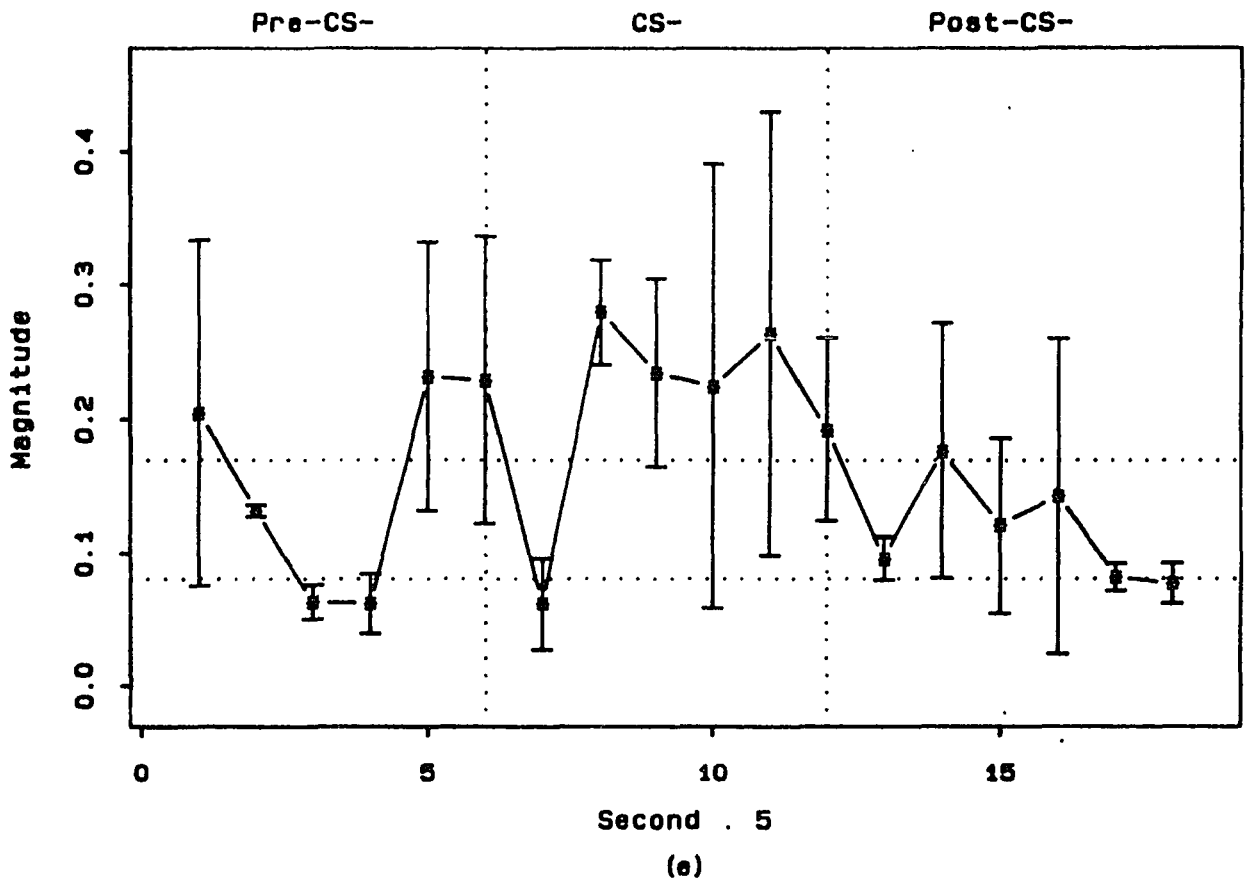

FIGURE D.8 (e) THE 5-SECOND AVERAGE OF (d) WITH STANDARD ERROR AND 95% CONFIDENCE INTERVAL.